TRANSITION METALS HOMEOSTASIS IN *STAPHYLOCOCCUS AUREUS*

By

HASSAN MOHAMMED JASIM AL-TAMEEMI

A dissertation submitted to the

School of Graduate Studies

Rutgers, The State University of New Jersey

In partial fulfillment of the requirements

For the degree of

Doctor of Philosophy

Graduate Program in Microbial Biology

Written under the direction of

Jeffrey M. Boyd

And approved by

_____

_____

_____

_____

New Brunswick, New Jersey

October 2019

ABSTRACT OF THE DISSERTATION

TRANSITION METALS HOMEOSTASIS IN *STAPHYLOCOCCUS AUREUS*

BY HASSAN MOHAMMED JASIM AL-TAMEEMI

DISSERTATION DIRECTOR:

JEFFREY M. BOYD

Staphylococcus aureus is a public health concern. It can evade the immune system and develop resistance to many antibiotic classes. The human immune system employs diverse mechanisms to overcome *S. aureus* infections including disrupting iron (Fe) and copper (Cu) homeostasis at the host-pathogen interface. The work presented herein described iron-sulfur (Fe-S) cluster synthesis as a potential antimicrobial target. We demonstrated that Suf (sulfur mobilization)-dependent Fe-S cluster synthesis is essential in *S. aureus*. Importantly, the Suf system is not present in mammals suggesting that it is a promising antibiotic target. A strain with decreased *suf* transcription exhibited phenotypes that are associated with impaired Fe-S protein maturation. These phenotypes included a reduction in the activity of Fe-S cluster-dependent enzymes and growth inhibition in media deficient in metabolites that require Fe-S enzymes for synthesis. The impairment in Fe-S cluster biogenesis led to increased sensitivity to reactive oxygen and reactive nitrogen species and decreased survival in human polymorphonuclear

leukocytes. We explored how copper harm *S. aureus*, by creating a Δ*copAB* Δ*copBL* strain (*cop*-) that was defective in removing copper from the cytosol. We isolated *cop*- strains with Tn insertions in *mntABC* that resist copper. When cultured with copper, strains containing the *mntA*::Tn mutation had less copper load than the parent strains. Manganese bound MntR repressed MntABC. The Δ*mntR* strain had reduced growth and increased copper load under copper stress. The introduction of the *mntA*::Tn allele annulled these phenotypes. Over-expression of MntABC amplified cellular copper load and sensitivity to copper. The *mntA*::Tn mutation presence also protected Fe-S enzymes from inactivation by copper. We also found that copper was not substantially inhibiting the growth of *S. aureus* by poisoning NrdEF under the growth conditions utilized; however, when NrdEF function was decreased by copper, the ribonucleotide reductase function is decreased by the addition of hydroxyurea. The introduction of a *mntA::Tn* allele improved growth of both Δ*copAZ* and Δ*copBL* strains from copper intoxication suggesting that the presence of a second copper detoxification system protects *S. aureus* from MntABC-dependent copper intoxication. The data presented are consistent with a model wherein copper enters *S. aureus* cells via the MntABC importer and poisons Fe-S enzymes. Taken together, the work presented in this thesis supports the viability of targeting Fe-S synthesis as a viable therapeutic approach and established a novel role for *mntABC* in copper homeostasis.

Acknowledgements

Ever since my graduation from The College of Veterinary Medicine in Iraq, I decided to pursue my postgraduate education in an American university. My country passed in several intermittent wars and sanctions which elongated my educational journey. I want to extend my appreciation to the many people who have helped me throughout my educational years in my home country and America. First and foremost, I would like to thank my advisor, Dr. Jeff M. Boyd, for accepting me in his lab, guiding me through the past years, and making this such a productive experience for me. In addition to a high caliber science, I learned the determination and dedication to science from his well-deserved journey to tenure-ship. I would also like to thank my thesis committee, Dr. Gerben Zylstra, Dr. Tamar Barkay, and Dr. Alvaro Toledo, for their support and invaluable feedback. Dr. Zylstra, I sincerely appreciate your help and advice during my study period. I am also in debt to Dr. Max M. Häggblom, the Department of Microbiology and Biochemistry, and the many Alumni and friends of the Department that, through their philanthropic donations, made fellowships, scholarships, and travel awards possible. I am blessed and thankful for the presence of Mrs. Alexandria Bachmann from the school of graduate studies in my life and for being a real Mom during the past years. My gratitude is also extended to Mrs. Marsha Nabors from university housing who was always supportive of Iraqi students. I would also like to acknowledge the present and past members of the Boyd Lab for their scientific support and for helping me at personal levels. I will miss you all and hope that one day we may cross paths again. I am in debt to my friend, Ameya Mashruwala, for

his scientific and personal advises while I was pursuing my research studies. I would further like to thank the government of Iraq for providing me with this educational opportunity. I will strive to continue to develop the education I have received here and to share the science with my academic community in Iraq.

And to my family. I cannot find enough words to thank my parents for everything that I achieved in life thus far. You were my motivation to continue across all hardships and I would not have been able to finish this work without your presence. To my wife, without your unwavering love, encouragement, and patience, I would have not reached to this point. The taste of success is meaningless without your presence in my life. Thank you. I dedicate this thesis to my family, especially my grandmother, who supported my early education and passed away while I was trying to achieve my educational goals.

Table of contents

List of tables

Chapter 1

Chapter 2

List of figures

Introduction

Chapter 1

Chapter 2

Concluding remarks and future directions

Preface

Chapter 1 has been published as : "The Suf iron-sulfur cluster biosynthetic system is essential in *Staphylococcus aureus*, and decreased suf function results in global metabolic defects and reduced survival in human neutrophils."

Roberts CA, Al-Tameemi HM, Mashruwala AA, Rosario-Cruz Z, Chauhan U, Sause WE, Torres VJ, Belden WJ, Boyd JM. *Infection and Immunity* 85 (6): e00100-17. https://doi.org/10.1128/IAI.00100-17. Hassan M. Al-Tameemi (A first co-author) contribution: Figures 1.4a, 1.5, 1.6, 1.7, 1.8,1.9, and (Table 1.4).

Chapter 2 is in preparation for publication as : *Staphylococcus aureus* lacking a functional MntABC manganese import system have increased resistance to copper. Hassan M. Al-Tameemi (A first author) contribution: All figures except Figure 2.5 A,B).

Introduction

General Overview of *Staphylococcus aureus*

Staphylococcus aureus is a Gram-positive bacterium isolated from wound suppurations in the 1880s by Sir Alexander Ogston (Ogston 1984). Since its discovery, it continues to be a significant human pathogen. Further evidence of its virulence was reported in 1941 when Skinner and Keefer reported that *S. aureus* associated bacteremia caused a mortality rate of 82% among 122 patients at Boston City Hospital (Skinner and Keefer 1941). After utilization of methicillin for treatment, the first β-lactamase-resistant penicillin was reported in 1961 in the United Kingdom (Jevons 1961). The health facilities associated methicillin resisting *Staphylococcus aureus* (MRSA) infections emerged in the 1960s in the United States (Tenover et al. 2006; Barrett et al.1968). Before the 1990s, most of the reported MRSA cases were related to health care settings, after which community-acquired MRSA (CA-MRSA) emerged (Tenover et al. 2006). These CA-MRSA strains are hypervirulent and cause skin and soft tissue infections (SSTIs). In many cases, infections often develop to a more invasive and systemic disease (David and Daum 2010). Armed by a wide range of virulence factors, *S. aureus* continues to be a threat to public health indicated by the annual reported morbidity and mortality cases by The Centers for Disease Control and Prevention (CDC). Antibiotic-resistant strains, including MRSA strains, are particularly worrisome (Turner et al. 2019). Due to the ability of this pathogen to rapidly evolve or acquires antibiotics resistance, treatment is becoming more complicated and an economic burden. Resistance to vancomycin, the backbone antibiotic for the treatment of

MRSA infections globally, is on the rise which signifies the need for investigating alternative antibiotics targets (Wilcox et al. 2019).

Methicillin resistance is attributed to *mecA* gene which is acquired by horizontal transfer of a mobile genetic element named Staphylococcal cassette chromosome *mec* (SCCmec) (Ito et al. 2009; Hartman and Tomasz 1981). The *mecA* gene encodes for the penicillin-binding protein 2a (PBP2a) enzyme, which is responsible for crosslinking the peptidoglycans in the bacterial cell wall. MRSA PBP2a has a low affinity for β- lactams antibiotics, which promotes resistance against this entire class of antibiotics (Turner et al. 2019; Hartman and Tomasz 1984; Ito et al. 2009).

It is estimated that up to >20% of the population are colonized with *S. aureus* (den Heijer et al. 2013) and 60% of people are considered intermittent carriers (Williams 1963; Kluytmans et al. 1997). *S. aureus* often found commensally in the nares, throat, axillae, rectum, anterior nares, extranasal sites, including the skin, perineum, pharynx, and groin. MRSA colonization increases the risk of infection especially for vulnerable and immune compromised categories (Carr et al. 2018; Smith et al. 2019).

S. aureus can resist and evade the host immune system. It poses a wide range of pathogenic factors such as immune evasive surface factors (capsule and protein A), toxins production (haemolysins and leukocidins), tissue invasion enzymes (hyaluronidase) and biofilm formation (Turner et al. 2019). To avoid the immune system and target antibiotics, small colony variants strains can be

selected for (Proctor et al. 1995) and may retain infection intracellularly (Ellington et al. 2006; Garzoni and Kelley 2009).

Once inside the host, pathogens are attacked by a wide variety of lethal immune responses. The pathogens also face a nutrients and metal restricted environment. The vertebrate's immune system developed metals sequestering mechanisms to limit bioavailability of metals like iron and manganese as well as to bombard pathogens with other metals such as copper (Becker and Skaar 2014; Rowland and Niederweis 2012).

In this context, due to their significant involvement during bacterial infection, the homeostasis and bioavailability of four major transition metals, iron (Fe), manganese (Mn), zinc (Zn), and copper (Cu), is crucial for pathogens survival (Salomon et al. 2011; Palmer and Skaar 2016).

Role of Iron in *S. aureus* infection

The uptake and use of iron in the metabolic and regulatory processes are vital for the progress of *S. aureus* infection (Mashruwala et al. 2016a; Posada et al. 2014; Roberts et al. 2017). The persistent necessity for iron by pathogens is due to the vast number of proteins that exploit the versatile redox potential of this inorganic element. Due to the difficulty to utilize the insoluble iron or ferric Fe(III) form, ferrous Fe(II) is the common form for bacterial biological processes (Cartron et al. 2006). During infection, free iron is sequestered by the host through several mechanisms. Of these, lactoferrin and transferrin iron-binding glycoproteins, found in the serum and mucosal secretions, makes iron limited for pathogens (Ellison 1994; Lin et al. 2014). Due to host limitation, pathogens, including *S. aureus*,

evolved complex strategies to acquire iron. While inside the host, *S. aureus* utilize two main tactics to access iron: siderophores (staphyloferrin A- encoded by *sfaABCD* , staphyloferrin B- encode by *sbnABCDEFGHI*), and the heme uptake from hemoglobin (Skaar et al. 2004; Beasley et al. 2009). Moreover, *S. aureus* can uptake exogenous Fe(III)-hydroxamate siderophores (Sebulsky et al. 2000).

The iron uptake processes are controlled by the iron-dependent ferric uptake regulator coded by the *fur* gene. Fur represses the Fur-regulated genes under iron repletion by binding to a consensus DNA sequence named the Fur box typically located upstream of the regulated genes (Horsburgh et al. 2001b; Johnson et al. 2011). The coordination of the metal co-repressor guides the conformational modification of the Fur regulator, which helps and stabilizes its contact with DNA. The geometry of Fur protein is governed by three metals binding sites which are thought to bind transition metals with higher affinity to iron (Xiong et al. 2000; Seo et al. 2014; Fillat 2014; Bags and Neilands 1987). Under iron-limited conditions*, S. aureus* redirects central metabolism into fermentative pathways (iron-sparing-response) in a Fur-dependent mechanism. It has been proposed that lactate production, during fermentative growth, lowers the pH and decrease iron binding affinity of host sequestering protein transferrin (Friedman et al. 2006). *S. aureus* utilizes other Fur family transcriptional regulators that senses metals and have overlapping roles such as PerR (reactive oxygen species (ROS) and Zur (zinc) (Horsburgh et al. 2002; Ando et al. 2003; Fillat 2014).

Almost all the iron inside the cells is combined into proteins utilizing iron-sulfur clusters (Fe-S clusters), heme, or as a mononuclear iron. A very limited

amount of non-incorporated iron exists inside of bacterial cells and has a tendency to catalyze harmful Fenton chemistry reactions (Keyer and Imlay 1996; Maringanti and Imlay 1999). After iron acquisition , iron is either integrated into its cognates targets or sequestered by ferritin FtnA (Horsburgh et al. 2001b; Morrissey et al. 2004), bacterioferritin comigratory protein (Bcp) (Horsburgh et al. 2001a), and the Dps homolog MrgA (Metallo regulated gene A) (Morrissey et al. 2004). These proteins are iron chelators and storage proteins with additional roles in protecting against ROS and DNA damage. PerR senses ROS and derepresses ROS responsive genes such as *katA, ahpCF, ftn,* and *mrgA* (Horsburgh et al. 2001a).

Iron-sulfur clusters:

Iron-sulfur (Fe-S) clusters are classified among the most ancient versatile inorganic cofactors found among all living organisms (Barras et al. 2005; Beinert 2000; Py and Barras 2010) . Due to their chemical versatility, Fe-S clusters can conduct various redox biological reactions (Roche et al. 2013; Py and Barras 2010; Sun et al. 2012). The rhombic [2Fe-2S] and cubane [4Fe-4S] clusters are the most prevalent forms in biological systems (Barras et al. 2005). Iron in these Fe-S clusters forms is either Iron Fe(II) or Fe(III) plus sulfide (S^{2-}) . They usually linked to thiolate ligand in the protein and therefore in most cases cysteine residues coordinate the iron in the cluster (Figure-A). However, histidinyl ligands can coordinate Fe-S clusters too (Beinert 2000; Py and Barras 2010).

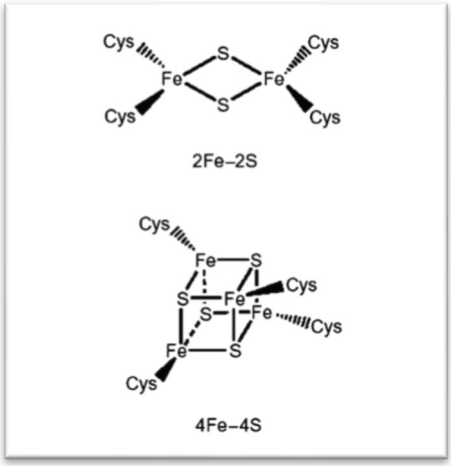

Figure-A : Schematic illustration of Fe-S clusters embedded in proteins by cysteine ligands. Top: rhombic, lower: cubane forms. Modified from (Barras et al. 2005).

Three Fe-S building machineries have been described in bacteria (Suf [sulfur mobilization], Isc, and Nif) (Zheng et al. 1998; Yuvaniyama et al. 2000; Takahashi and Tokumoto 2002). *S. aureus* utilizes the Suf machinery, composed of the SufCDSUB proteins, to synthesize Fe-S clusters from monoatomic Fe^{2+}, S^0, and electrons (Mashruwala et al. 2015b). After synthesis, the Fe-S cluster is handed to either an apoprotein or Fe-S cluster carriers that deliver the cofactor to the target apoprotein (Figure-B.a. , B.b).(Wollers et al. 2010; Chahal and Outten 2012; Mashruwala et al. 2015b).

B.a.

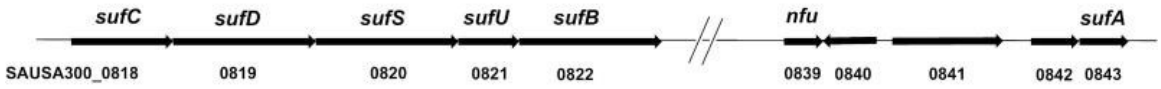

B.b.

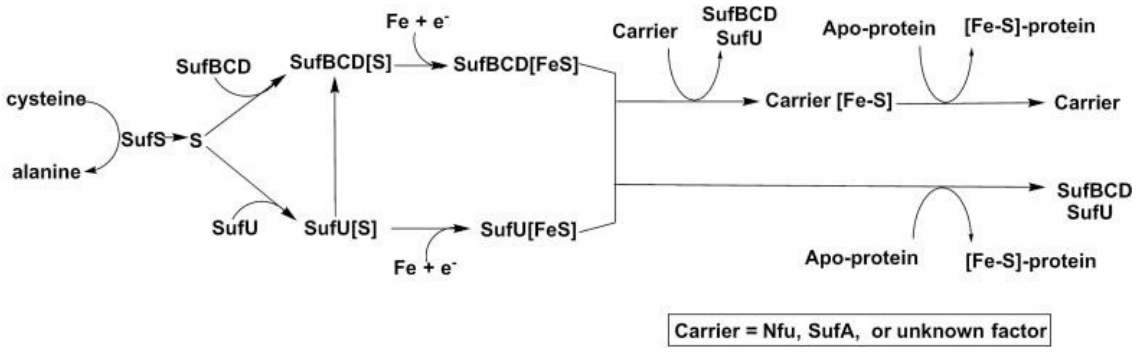

Figure-B: Fe-S cluster biosynthesis in *S. aureus* USA300_FPR3757: Modified from (Mashruwala et al. 2015b).

Panel B.a. - Chromosomal locations of *S. aureus* Fe-S cluster genes (*sufCDSUB* operon) and genes coding for the Fe-S cluster carrier molecules *nfu* and *sufA*.

Panel B.b: Model for Fe-S cluster biogenesis and trafficking in *S. aureus*. SufS donate S^0 for Fe-S cluster biosynthesis. Fe-S clusters are built on the SufBCD or SufU scaffolds. Build clusters are transferred to either 1) an apo-protein, or 2) an Fe-S cluster carrier molecule (SufA and Nfu) for delivery to a target apo-protein.

Copper importance for *S. aureus*:

Copper is an essential metal for many organisms (Andreini et al. 2008). Compared to other transition metals, copper uptake pathways are the least understood in bacterial pathogens (Begg 2019), with only argued non-specific copper uptake pathway through porins (Speer et al. 2013).

Copper has two oxidation states: water- insoluble reduced Cu (I) (cuprous) and water-soluble oxidized copper (II) (cupric) (Festa and Thiele 2011). Both copper forms can bind organic molecules effectively and form many organic complexes (Whellan et al. 2014). These characteristic features allowed copper (I) to bind to soft bases such as thiols. Whereas, copper (II) can bind additional ligands, including sulphate and nitrate. Copper is typically bound to proteins through cysteine, methionine, or histidine side chains (Osman and Cavet 2008; Festa and Thiele 2011; Whellan et al. 2014; Rubino et al. 2011). The free unbound copper is not favored inside the cell, and its concentration is strictly regulated. While maintaining a relatively stable quota of copper for cellular processes, bacteria sense and limit intracellular free copper at zeptomolar levels which render cytosolic environment virtually free of “free” or non-chelated copper (Finney and O’Halloran 2003; Changela et al. 2003).

The molecular mechanism(s) of copper killing is not entirely clear, and it is likely multifaceted (Begg 2019). In support of this, copper stress involves perturbations of many stress and non-stress regulons resulting in multi-dimensional responses (Baker et al. 2010; Chillappagari et al. 2010; Moore et al. 2005; Quintana et al. 2017). Copper can cause hydroxyl radicals through Haber–

Weiss reaction and Fenton chemistry reaction (Gunther et al. 1995; Cervantes-Cervantes et al. 2005). However, it has been found that copper is more toxic anaerobically which suggests additional mechanisms for copper toxicity (Tan et al. 2017; Macomber and Imlay 2009). Moreover, studies indicated that the toxicity of copper is not entirely attributed to ROS and Fenton chemistry (Macomber et al. 2007; Sarah and Keevil 2016; Pham et al. 2013).

Copper can bind to adventitious sites in proteins, nucleic acids, polysaccharides and lipids, causing the dislocation of native metal ions, and/or alterations to their structure and function (Macomber and Imlay 2009; Hong et al. 2012). In *Pneumococcus,* copper inhibited the essential aerobic manganese-dependent nucleotide synthesis pathway and increased the expression of the anaerobic pathway (Johnson et al. 2015b). Copper ions have been shown to damage the outer and/or inner membranes of bacteria (Hong et al. 2012; Peters et al. 2018).

There are two basic mechanisms for tolerance of copper in bacteria. First, the transmembrane copper exports (P1B-type ATPases like CopA and CopB transporters) function to export copper as to maintain a copper free cytoplasm (Rosario-Cruz et al. 2019).

Copper is transported and handed to the target proteins, including CsoR and cytoplasmic amino terminal of CopA exporter, by cytoplasmic CopZ chaperons (Singleton et al. 2009; Sitthisak et al. 2007; Quintana et al. 2017). Second, the cysteine-rich metallothioneins tightly bind copper ions by sequestering copper and limiting its toxicity (Shi et al. 2014). Other protection mechanisms were proposed

such as the use of siderophore-mediated protection by yersiniabactin in *E. coli* which can bind to copper (II) and prevent its reduction to copper (I) (Chaturvedi et al. 2012), and the oxidation of copper (I) by multicopper oxidases to copper (II) ion. These multicopper oxidases work by oxidizing toxic copper (I) to less toxic copper (II) (Djoko et al. 2010).

Staphylococcus aureus has an operon encoding for P1-type ATPase protein (CopA) and a downstream copper chaperone protein (CopZ). Some strains possess an additional copper P1-type ATPase (CopB) transporter (Rosario-Cruz et al. 2019) and a multicopper oxidase (Mco) (Sitthisak et al. 2005). The CsoR copper response regulator senses copper levels in *S. aureus*.

Copper-free CsoR acts as a repressor for the transcription of the genes encoding the transmembrane copper exporters (CopA and CopB transporters), external copper binding lipoprotein CopL, and CopZ chaperone that is thought to shuttle copper to the transporters (Rosario-Cruz et al. 2019; Baker et al. 2011).

The importance of manganese for *S. aureus*:

Manganese (Mn) has a vital role in the virulence of many bacterial pathogens. Lacking intracellular manganese (II) affects manganese-dependent enzymes that are involved in cellular process such as transcription, metabolism, and defense against oxidative stress (Grunenwald et al. 2019; Juttukonda and Skaar 2015). Humans immune system limit manganese and zinc in the site of infection. Neutrophils produce calprotectin (CP) protein at the site of infection to chelates manganese and zinc (Corbin et al. 2008). Two main classes of manganese transporters have been found in bacteria: natural resistance-

associated macrophage proteins (NRAMP) H^{+}- Mn^{2+} and the ATP binding (ABC) permease. Almost all sequenced bacterial geneomes encode both or one of these systems (Papp-Wallace and Maguire 2006). In *S. aureus* manganese is senesced by the transcriptional regulator MntR, which acts as a negative and positive regulator of the manganese importers MntABC and MntH (NRAMP), respectively (Ando et al. 2003; Horsburgh et al. 2002). MntH is constitutively expressed in Mn (II) replete conditions, with relatively modest modulation of expression in response to manganese (II) availability. Whereas MntABC is proposed to be the primary manganese (II) importer when cells are subjected to manganese limitations (Ahuja et al. 2015; Radin et al. 2019).

In *S. aureus,* MntABC consists of the ATP-binding protein MntA, the permease MntB, and the metal binding MntC (Anderson et al. 2012; Cockayne et al. 1998; Horsburgh et al. 2002). The membrane-anchored MntC chelate manganese (II) from the host environment and deliver it to the integral membrane transporter, MntB (Figure-C). MntC, is highly conserved in *Staphylococcus* (Anderson et al. 2012). It was initially proposed to be an iron transport (Stoll et al. 2005; Müller et al. 2010; Cockayne et al. 1998). Typically, the metal binding site of manganese (II) binding proteins is coordinated by two histidine residues, a glutamate and aspartate residue. *S. aureus* MntC manganese (II) binding site is coordinated by H50, H123, E189, and D264 residues (Ahuja et al. 2015; Gribenko et al. 2013; Handke et al. 2018).

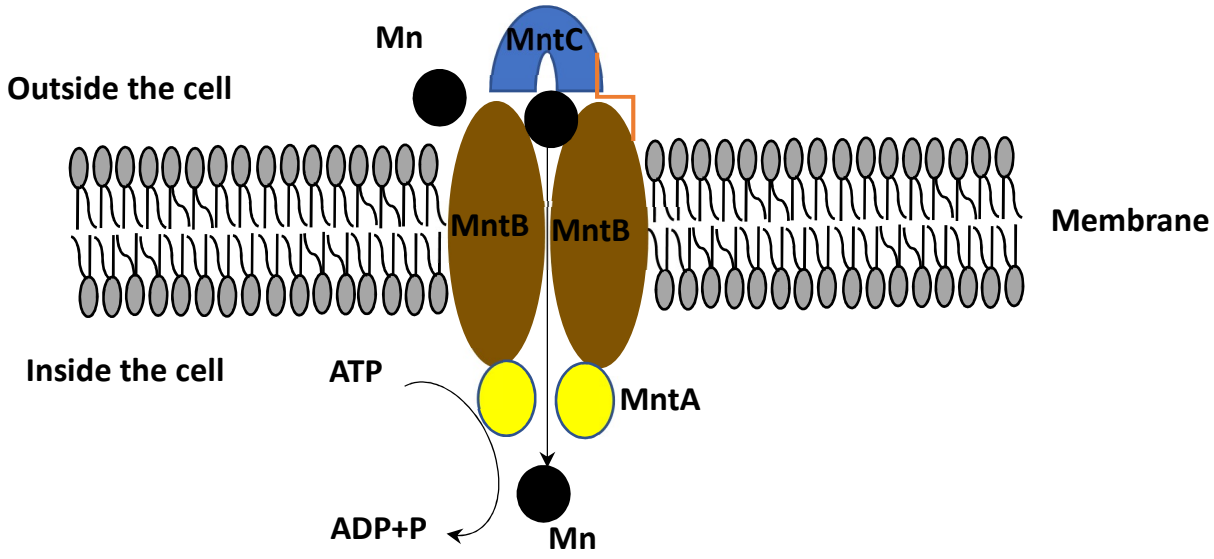

Figure-C: Schematic representation of MntABC importer. The membrane-anchored MntC (blue) chelate manganese (II) (black circle) from the environment and deliver it to the integral membrane transporter MntB (brown). The MntA ATPase (Yellow) provides the energy for conformational changes necessary for manganese (II) uptake.

Response of *S. aureus* to reactive oxygen and maintenance of a reduced intracellular environment:

As a facultative anaerobic pathogen, *S. aureus* must be able to circumvent the endogenous and exogenous reactive oxygen (ROS) and reactive nitrogen species (RNS). Oxygen reactive by-products, such as superoxide anion radical ($^{\cdot}O^{2}$), hydrogen peroxide (H_2O_2), and the extremely reactive hydroxyl radicals ($^{\cdot}OH$), are constantly produced during aerobic growth. These ROS can target macromolecules, DNA, proteins and lipids in cells causing reversible and irreversible damage (Mashruwala and Boyd 2017; Sun et al. 2012; Imlay 2003; Kashmiri and Mankar 2014; Jang and Imlay 2007; Roberts et al. 2017; Arce

Miranda et al. 2011). *S. aureus* monitors the levels of these free radical oxidants constantly and employs antioxidants mechanisms to prevent oxidative stress (Mashruwala and Boyd 2017). These mechanisms include, production of the antioxidant pigment staphyloxanthin (Clauditz et al. 2006), and expression of detoxification enzymes. The primary detoxification enzymes include catalases (Mashruwala and Boyd 2017), superoxide dismutases (Garcia et al. 2017), and peroxiredoxins such the alkyl hydroperoxide reductase (AhpCF) (Horsburgh et al. 2001a). Furthermore, survival inside the host requires the ability to resist nitrogen intermediates such as nitric oxide (Grosser et al. 2018). Due to the harmful effect of ROS to iron-sulfur clusters and proteins, *S. aureus* utilizes systems for buffering and repair (Mashruwala and Boyd 2017; Posada et al. 2014). When ROS levels increase, transition metals can facilitate redox reactions and facilitate ROS generation and Fenton chemistry (Imlay 2003). Bacteria employ mechanisims for exporting and/or sequestration to limit these metals toxic effect especially in the presence of oxidative stress (Gralnick and Downs 2003; Horsburgh et al. 2001a; Martin and Giedroc 2016).

The cytoplasm of bacteria is reduced to maintain the protein thiols in a reduced state (Fahey 2013; Prinz et al. 1997). This reduced state is maintained through thioredoxin and glutaredoxin systems (Prinz et al. 1997), the low-molecular-weight thiol reductants (coenzyme A (CoASH) (Lee et al. 2007; delCardayre et al. 1998) and bacillithiol (BSH) (Fang and Dos Santos 2015; Rosario-Cruz et al. 2015; Newton et al. 2009). *S. aureus* lacks the glutathione pathway (Diep et al. 2006; Posada et al. 2014; Rosario-Cruz et al. 2015) and relays

heavily on the thioredoxin and BSH pathways to conduct the thiol-disulfide redox cycling reactions to maintain a reduced cytoplasm (Rosario-Cruz et al. 2015). The genes encoding Thioredoxin (*trxA)* and thioredoxin reductase (*trxB)* are induced during oxidative stress and when disulfide bonds are oxidized (Uziel et al. 2004; Ballal and Manna 2010). Copper can also cause thiol oxidation in *S. aureus* (Baker et al. 2010). In *S. aureus*, *trxB* transcription is negatively regulated by PerR (Horsburgh et al. 2001a). Non-protein thiols, such as BSH and Cys may chelae intracellular copper and prevent it from damaging cellular macromolecules (Fang and Dos Santos 2015).

The role of metals in Phagocytosis:

Inside the phagosome, macrophages limit iron, manganese, and zinc but simultaneously bombard the pathogen with copper. Macrophages and neutrophils utilize the oxidative burst to kill pathogen. This process involves generation of superoxide via an NADPH-dependent oxidase (NOX). The unstable super oxide (O^{2-}) can react with a variety of cellular targets or can dismutate into H_2O_2 or interact with nitric oxide (NO) to form peroxynitrite (ONOO−), which further damages cells components. Hydrogen peroxide can be reduced to other reactive oxygen species (ROS), such as hydroxyl radicals (OH·) or hypochlorite (OCl^-) and chloramines through the myeloperoxidase (MPO) complex (Uribe-Querol and Rosales 2017). Dislocation of transition metals such as iron from their cognate proteins can cause Fenton chemistry resulting in the production of hydroxyl radicals (OH·). Elemental analysis for phagosomal vacuole showed that copper levels rise from 25 to 500 μM after phagocytosis of *M. tuberculosis.* The more

virulent strains accumulated more copper in the phagosomal vacuole which indicate how copper killing mechanism is an important defense element for the phagocytic cells (Wagner et al. 2005). *S. aureus* can resist and evade phagocytic killing through sophisticated mechanisms. Studies proposed that *S. aureus* can survive intracellularly in the phagocytic cells and is intracellular pathogen (Ellington et al. 2006; Garzoni and Kelley 2009).

There are limited number of cellular processes that can be targeted by antimicrobials. Metals associated processes are essential for all pathogens including *S. aureus.* Understanding these processes is a promising approach for prevention and therapy. *S. aureus* metals associated processes and metals homeostasis of *S. aureus* is the focus of this study.

Research Goal and Objectives.

The goal of this work was to identify and characterize viable targets for antimicrobials in *S. aureus* and to understand molecular response at the host-pathogen interface when confronting copper stress.

Chapter 1: Examine the iron-sulfur cluster biogenesis as a potential target for antimicrobial therapy.

Chapter 2: Describes *S. aureus* copper homeostasis and a novel role for the MntABC importer in copper uptake.

Chapter 1

The Suf Iron-Sulfur Cluster Biosynthetic System Is Essential in *Staphylococcus aureus*, and Decreased Suf Function Results in Global Metabolic Defects and Reduced Survival in Human Neutrophils.

https://doi.org/10.1128/IAI.00100-17.

Abstract

Staphylococcus aureus remains a causative agent for morbidity and mortality worldwide. This is in part a result of antimicrobial resistance, highlighting the need to uncover novel antibiotic targets and to discover new therapeutic agents. In the present study, we explored the possibility that iron-sulfur (Fe-S) cluster synthesis is a viable antimicrobial target. RNA interference studies established that Suf (sulfur mobilization)-dependent Fe-S cluster synthesis is essential in *S. aureus*. We found that *sufCDSUB* were cotranscribed and that *suf* transcription was positively influenced by sigma factor B. We characterized an *S. aureus* strain that contained a transposon inserted in the intergenic space between *sufC* and *sufD* (*sufD**), resulting in decreased transcription of *sufSUB*. Consistent with the transcriptional data, the *sufD** strain had multiple phenotypes associated with impaired Fe-S protein maturation. They included decreased activities of Fe-S cluster-dependent enzymes, decreased growth in media lacking metabolites that require Fe-S proteins for synthesis, and decreased flux through the tricarboxylic acid (TCA) cycle. Decreased Fe-S cluster synthesis resulted in sensitivity to reactive oxygen and reactive nitrogen species, as well as increased DNA damage and impaired DNA repair. The *sufD** strain also

exhibited perturbed intracellular nonchelated iron pools. Importantly, the *sufD** strain did not exhibit altered exoprotein production or altered biofilm formation, but it was attenuated for survival upon challenge by human polymorphonuclear leukocytes. The results presented are consistent with the hypothesis that Fe-S cluster synthesis is a viable target for antimicrobial development.

Introduction

Staphylococcus aureus is a human commensal that causes morbidity and mortality worldwide. While it is responsible for low-morbidity maladies, such as folliculitis, it is also capable of causing fatal afflictions, such as endocarditis, bacteremia, and toxic shock syndrome (Klevens 2007; Daum 2007). Bacterial antibiotic resistance continues to increase and to be problematic. Infections caused by antibiotic-resistant *S. aureus* result in increased mortality, increased stress on the health care system, and an increased financial burden (Lodise and McKinnon 2007; Cosgrove et al. 2003). Current FDA-approved antibacterials target a limited number of metabolic processes (Lewis 2013). Developing antibacterials that target alternate processes would expand treatment options and aid in multidrug therapy. These facts highlight the need for (i) continued investigations into novel antimicrobial targets and (ii) the discovery of new antimicrobials.

Iron (Fe) is a required nutrient for human bacterial pathogens. Not surprisingly, *S. aureus* strains defective in acquiring or processing intracellular iron have decreased virulence (Skaar et al. 2004; Mashruwala et al. 2015b). Upon acquisition, *S. aureus* uses iron to metalate proteins, produce heme, and synthesize inorganic iron-sulfur (Fe-S) cluster prosthetic groups. Three Fe-S cluster synthesis machineries (Suf [sulfur mobilization], Isc, and Nif) that are, for the most part, functionally redundant but biochemically distinct have been described in bacteria (Zheng et al. 1998; Yuvaniyama et al. 2000; Takahashi and Tokumoto 2002). *S. aureus* utilizes the SufCDSUB machinery to synthesize Fe-S

clusters from monoatomic Fe^{2+}, S^0, and electrons (Mashruwala et al. 2015b). SufBCD acts as a molecular scaffold for Fe-S cluster synthesis (Wollers et al. 2010). SufC is an ATPase that has homology with membrane-associated ATPases, SufD participates in iron acquisition, and SufB is thought to be the site of Fe-S cluster synthesis (Nachin et al. 2001; Saini et al. 2010; Layer et al. 2007). SufS is a cysteine desulfurase that catalyzes the removal of elemental sulfur from cysteine, producing alanine and a SufS-bound persulfide (Selbach et al. 2010). The persulfide is transferred to SufU, which is a sulfur transfer protein that provides the sulfur to SufBCD (Selbach et al. 2014) After synthesis, the Fe-S cluster is transferred directly to either an apoprotein or an Fe-S cluster carrier that traffics the cofactor to the target apoprotein (Wollers et al. 2010; Chahal and Outten 2012). SufA and Nfu function as Fe-S cluster carriers in *S. aureus* (Mashruwala et al. 2015b; Rosario-Cruz et al. 2015). Genetic evidence suggests that SufT and bacillithiol also have roles in the maturation of Fe-S proteins (Rosario-Cruz et al. 2015; Mashruwala et al. 2016a; Rosario-Cruz and Boyd 2016).

The SufCDSUB Fe-S cluster synthesis machinery is fundamentally different from the synthesis machinery used by mammals. Mammals synthesize Fe-S clusters in two cellular locations (Lill 2009). In mammals, Fe-S clusters are synthesized in mitochondria using machinery that is similar to the bacterial Isc system, as well as in the cytosol using the cytosolic iron-sulfur cluster assembly (CIA) machinery, which does not share homology with described bacterial synthetic systems. Therefore, if a therapeutic agent that inhibits SufCDSUB is developed, it is unlikely that the agent would affect the essential process of Fe-S

cluster synthesis in humans. Proteins containing Fe-S prosthetic groups are widely distributed throughout the proteomes of most organisms and are necessary for diverse cellular processes. Because of the substantial reliance on Fe-S proteins, we hypothesize that disruption of Fe-S cluster synthesis in *S. aureus* will result in metabolic standstill and eventual cell death. This hypothesis is supported by results from high-density transposon mutant screens showing that the *sufCDSUB* gene products are important for *S. aureus* fitness and possibly survival (Valentino et al. 2014; Santiago et al. 2015; Chaudhuri et al. 2009).

This study was initiated to determine if Fe-S cluster biogenesis is a viable antimicrobial target in *S. aureus*. RNA interference studies confirmed that the Suf Fe-S cluster biosynthetic system is essential for *S. aureus* viability. An *S. aureus* strain with decreased *sufSUB* transcription had a decreased capability to mature Fe-S proteins. Decreased Suf function resulted in global metabolic defects and reduced survival in human polymorphonuclear neutrophils (PMNs), but it did not alter biofilm formation or exoprotein production.

Results

Expression of antisense RNAs to the *sufC* or *sufU* transcripts decreases *S. aureus* viability.

The conditional expression of an antisense RNA targeted to a corresponding mRNA is an effective means to deplete cells of a specific gene product (Ji et al. 2002). The essentiality of Suf was examined using mRNA depletion. DNA fragments corresponding to *sufC* or *sufUB* were shotgun cloned into a plasmid under the transcriptional control of an anhydrotetracycline (Atet)-inducible promoter. Two clones corresponding to *sufC* and two clones corresponding to *sufU* that resulted in decreased growth in tryptic soy broth (TSB) medium upon expression of the plasmid insert were isolated. The plasmids contained fragments that expressed an RNA that was antisense to the 3′ coding region of either the *sufC* or *sufU* mRNA. *sufC* is 762 nucleotides in length, and the p*sufC*KD plasmids contained fragments corresponding to bases 515 to 762 (p*sufC*KD1) and 572 to 750 (p*sufC*KD2). *sufU* is 465 nucleotides in length, and one clone contained a fragment corresponding to bases 216 to 465 plus 32 bp of intergenic *sufUB* DNA (p*sufU*KD1) while the second clone corresponded to bases 353 to 465 plus 32 bp of intergenic *sufUB* DNA (p*sufU*KD2). *S. aureus* strain RN4220 containing the empty vector or the p*suf*KD plasmids did not exhibit growth abnormalities when cultured on solid medium lacking inducer (Figure 1.1). As the concentration of Atet was increased, viability decreased in the cells containing p*suf*KD plasmids, but not in cells containing the empty vector. The efficiency of the knockdown plasmids was decreased in *S. aureus* strain LAC, and this effect was

independent of SigB or Agr, which are known to be defective in RN4220 (data not shown) (Traber and Novick 2006; Nair et al. 2011). It is currently unknown why the plasmids behave differently in these two genetic backgrounds.

A transposon insertion between *sufC* and *sufD* results in decreased transcription of downstream *suf* genes.

Two strains that contain *bursa aurealis* mariner-based transposons inserted into the *sufCDSUB* operon between annotated genes were obtained (Fey et al. 2013). The transposons were located 62 and 63 bp upstream of *sufD* (*sufD**) or *sufS* (*sufS**), respectively (Figure 1.2A). We were able to reconstruct the *sufD** strain in the *S. aureus* LAC background, but we were unable to reconstruct the *sufS** strain. Therefore, the *sufS** strain is not discussed further in this study. We assessed the effects of the *sufD** transposon on transcription of *sufCDSUB*. The transcripts corresponding to the gene upstream of the *sufD** transposon were increased (Figure 1.2B). In contrast, there was no effect on the *sufD* transcript, but the transcripts corresponding to *sufSUB* were decreased.

***sufCDSUB* are cotranscribed, and transcription is modulated by sigma factor B (σ^B).**

A previously published transcriptome sequencing (RNA-seq) data set (Osmundson et al. 2013) was analyzed to further understand how the *sufD** transposon decreased transcription of *sufSUB*. The reads that mapped to *sufCDSUB* were relatively evenly distributed (Figure 1.3A), leading to the hypothesis that *sufCDSUB* are transcribed as an operon using a common promoter. To test this, a cDNA library was generated from DNase-treated wild-type

(WT) RNA. We used oligonucleotides that bridged various *suf* genes to test whether multiple genes existed on the same cDNA (Figure 1.3B). The resulting amplicons suggested that *sufCDSUB* are cotranscribed. As a control, we included a condition under which reverse transcriptase was not added to rule out possible DNA contamination. Reaction mixtures lacking reverse transcriptase did not generate any detectable product, indicating that the amplicons were not the result of contaminating genomic DNA (Figure 1.3B).

The reads from the RNA-seq experiment (Osmundson et al. 2013) were further analyzed to ascertain the transcription start site and to determine the extent of the *suf* 5′ untranslated region (UTR). The distal reads started at an adenine located 82 bp upstream from the predicted translation start site (Figure 1.3C). This analysis allowed us to identify putative σ^A and σ^B recognition sequences 14 and 28 bp upstream from the proposed transcription start site, respectively (Pané-Farré et al. 2006).

Sigma factor B is a general stress response transcriptional regulator in *S. aureus* (Gertz et al. 2000). The transcriptional activity of *sufC* was monitored in the WT and Δ*sigB* strains during growth. The transcriptional activity of *sufC* was decreased in the Δ*sigB* strain (Figure 1.3D), confirming that SigB positively influences *sufC* transcription.

Decreased *suf* transcription results in lower activities of Fe-S cluster-requiring enzymes.

Aconitase (AcnA) requires an Fe-S cluster for function (Kennedy et al. 1983). The AcnA activity in the *sufD** strain was ~20% of that in the WT (Figure

1.4A). Returning *sufCDSUB* to the chromosome of the *sufD** strain at a secondary location via episome (*sufD** *suf*$^{+}$) fully restored AcnA activity.

S. aureus increases the transcription of genes necessary to metabolize reactive oxygen species (ROS) when cultured under high aeration, suggesting that endogenous ROS accumulates under these growth conditions (Mashruwala and Boyd 2017). Consequently, *S. aureus* strains deficient in the maturation of Fe-S proteins or scavenging endogenously produced ROS display severe defects in AcnA activity when the dioxygen tension is increased (Mashruwala et al. 2016a). The effect of dioxygen tension on AcnA activity in the WT, Δ*acnA*, and *sufD** strains was assessed. A *sodA*::Tn mutant that lacks the major superoxide dismutase was included as an experimental control. To modulate the concentration of dioxygen in the culture medium, we varied the ratio of liquid medium volume to culture vessel to gaseous headspace (HV ratio). The higher the HV ratio, the higher the concentration of dissolved dioxygen (Ledala et al. 2014). The *sodA*::Tn mutant had decreased AcnA activity when cultured at an HV ratio of 20, but the AcnA activity was comparable to that of the WT when cultured at an HV ratio of 2.5 (Figure 1.4B). AcnA activity was greatly decreased in the *sufD** strain, and AcnA activity was not significantly altered as the culture HV ratio was varied.

Like AcnA, the enzyme glutamate synthase (GOGAT, or GltBD) requires Fe-S clusters for function (Vanoni and Curti 2008). The *sufD** strain displayed ~25% of the GOGAT activity of the WT (Figure 1.4C). Taken together, these findings suggest the *sufD** strain has decreased Fe-S enzyme activity and that the

Suf system is the dominant Fe-S cluster synthetic system under multiple culture conditions.

Decreased Suf function results in a reduced rate of carbon flux through the TCA cycle.

AcnA catalyzes the first committed step in the tricarboxylic acid (TCA) cycle and therefore acts as a gatekeeper for flux through the TCA cycle. We tested the hypothesis that TCA cycle function would also be decreased in the *sufD** strain.

The WT, Δ*acnA*, and *sufD** strains were cultured in TSB, and growth was monitored over time. The growth rates of the WT, *sufD**, and Δ*acnA* strains were similar during the exponential growth phase (<6 h) (Figure 1.5A). During the postexponential growth phase (>6 h), the WT and *sufD** strains displayed slower growth, but the *sufD** strain displayed an extended lag phase before postexponential growth commenced. The Δ*acnA* strain did not grow after this time, confirming that growth beyond this inflection point requires TCA cycle function. The *sufD** *suf*+strain did not display growth abnormalities in TSB (data not shown).

The activity of AcnA was also monitored at specific time points throughout growth. AcnA activity was decreased in the *sufD** strain throughout growth (Figure 1.5B). The largest difference in AcnA activity between the WT and *sufD** strains occurred at the start of postexponential outgrowth (~8 h). Acetate accumulation in culture media from all strains was examined. Consistent with decreased TCA cycle function, acetate uptake was decreased and was nonexistent in the *sufD** and Δ*acnA* strains, respectively (Figure 1.5C). All the strains acidified the culture medium at similar rates during the initial growth period. After ~6 h, the WT

and *sufD** strains basified the medium, but the rate of basification was lower in the *sufD** strain (Figure 1.5D). The pH of the medium used to culture the Δ*acnA* strain did not increase after the initial acidification. Taken together, these findings are consistent with the hypothesis that the decreased AcnA activity of the *sufD** strain resulted in decreased flux through the TCA cycle.

Decreased Fe-S cluster synthesis results in decreased growth in media lacking specific amino acids or lipoic acid.

We assayed the growth of the WT, *sufD**, and *sufD** *suf*$^{+}$ strains on chemically defined solid media. The *sufD** strain grew poorly on chemically defined media supplemented with the 20 canonical amino acids (20 aa medium), whereas the *sufD** *suf*$^{+}$ strain grew like the WT. The enzyme lipoyl synthase requires Fe-S clusters (Ollagnier-de Choudens and Fontecave 1999). Supplementing the 20 aa growth medium with lipoic acid alleviated this growth defect of the *sufD** strain. Isoleucine, leucine, and glutamate/glutamine synthesis also requires Fe-S enzymes(Flint and Emptage 1988; Hentze and Argos 1991; Miller 1974). Compared to the WT, the *sufD** strain displayed poor to no growth on chemically defined solid medium containing lipoic acid but lacking isoleucine, leucine, or glutamate and glutamine (Figure 1.6). These phenotypes could be genetically complemented.

Decreased Suf function results in increased DNA damage and a decreased ability to repair damaged DNA.

The DNA repair enzymes MutY (Porello et al. 1998), Nth (Fu et al. 1992), and AddAB (Yeeles et al. 2009) require an Fe-S cluster for function. Mutations

in *rpoB*, which encodes RNA polymerase, provide resistance to rifampin (Rif) (Ezekiel and Hutchins 1968). The rate of spontaneous Rif resistance was determined for the WT and *sufD** strains by plating upon tryptic soy agar (TSA) with or without rifampin. The *sufD** strain had an ~20-fold increase in rifampin-resistant cells compared to the WT strain (Figure 1.7A).

We next examined if one or more of the described Fe-S cluster-requiring DNA repair enzymes had a role in preventing *rpoB* mutations when cultured under standard laboratory conditions. The rate of rifampin resistance was determined in the WT, *mutY*::Tn, *nth*::Tn, and *addB*::Tn mutant strains. The *mutY*::Tn, *nth*::Tn, and *addB*::Tn strains had increased rates of rifampin resistance (Figure 1.7B). We next assayed the susceptibility of the WT, *sufD**, and *sufD* suf*$^{+}$ strains to chemical mutagens. The *sufD** strain had increased sensitivity to methyl methanesulfonate (MMS) (Figure 1.7C) and diethyl sulfate (DES) (Figure 1.7D) compared to the WT and *sufD* suf*$^{+}$ strains. We also examined the necessity for Fe-S cluster-requiring DNA repair proteins for growth in the presence of MMS or DES. The *nth*::Tn and *mutY*::Tn strains showed resistance to MMS and DES similar to that of the WT (Figure 1.7E and F), but the *addB*::Tn strain displayed greatly increased sensitivity to both mutagens.

We sought genetic evidence to lend support to the hypothesis that decreased Fe-S cluster assembly resulted in decreased AddAB activity and increased sensitivity to DNA-damaging agents. Despite multiple attempts, we were unsuccessful in constructing the *sufD* addB*::Tn double-mutant strain, suggesting that the strain may not be viable. However, we were able to create a Δ*nfu addB*::Tn

double mutant. Like the *sufD** strain, the Δ*nfu* strain displayed increased sensitivity to MMS and DES (Figure 1.7E and F). The phenotypic effects of the Δ*nfu* and *addB*::Tn mutations were not additive. Although not conclusive, these data are consistent with the hypothesis that defects in Fe-S cluster assembly result in diminished ability to repair damaged DNA because of decreased functionality of Fe-S clusters requiring DNA repair enzymes.

Decreased Suf function increases sensitivity to reactive oxygen and reactive nitrogen species.

Oxidation of solvent-accessible Fe-S clusters can result in cluster disintegration and impaired protein function. Proteins requiring Fe-S cluster cofactors are targets for ROS and reactive nitrogen species (RNS) (Jang and Imlay 2007; Duan et al. 2009).

The growth of the *sufD** strain in the presence of methyl viologen was monitored. Methyl viologen is a redox cycling agent that produces superoxide. The *sufD** strain had decreased growth when plated upon solid medium containing methyl viologen (Figure 1.8A), and the phenotype could be genetically complemented. A strain lacking the major superoxide dismutase (*sodA*::Tn) displayed decreased growth, verifying superoxide generation. The *sufD** strain also displayed decreased survival after challenge with a bolus of hydrogen peroxide (H_2O_2), and the phenotype could be genetically complemented (Figure 1.8B). A *katA*::Tn strain that is unable to produce functional catalase also displayed decreased survival upon H_2O_2 challenge.

Next, we examined the effects of RNS on the *sufD** strain. We examined the growth profiles of WT, *sufD**, and *sufD** *suf*+ strains in chemically defined medium in the presence and absence of nitroprusside, which interacts with intracellular thiols, resulting in the release of RNS (Grossi and D'Angelo 2005). The *sufD** mutant had a severe growth defect when exposed to nitrosative stress, and the phenotype could be genetically complemented (Figure 1.8C).

The *sufD strain has altered iron homeostasis.**

An *S. aureus* strain lacking the Fe-S cluster maturation factor Nfu is perturbed in intracellular iron homeostasis. We examined whether defective Fe-S cluster synthesis also results in perturbed intracellular iron homeostasis. Growth of the WT, *sufD**, and *sufD** *suf*+ strains was monitored in the presence of 2,2-dipyridyl (DIP), which is a cell-permeable divalent metal chelator with specificity for iron (Rauen et al. 2007). An *fhuC*::Tn mutant that is defective in iron scavenging was included as an experimental control (Speziali et al. 2006). The *sufD** and *fhuC*::Tn strains displayed decreased growth compared to the WT when cultured in the presence of DIP, and the phenotype of the *sufD** mutation could be genetically complemented (Figure 1.9A).

The antibiotic streptonigrin, in combination with iron and an intracellular electron donor, causes DNA damage resulting in cell death (Bolzán and Bianchi 2001). Higher incidences of cell death are correlated with an increased concentration of nonchelated intracellular iron (White and Yeowell 1982). The *sufD** strain displayed increased sensitivity to growth in the presence of

streptonigrin, and the phenotype could be genetically complemented (Figure 1.9B).

Streptonigrin, in conjunction with iron, can catalyze double-stranded DNA breaks (DeGraff et al. 1994). Strains defective in Fe-S cluster assembly were defective in repairing damaged DNA (Figure 1.7). We examined whether the increased streptonigrin sensitivity of strains defective in maturing Fe-S proteins was the result of defective DNA repair. The streptonigrin sensitivities of the *nth*::Tn, *mutY*::Tn, and *addB*::Tn strains were determined. The *nth*::Tn and *mutY*::Tn mutants had streptonigrin sensitivities similar to that of the WT, but the *addB*::Tn mutant displayed increased sensitivity to streptonigrin (Figure 1.9C). The streptonigrin sensitivities of the Δ*nfu* and Δ*nfu addB*::Tn mutants were also assessed. The streptonigrin sensitivity phenotypes attributed to the Δ*nfu* and *addB*::Tn mutations were additive. These findings suggested that the streptonigrin sensitivity phenotype of strains defective in Fe-S cluster assembly was not exclusively due to defective AddAB function.

Exoprotein production and biofilm formation are not significantly altered in the *sufDmutant.**

S. aureus produces and secretes a number of exoproteins, including toxins, adhesins, proteases, and invasins that are crucial for pathogenesis (Bartlett and Hulten 2010). The total abundance of exoproteins was quantified in the spent culture medium obtained from the WT and *sufD**strains. *S. aureus* strains lacking a functional Agr system are deficient in exoprotein production, and therefore, an *agrA*::Tn strain was included as a control (Recsei et al. 1986) . The *agrA*::Tn

strain had decreased exoprotein production, and the phenotype of the *sufD** strain was not statistically significant (*P* = 0.049) (Figure 1.10A).

The activities of hemolytic toxins present in the spent media from WT and *sufD** strains were assessed by examining the ability of spent culture medium to lyse rabbit erythrocytes. An *agrA* mutant has decreased production of hemolytic toxins and was included as a control (Recsei et al. 1986). The WT and *sufD** strains showed similar hemolytic activities (Figure 1.10B), whereas exoproteins from the *agrA*::Tn mutant did not cause detectable lysis.

S. aureus forms surface-associated communities referred to as biofilms. Biofilm-associated cells serve as the etiologic agents of recurrent staphylococcal infections (Otto 2008). Biofilm formation was monitored aerobically using the WT and *sufD** strains. The *agrA*::Tn and Δ*sigB* strains were included as experimental controls for increased and decreased biofilm formation, respectively(Lauderdale et al. 2009; Boles and Horswill 2008). The WT and *sufD** strains formed similar amounts of biofilm, whereas the *agrA*::Tn and Δ*sigB* strains formed more and less biofilm than the WT, respectively (Figure 1.10C).

Effective Fe-S cluster biosynthesis is necessary for survival in human PMNs.

PMNs phagocytize invading bacteria and subject them to toxic chemical species, including ROS (Nauseef 2007). The finding that strains defective in Fe-S cluster synthesis have global metabolic defects, including increased sensitivity to ROS and increased nonchelated Fe, led us to hypothesize that decreased Fe-S cluster synthesis would result in decreased survival in human PMNs.

We examined the abilities of the WT, *sufD**, and *lacB*::Tn strains to survive challenge by human PMNs. The *lacB*::Tn strain was included to evaluate the contribution of the *bursa aurealis* transposon to bacterial survival. The strains were individually combined with human PMNs, and bacterial survival was monitored at various time points. The *sufD** strain had decreased survival compared to that of the WT upon challenge with PMNs (Figure 1.11). The survival of the *lacB*::Tn strain was indistinguishable from that of the WT. Moreover, while the WT and *lacB*::Tn strains were able to rebound (120 and 180 min), minimal growth rebound was observed with the *sufD** strain.

Discussion

The present study confirmed that the Suf Fe-S cluster synthesis system is essential for *S. aureus* under standard laboratory growth conditions. These findings imply that Suf is the only Fe-S cluster synthesis system required for growth under these conditions (Mashruwala et al. 2015b). Therefore, if a therapeutic agent is developed that inhibits SufCDSUB, there may not be an alternate synthesis system that can compensate for its loss. Similar to *S. aureus*, a majority of bacterial species are predicted to utilize only one Fe-S cluster biosynthetic system, and the Suf system is the most widely distributed (Boyd et al. 2014). Data from genetic screens suggest that Fe-S cluster synthesis is also required for fitness or survival of a number of additional human bacterial pathogens during routine laboratory growth (Table 1.4), including *Mycobacterium tuberculosis* and the ESKAPE pathogens *Enterococcus faecalis*, *Pseudomonas aeruginosa*, and *Acinetobacter baumannii*. Not surprisingly, bioinformatics analysis suggests that the individual

genomes of these organisms encode only one described Fe-S cluster synthetic system.

Unlike *S. aureus*, some bacteria utilize multiple Fe-S cluster assembly machineries (e.g., Suf and Isc) that are biochemically dissimilar but, for the most part, functionally redundant (Py and Barras 2010). Lesions in genes necessary for the function of an individual Fe-S cluster synthesis system are not lethal in these organisms (*Escherichia coli* and *Klebsiella pneumoniae*) (Table 1.4) (Bachman et al. 2015; Baba et al. 2006); therefore, therapeutic agents targeting a single Fe-S cluster synthesis system would be less effective in preventing the growth or survival of these bacteria.

Iron-sulfur cluster synthesis is also essential in mammals, but importantly, mammals use Fe-S cluster synthesis machinery that is primarily different from the Suf system reviewed in (Lill 2009). This decreases the likelihood that a potential therapeutic agent that inhibits Suf function would have adverse effects on Fe-S cluster synthesis in mammals.

We utilized an *S. aureus* strain (*sufD**) with decreased transcription of *sufSUB* to examine the effects of decreased Suf function on *S. aureus* physiology. Not surprisingly, the strain had decreased activities of Fe-S cluster-dependent enzymes and global metabolic defects. Decreased Fe-S cluster synthesis reduced growth on media lacking metabolites that require Fe-S proteins for synthesis. Protein-associated and solvent-exposed Fe-S clusters are a primary target of ROS and RNS damage (Jang and Imlay 2007; Duan et al. 2009; Flint et al. 1993), and the *sufD** strain displayed increased sensitivity to H_2O_2, methyl

viologen, and nitroprusside. Decreased Suf function also resulted in reduced flux through the TCA cycle and a destabilized nonchelated iron pool. The *sufD** strain had increased mutagenesis and decreased ability to repair DNA, which were likely the result of decreased AddAB and Nth activities.

Two scenarios could explain the essentiality of SufCDSUB for *S. aureus* survival during standard laboratory growth. There may be a described or unidentified essential Fe-S protein(s). To examine this, we analyzed the results from high-density transposon screens in hopes of determining why Suf is essential in *S. aureus* (Valentino et al. 2014; Santiago et al. 2015; Chaudhuri et al. 2009). With the exception of Fe-S cluster synthesis proteins, the only described Fe-S proteins predicted to be essential are those encoded by *fdx* (ferredoxin) , *hemH* (ferrochelatase), and *addB* (DNA helicase/exonuclease). Fdx and AddB were reported to be essential in one of the three studies, whereas HemH was reported to be essential in two of the studies. Here, we report that the LAC *addB*::Tn mutant is viable. Alternatively, the wide variety of metabolic defects resulting from defective Fe-S protein maturation may result in metabolic standstill and cell death. The numerous metabolic defects of the *sufD** strain support this argument. If the inhibition of numerous metabolic functions leads to the death of cells lacking Suf function, it lowers the probability that a mutation will arise, other than mutations that affect SufCDUSB function, which would provide metabolic bypass to these processes.

Decreased Fe-S cluster synthesis did not alter exoprotein accumulation, alpha-toxin production, or biofilm formation. However, the *sufD** strain displayed

decreased survival in human PMNs. Further emphasizing the importance of Fe-S protein maturation for pathogenesis, an *S. aureus* strain lacking the Fe-S cluster carrier Nfu also displayed decreased survival in PMNs and decreased tissue colonization in a mouse model of infection (Mashruwala et al. 2015b). A recent study used transposon sequencing (Tn-seq) to identify *S. aureus* genes that are necessary for fitness in various models of infection (Valentino et al. 2014). A number of described Fe-S proteins were required for fitness, including AddAB, Nth (DNA repair), MiaB (RNA modification), AcnA, Fdx, SdaA (central metabolism), HemN, and HemH (heme synthesis). The Nfu, SufA, and SufT Fe-S protein assembly factors were also required for fitness during infection (Valentino et al. 2014).

In summary, the data presented in the present study confirm that Suf-dependent Fe-S cluster biosynthesis is essential for *S. aureus* survival under standard laboratory conditions. We show that an *S. aureus* strain with decreased Suf function has broad metabolic defects and reduced survival upon challenge with human PMNs. The mutant strains and genetic constructs described comprise a valuable toolbox for the identification of potential Suf inhibitors and for further characterization of Fe-S cluster assembly in *S. aureus*.

Materials and methods

Materials.

Phusion DNA polymerase, deoxynucleoside triphosphates, the quick DNA ligase kit, and restriction enzymes were purchased from New England BioLabs. The plasmid miniprep kit, gel extraction kit, and RNA Protect were purchased from Qiagen. TRIzol and High-Capacity cDNA reverse transcription kits were purchased from Life Technologies. Oligonucleotides, obtained from Integrated DNA Technologies, are listed in (Table 1.1) DNase I was purchased from Ambion. Lysostaphin was purchased from Ambi Products. TSB was purchased from MP Biomedical. Difco BiTek agar was added (15 g liter^{-1}) for solid medium. Unless otherwise stated, all chemicals were purchased from Sigma-Aldrich and were of the highest purity obtainable.

Table 1.1: Primers used in this study.

Name	Sequence
sufDfwdRT	CAAGTTGATGATAATGCATCGAAAG
sufDrevRT	ATGGTTCATAAGAGCGTCTGCTAA
sufSfwdRT	AACCATTGCAGAAATAGCTCATCA
sufSrevRT	GCTTGCGCCCCATCAAC
sufUfwdRT	AATGGCAAGTGCATCGATGA
sufUrevRT	GCATTGCTTCTCCAAGTGAATG
sufBfwdRT	CTGTTGTGGAAATCATTGTGCAT
sufBrevRT	GTTCGCCCAGTTTTGAATCG
sufCRT5	GATGAAATCGATTCAGGGTTAGACA
sufCRT3	TTCCCCACGCATTTGGTTA
sufCup	TTATTCAGCTGAACCGAACTCTTC
sufCdwn	CTCGTTCCCATAGCAAAACCT
sufUBup	GTATTTGTGTTGTCGCTTTATCCACC
sufUBdwn	CGGGTCTATGACAGTAGATATG
pML100rev	GCCTGCAGGTCGACTCTAGAGG
pML100for	GGCGTATCACGAGGCCCTTTCG
sufinternal5	GACGTTAATGAAGTAATCAAGGATTTTCCGATATTAGA
sufinternal3	TCTAATATCGGAAAATCCTTGATTACTTCATTAACGTC
pLLYCC5	CTGTAATGGGCCCAATCACTAGTGAATTCCCGAAGCGGTGGCACT TTTCGGGGAAA
sufYCC3	TCTCACGACGTTTTTGGCCGGTACCACGCGTTCCGGACTATATTA CCCTGTTATCCCTA
YccSuf	TAGGGATAACAGGGTAATATAGTCCGGAACGCGTGGTACCGGCCA AAAACGTCGTGAGA
sufpLL39	GTGCTAAAGAAGTTGTAGGTAATAAAAAAGCTTGCTAGCCGGAAG TCAAGAATGGCTTA

Bacterial growth and media.

The chemically defined minimal medium was described previously (Mashruwala et al. 2016a) and where noted was supplemented with 0.5 μg ml^{-1} lipoic acid. *S. aureus*strains cultured in TSB were grown at 37°C with shaking at 200 rpm in 10-ml culture tubes containing 1 ml of liquid medium unless otherwise stated. Top agar overlays were made by diluting overnight cultures grown in TSB (1:100 in phosphate-buffered saline [PBS]) and then adding 100 μl to 4 ml of 3.5% TSA before pouring it on top of TSA plates. Where noted, 1 μl of 2.5-mg ml^{-1} streptonigrin dissolved in dimethyl sulfoxide (DMSO), 4 μl of neat diethyl sulfate, or 2 μl of neat methyl methanesulfonate was spotted in the centers of the plates. Antibiotics were added to TSB at the following concentrations: 3 to 5 ng ml^{-1} Atet, 30 μg ml^{-1} chloramphenicol (Cm), 1.25 μg ml^{-1} Rif, and 10 μg ml^{-1} erythromycin (Erm). To maintain plasmids, the medium was supplemented with 15 μg ml^{-1} or 5 μg ml^{-1} Cm or Erm, respectively. Methyl viologen and 2,2-dypyridyl were added to solid media at 40 mM and 900 mM, respectively.

Liquid phenotypic analysis was conducted in 96-well microtiter plates containing 200 μl of medium per well using a BioTek 808E visible absorption spectrophotometer, and culture densities were read at 600 nm. The cells used for inoculation were cultured for 18 h in TSB medium, and the cells were washed with PBS. The optical densities (OD) of the cell suspensions were adjusted to 2.5 (A_{600}) with PBS. Two microliters of the washed cells was added to 198 μl of medium. Where noted, sodium nitroprusside was added to liquid media at 15 mM.

Genetic and recombinant DNA techniques.

The bacterial strains and plasmids used in this study are listed in Tables 1.2 and 1.3. Unless otherwise noted, these strains, including the *sufD** strain, were constructed in the community-associated methicillin-resistant *S. aureus* (MRSA) USA300 strain LAC (JMB strains) that had been cured of the plasmid conferring resistance to erythromycin (pUSA03) (Pang et al. 2014). All transductions were conducted using phage 80α (Novick 1963). All the *S. aureus* mutant strains and plasmids were verified using PCR or by sequencing PCR products or plasmids. All DNA sequencing was performed by Genewiz (South Plainfield, NJ).

Table 1.2 : Strains used in this study.

Strain name	Genotype	Source/reference
WT	USA300_LAC	(Boles et al. 2010)
JMB1102	Δ*sigB* (SAUSA300_2022)	(Lauderdale et al. 2009)
JMB1163	Δ*acnA*::*tetM* (SAUSA300_1246)	(Sadykov et al. 2010)
JMB1165	Δ*nfu* (SAUSA300_0839)	(Mashruwala et al. 2015b)
JMB2078	*kat*::Tn (*ermB*) (SAUSA300_1232)	V. Torres
JMB2763	*nth*::Tn (*ermB*) (SAUSA300_1343)	(Fey et al. 2013)
JMB2726	*mutY*::Tn (*ermB*) (SAUSA300_1849)	(Fey et al. 2013)
JMB2950	*agrA*::Tn (*ermB*) (SAUSA300_1992)	(Fey et al. 2013)
JMB3298	*addB*::Tn (*ermB*) (SAUSA300_0869)	(Fey et al. 2013)
JMB5853	*sodA*::Tn (*ermB*) (SAUSA300_1513)	(Fey et al. 2013)
None	*sufD**::Tn (*ermB*) (Figure 1.2A)	P. Fey
None	*sufS**::Tn (*ermB*) (Figure 1.2A)	P. Fey
JMB8464	*sufD**::Tn (*ermB*)	This study
JMB8472	*sufD**::Tn (*ermB*), pLL39_*sufCDSUB*	This study
JMB7237	*lacB*::Tn (*ermB*) (SAUSA300_2154)	(Fey et al. 2013)
JMB7525	*fhuC*::Tn (*ermB*) (SAUSA300_0633)	(Fey et al. 2013)
JMB7592	Δ*nfu addB*::Tn (*ermB*)	This study
RN4220	Restriction minus	(Kreiswirth et al. 1983)
E. coli PX5	Used for gene cloning	Protein Express

Table 1.3 : Plasmids used in this study.

Plasmid name	Insert	Function	Reference
pCM11_*sufC*p	*sufC* promoter	*sufC* transcriptional activity	(Mashruwala et al. 2016b)
pML100	None	Gene expression	(Lei et al. 2011)
p*sufC*KD1	*sufC* DNA	Suf depletion	
p*sufC*KD2	*sufC* DNA	Suf depletion	
p*sufU*KD1	*sufU* DNA	Suf depletion	
p*sufU*KD2	*sufU* DNA	Suf depletion	
pLL39	None	Genetic complementation	(Luong and Lee 2007)
pLL39_*sufCDSUB*	*sufCDSUB*	Genetic complementation	
pCR2.1_TOPO	None	Cloning	

The Suf depletion plasmids were created as described previously (Eidem et al. 2015). Briefly, the *sufC* gene and its 5′ untranslated region were amplified using the sufCup and sufCdwn primers. The *sufUB*amplicon was created using the sufUBup and sufUBdwn primers. The resulting amplicons were gel purified and treated with 0.03 U DNase I (Ambion, Carlsbad, CA) for 5 min. The digested DNAs were separated using agarose gel chromatography, and DNAs of approximately 250 bp were purified. The purified fragments were treated with T4 DNA polymerase (NEB, Ipswich, MA) and subsequently treated with *Taq* DNA polymerase (NEB). The DNA fragments were cloned into pCR2.1_TOPO (Thermo-Fisher). After transformation and selection, the colonies were pooled and the plasmids were purified. The plasmids were digested with EcoRI, and the insert fragments were gel purified and subsequently subcloned into pML100 (Lei et al. 2011). After

transformation and selection, colonies containing pML100 were pooled, and plasmids were purified and transformed into *S. aureus* RN4220 and plated on TSA-Cm. Individual chloramphenicol-resistant RN4220 colonies were inoculated into 200 µl of TSB-Cm medium in 96-well microtiter plates and cultured overnight. The cells were subcultured into liquid TSB media with and without Atet, and strains with decreased growth in the presence of Atet were retained. Four positive clones were identified, and the inserts were confirmed by DNA sequencing. The pLL39_*sufCDUSB* plasmid was created using yeast recombinational cloning as previously described (Joska et al. 2014; Mashruwala et al. 2015a). The amplicons for pLL39_*sufCDSUB* were created using the following primer pairs: pLLYCC5 and sufYCC3, YccSuf and Sufinternal3, and Sufinternal5 and sufpLL39. pLL39 was linearized using SalI.

RNA-seq analysis of the *suf* operon.

RNA-seq data were downloaded from the Gene Expression Omnibus (GEO) (accession number GSE48896), corresponding to NCTC8325-4 (Osmundson et al. 2013). The downloaded Sequence Read Archive (SRA) files were converted to fastq format using the SRA toolkit and then mapped to the *S. aureus* genome using Tophat (Trapnell et al. 2012, 2010). The resulting bam files were sorted and indexed using SAMtools (Li et al. 2009) and then converted to tdf format using Integrative Genomics Viewer (IGV) tools (Robinson et al. 2011). The image of the *suf* operon was acquired using IGV (Robinson et al. 2011).

Protein analysis and GOGAT assays. GOGAT assays were conducted as previously described with slight modifications(Rosario-Cruz et al. 2015). Briefly,

strains were cultured overnight in TSB, and the cells were pelleted by centrifugation and resuspended in PBS (1:1). The resuspended cells were used to inoculate 5 ml (in a 30-ml tube) of chemically defined medium containing 20 aa and lipoic acid to an OD of 0.1 (A_{600}). Strains were cultured at 37°C with shaking to an OD of 0.8 (A_{600}), and the cells were harvested by centrifugation and resuspended in lysis buffer (50 mM Tris-HCl, pH 7.7). The cells were lysed anaerobically by the addition of 4 µg lysostaphin and 8 µg DNase. The cells were incubated at 37°C until full lysis was observed (~1 h). The cell debris was removed by centrifugation. GOGAT was assayed by the addition of 60 µl of 50 mM glutamine (pH 7.7), 60 µl of 5 mM α-ketoglutarate (pH 7.7), 60 µl of cell extract, and 60 µl of 0.75 mM NADP (NADPH) to 600 µl of lysis buffer. GOGAT activity was determined by monitoring the rate of NADPH oxidation at 340 nm for 5 min (extinction coefficient at 340 nm [ε_{340}] = 6.22 mM^{-1} cm^{-1} (Dougall 1974).

Aconitase assays.

AcnA assays were conducted as previously described with slight modifications (Mashruwala et al. 2016a). Strains were cultured overnight in TSB before diluting them in fresh TSB to an optical density of 0.1 (A_{600}). The cultures were diluted in 0.5 ml or 4 ml of TSB in 10-ml culture tubes. The cells were cultured for 8 h (Figure 1.4), or samples were removed throughout growth (Figure 1.5) before they were harvested by centrifugation, and the cell pellets were stored at −80°C. The cells were thawed anaerobically, resuspended with 200 µl of AcnA buffer (50 mM Tris, 150 mM NaCl, pH 7.4), and lysed by the addition of 4 µg lysostaphin and 8 µg DNase. The cells were incubated at 37°C until full lysis was

observed (~1 h). The cell debris was removed by centrifugation, and AcnA activity was assessed as previously described (Kennedy et al. 1983).

Protein concentration determination. The protein concentration was determined using a copper-bicinchoninic acid-based colorimetric assay modified for a 96-well plate(Olson and Markwell 2007).

RNA isolation and quantification of mRNA transcripts. Bacterial strains were cultured overnight in TSB (~18 h) and diluted in 80 ml of fresh TSB to a final OD of 0.05 (A_{600}) in 300-ml flasks in order to mimic the growth conditions used for the growth and acetate accumulation experiments shown in (Figure 1.5) The cells were cultured for 8 h before harvesting by centrifugation. The cells were treated with RNAProtect (Qiagen) for 10 min at room temperature and pelleted by centrifugation, and the cell pellets were stored at −80°C. The pellets were thawed and washed twice with 0.5 ml of lysis buffer (50 mM RNase-free Tris, pH 8). The cells were lysed by the addition of 20 μg of lysostaphin and incubated for 30 min at 37°C. RNA was isolated using TRIzol reagent (Ambion-Life Technologies) according to the manufacturer's instructions. DNA was digested with the Turbo DNA-free kit (Ambion-Life Technologies). The cDNA libraries were constructed using isolated RNA as a template and a High Capacity RNA-to-cDNA kit (Applied Biosysytems). An Applied Biosystems StepOnePlus thermocycler and Power SYBR green PCR master mix (Applied Biosystems) were used to quantify DNA abundance. The primers for quantitative real-time PCR of the *sufC*, *sufD*, *sufS*, *sufU*, and *sufB*transcripts, designed using Primer Express 3.0 software from Applied Biosystems, are listed in (Table 1.1)

H_2O_2 killing assays.

Bacterial strains were cultured for 12 h in TSB. The cells were pelleted by centrifugation and resuspended in an equal volume of PBS. The optical densities of the strains were adjusted to an OD of 0.7 (A_{600}) in a total volume of 1 ml of PBS. The cells were subsequently challenged with a bolus of H_2O_2 (500 mM) and incubated for 1 h at room temperature. Fifty microliters of the reaction mixture was diluted 1:20 in PBS buffer containing catalase (1,300 units ml^{-1}) and incubated for 5 min. Cell viability was visualized by serial dilution of cells and spot plating upon TSA.

Determination of pH profiles and acetic acid concentrations in spent media.

Strains cultured overnight in TSB (~18 h) were diluted in 80 ml of fresh TSB to a final OD of 0.05 (A_{600}) in 300-ml flasks. At the indicated times, aliquots of the cultures were removed, the culture OD (A_{600}) was determined, and the cells and culture media were partitioned by centrifugation at 14,000 rpm for 1 min. Two milliliters of either the culture supernatant or sterile TSB, which served to provide a pH reading for the point of inoculation, were combined with 8 ml of distilled and deionized water, and the pH was determined using a Fisher Scientific Accumet AB15 pH mV meter. The concentration of acetic acid in the spent medium was determined using a BioVision acetate colorimetric assay kit (K658) according to the manufacturer's instructions.

Static model of biofilm formation. Biofilm formation was examined as described previously, with minor changes (Mashruwala et al. 2016a; Lauderdale et al. 2009). Briefly, overnight cultures were diluted in biofilm medium to a final optical density

of 0.05 (A_{590}), added to the wells of a 96-well microtiter plate, and incubated statically at 37°C for 22 h. Prior to harvesting the biofilms, the optical densities (A_{590}) of the cultures were determined. The plate was subsequently washed with water, the biofilms were heat fixed at 60°C, and the plates were allowed to cool to room temperature. The biofilms were stained with 0.1% crystal violet and washed to remove unbound stain. The plates were dried and subsequently destained by the addition of 33% acetic acid, and the absorbance at 570 nm of the resulting solution was recorded. The absorbance (A_{570}) was standardized to an acetic acid blank and subsequently to the optical density of the cells upon harvest. Finally, the data were normalized with respect to the WT strain to obtain relative biofilm formation.

Total exoprotein analyses.

Spent medium supernatants were obtained from overnight cultures, filter sterilized with a 0.22-μm-pore-size syringe filter, and standardized with respect to culture optical densities (A_{600}), as previously described (Mashruwala et al. 2016b). Exoproteins were extracted from the spent medium supernatant using standard trichloroacetic acid precipitation. The resultant protein pellets were resuspended, and protein concentrations were determined using a biuret assay. The data were subsequently normalized with respect to the WT strain.

Hemolysis assays. The hemolytic activities of staphylococcal exoproteins were determined as previously described(Blevins et al. 2002). The data were subsequently normalized with respect to the WT strain.

Mutagenesis frequency.

Overnight cultures (n = 10) were grown in TSB medium before dilution (1:100) in fresh TSB (A_{600}, ~0.1). The cells were cultured with shaking for 48 h at 37°C. One hundred microliters of culture was spread plated on TSA supplemented with 1.25 μg $ml^{-1}$of rifampin, and CFU were determined after 36 h of incubation. Cultures were also serially diluted and spot plated on TSA to determine total CFU. The mutagenesis frequency was calculated by dividing the number of rifampin-resistant colonies by the total number of CFU.

Transcriptional reporter analyses.

Strains containing the p*sufC*p (Mashruwala et al. 2016a) transcriptional reporter plasmid were grown in TSB-Erm medium overnight. The cultures were then diluted (1:100) in 5 ml of fresh TSB-Erm and allowed to grow for 30 h, during which 200-μl aliquots were removed at various time points and fluorescence and culture OD (A_{600}) were measured with a PerkinElmer HTS 7000 Bio Assay reader. Green fluorescent protein (GFP) was excited at 485 nm, and emission was read at 535 nm. Fluorescence was standardized with respect to the culture OD.

Opsonophagocytic killing assay.

Strains were cultured overnight in TSB and subcultured in TSB (1:100) the following day for 3 h. Human primary PMNs were isolated by dextran gradient as described previously (DuMont et al. 2013). Prior to infection, 96-well plates were coated with 20% human serum in RPMI 1640 (10 mM HEPES plus 0.1% human serum albumin [HSA]) for 30 min at 37°C. Following subculture of the bacteria, the

strains were opsonized with 20% human serum for 30 min at 37°C, washed, and diluted to an approximate density of 2.5×10^7 CFU ml^{-1}. Approximately 250,000 PMNs per well in a 96-well plate were infected with approximately 2.5×10^6 CFU to generate a multiplicity of infection (MOI) of 10. With the exception of time zero, the infections were centrifuged at 1,500 RPM for 7 min to synchronize the bacteria with the PMNs. During centrifugation, 1% saponin was added to the time zero infections to lyse the PMNS, and CFU were then determined by serial dilution and plating on TSA. This procedure was followed for the remaining time points up to 180 min. Blood samples were obtained from anonymous healthy donors as buffy coats (New York City Blood Center). The New York City Blood Center obtained written informed consent from all participants involved in the study. The research was approved by the New York University School of Medicine institutional human subjects board.

Bioinformatic and statistical analyses.

The analyses presented in (Table 1.4) were generated by first using BLAST(Altschul et al. 1990) to identify the homologues of *S. aureus* SufBCD, *E. coli* IscU, or *Azotobacter vinelandii* NifU in the genomes of various bacterial pathogens. The corresponding locus tags were then used to determine whether the genes were predicted to be essential, using published data sets. The data presented were analyzed and plotted using SigmaPlot version 12, and statistical analyses were conducted using Microsoft Excel.

Table 1.4: Fe-S biosynthesis systems in select bacterial strains

Bacterial species	**Fe-S assembly machinery**	**Fe-S biogenesis system predicted to be essential**	**Reference**
Acinetobacter baumannii ***a***	Isc	Yes	(Gallagher et al. 2015)
Bacillus subtilis	Suf	Yes	(Kobayashi et al. 2003)
Bacteroides fragilis	Suf	Yes	(Veeranagouda et al. 2014)
Burkholderia pseudomallei	Suf and Isc	Yes *c*	(Moule et al. 2014)
Campylobacter jejuni	Nif	Yes	(Metris et al. 2011)
Clostridium difficile	Suf	Yes	(Dembek et al. 2015)
Enterococcus faecalis ***a***	Suf	Yes *b*	(Garsin et al. 2004)
Escherichia coli	Suf and Isc	No	(Baba et al. 2006)
Francisella novicida	Suf	Yes	(Gallagher et al. 2007)
Haemophilus influenzae	Isc	Yes	(Akerley et al. 2002)
Helicobacter pylori	Nif	Yes	(Salama et al. 2004)
Klebsiella pneumoniae ***a***	Suf, Nif and Isc	No	(Bachman et al. 2015)
Mycobacterium tuberculosis	Suf	Yes	(Huet et al. 2005)
Porphyromonas gingivalis	Suf	Yes	(Klein et al. 2012)
Pseudomonas aeruginosa ***a***	Isc	Yes	(Lee et al. 2015)
Salmonella enterica	Suf and Isc	No	(Knuth et al. 2004)
Staphylococcus aureus ***a***	Suf	Yes	(Valentino et al. 2014)
Streptococcus pneumoniae	Suf	Yes	(van Opijnen and Camilli 2012)
Streptococcus pyogenes	Suf	Yes	(Le Breton et al. 2015)
Vibrio cholerae	Isc	Yes	(Kamp et al. 2013)

a ESKAPE pathogen, capable of escaping the biocidal effects of antibiotics.

b Limited data set.

c The IscS cysteine desulfurase is predicted to be essential.

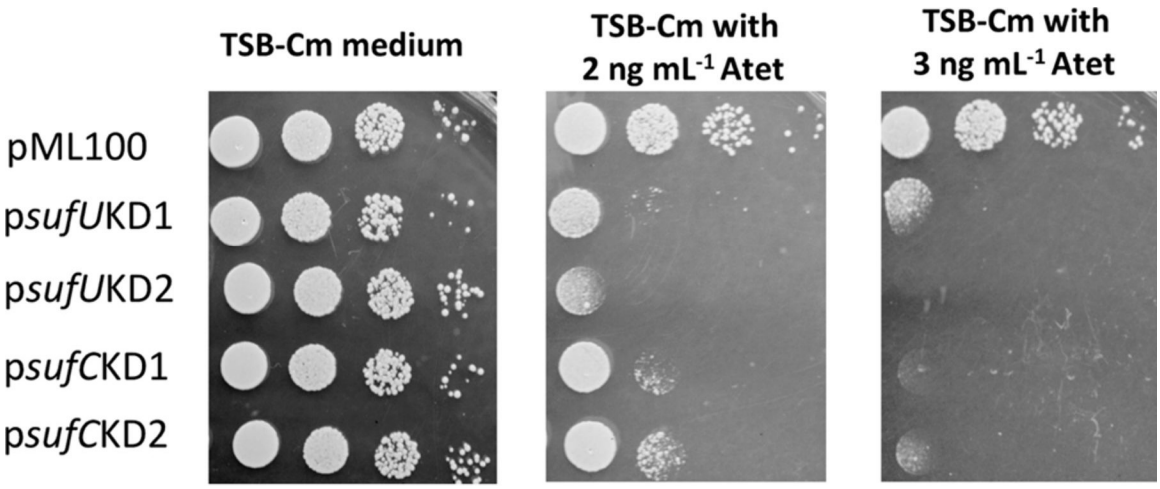

Figure 1.1: *sufC or sufU* depletion decreases *S. aureus* viability. *S. aureus* RN4220 containing *pML100* (empty vector), p*sufU*KD1, p*sufU*KD2, p*sufC*KD1, or p*sufC*KD2 was serially diluted and spot plated on TSA-chloramphenicol medium with and without Atet (inducer). Images from a representative experiment are shown.

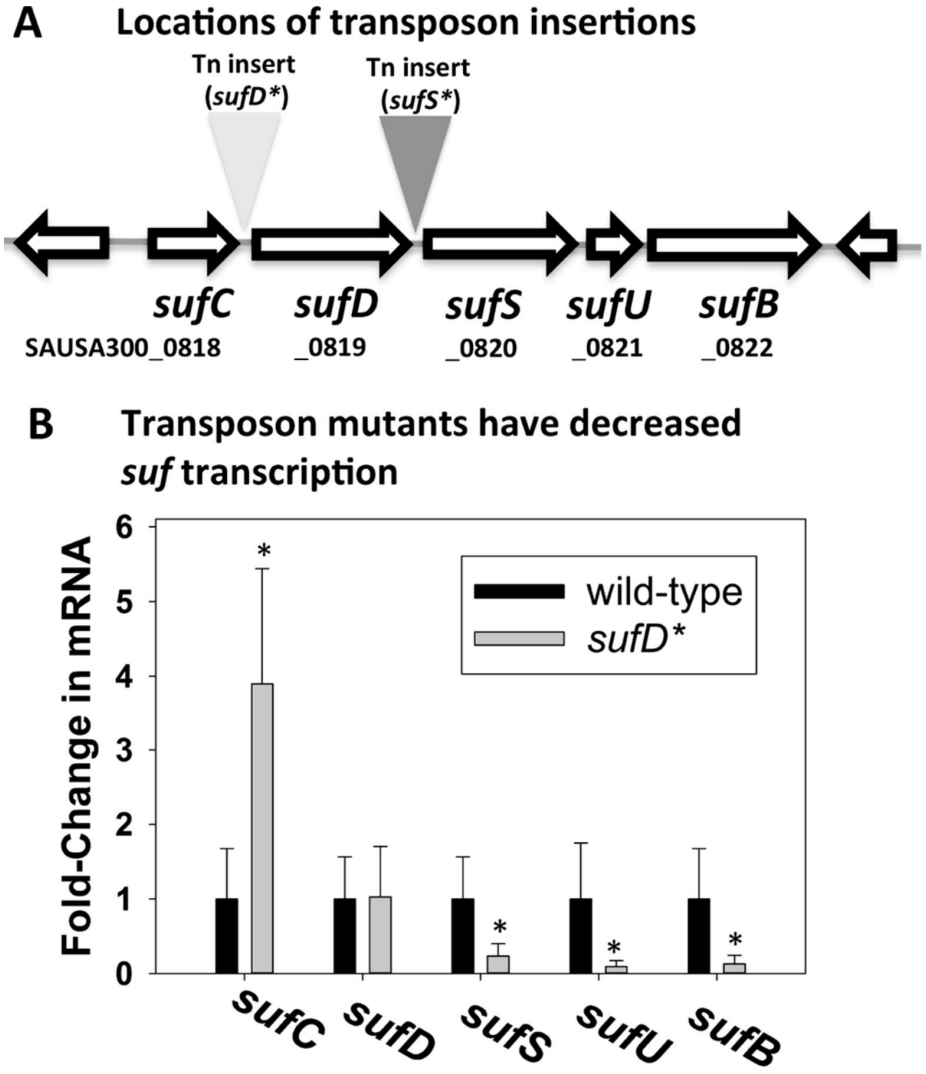

Figure 1.2: A transposon insertion between *sufC* and *sufD* decreases transcription of *sufSUB*. (A) Locations of the individual *sufS** and *sufD** transposon insertion sites. The *sufS** transposon insertion is located between *sufD* and *sufS*, and the *sufD** transposon insertion is located between *sufC* and *sufD*. (B) The *sufD** insertion decreases transcription of *sufSUB*. Total RNA was isolated from the WT and *sufD** strains, and the transcription of the individual *sufCDSUB*genes was quantified. The data represent average mRNA abundances from cells cultured in biological triplicates; cDNA libraries were analyzed in duplicate. The error bars represent standard deviations; *, $P < 0.05$ relative to the WT strain using a two-tailed Student *t* test.

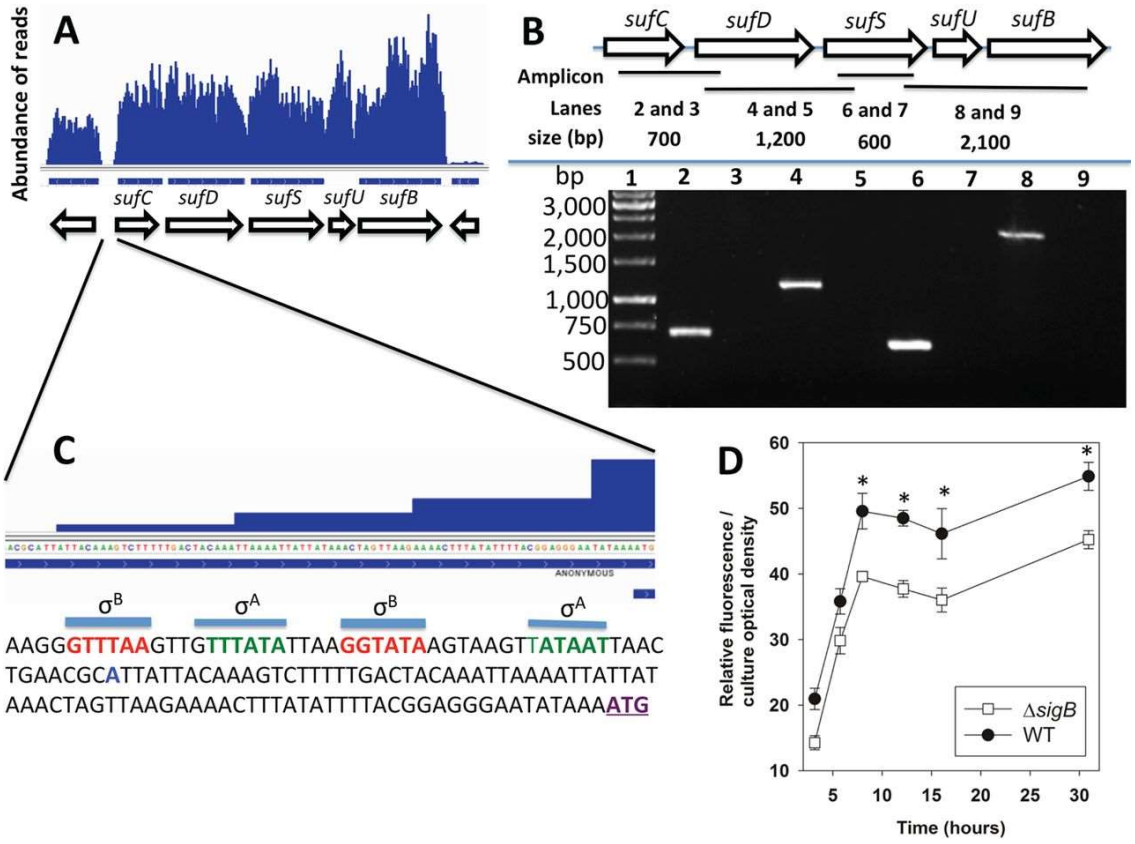

Figure 1.3 The *sufCDSUB* genes are cotranscribed, and transcription is positively influenced by sigma factor B. (A) Analysis of a previously published RNA-seq data set (Osmundson et al. 2013) indicating that *sufCDSUB* are cotranscribed. (B) The *suf* genes are cotranscribed. (Top) Schematic of the *suf* operon; the locations of the amplicons are shown as black bars, and the predicted sizes of the amplicons (generated using the following primer pairs: lanes 2 and 3, sufCRT5 and sufDrevRT; lanes 4 and 5, sufDfwdRT and sufinternal3; lanes 6 and 7, sufinternal5 and sufSrevRT; lanes 8 and 9, sufSfwdRT and sufBrevRT) are shown. (Bottom) Amplicons were generated from cDNA libraries using RNAs isolated from the WT and separated using agarose gel electrophoresis. The samples analyzed in lanes 3, 5, 7, and 9 were generated using a template that was not treated with reverse transcriptase. (C) The promoter of the *suf* operon contains potential sigma factor A (green) and sigma factor B (red) recognition sites. The predicted transcriptional start site is shown in blue and was determined by analyzing previously

published RNA-seq data (Osmundson et al. 2013). The annotated *sufC* translational start site is in purple and underlined. (D) The transcriptional activity of the *sufC* promoter is modulated by sigma factor B (SigB). The transcriptional activity of *sufC* was monitored in the WT and Δ*sigB* strains containing pCM11_*suf*. The data shown represent the averages of biological triplicates with standard deviations. *, $P < 0.05$ relative to the WT strain, using a two-tailed Student *t* test.

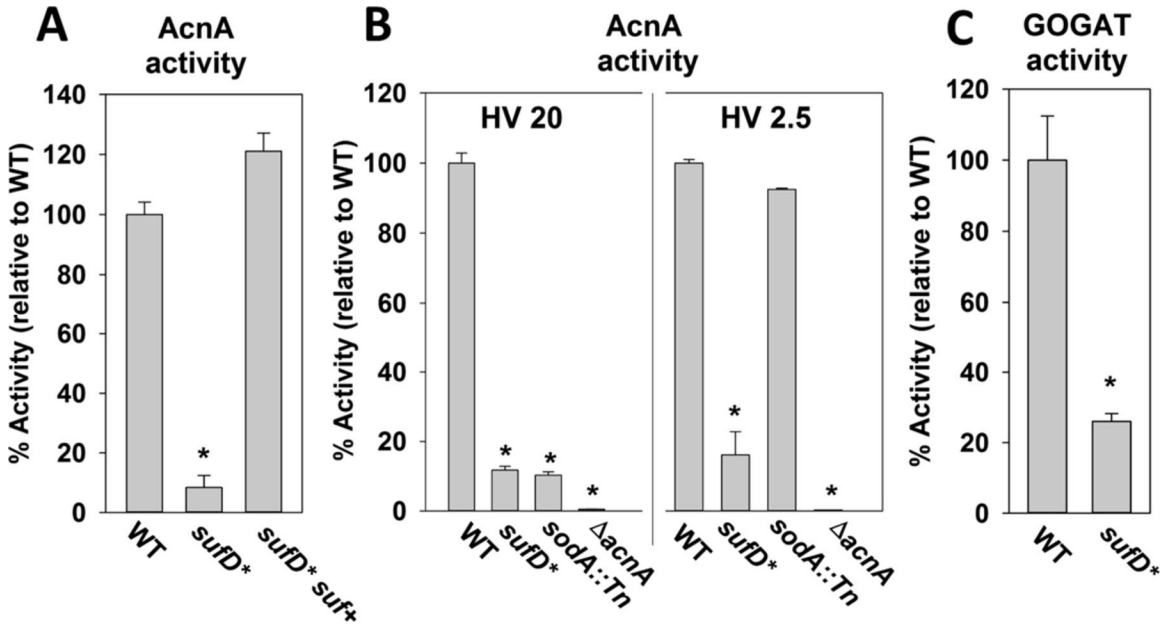

Figure 1.4 Iron-sulfur cluster-requiring proteins have decreased activity in *S. aureus* strains with decreased *suf* transcription. (A) AcnA activity was assessed in the WT, *sufD**, and *sufD** *suf*+strains. (B) AcnA activity is decreased in the *sufD** strain irrespective of culture aeration. The AcnA assays were conducted in cell lysates from the WT, *sufD**, *sodA*::Tn, and Δ*acnA* strains cultured in TSB with altered HV ratios. (C) Glutamate dehydrogenase activities were assessed in the WT and *sufD** strains. The data shown represent the averages of biological triplicates with standard deviations. *, $P < 0.05$ relative to the WT strain using a two-tailed Student *t* test.

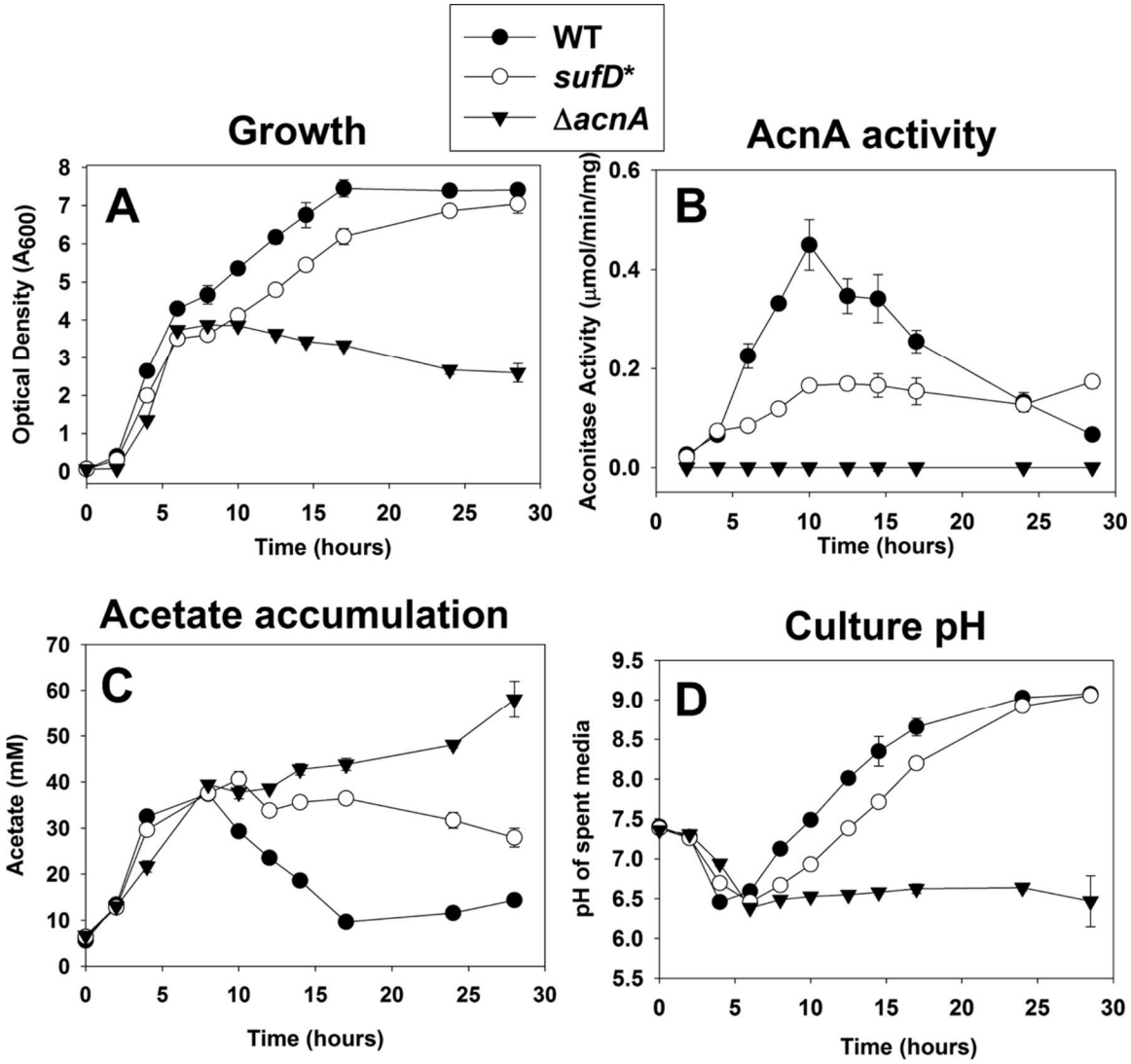

Figure 1.5 Decreased Suf function results in a reduced rate of carbon flux through the TCA cycle. (A) Growth profiles of the WT, *sufD**, and Δ*acnA* strains. (B) AcnA activity throughout growth. (C) Concentrations of acetate in culture supernatants throughout growth. (D) Spent medium pH throughout growth. The data represent averages of biological triplicates with standard deviations.

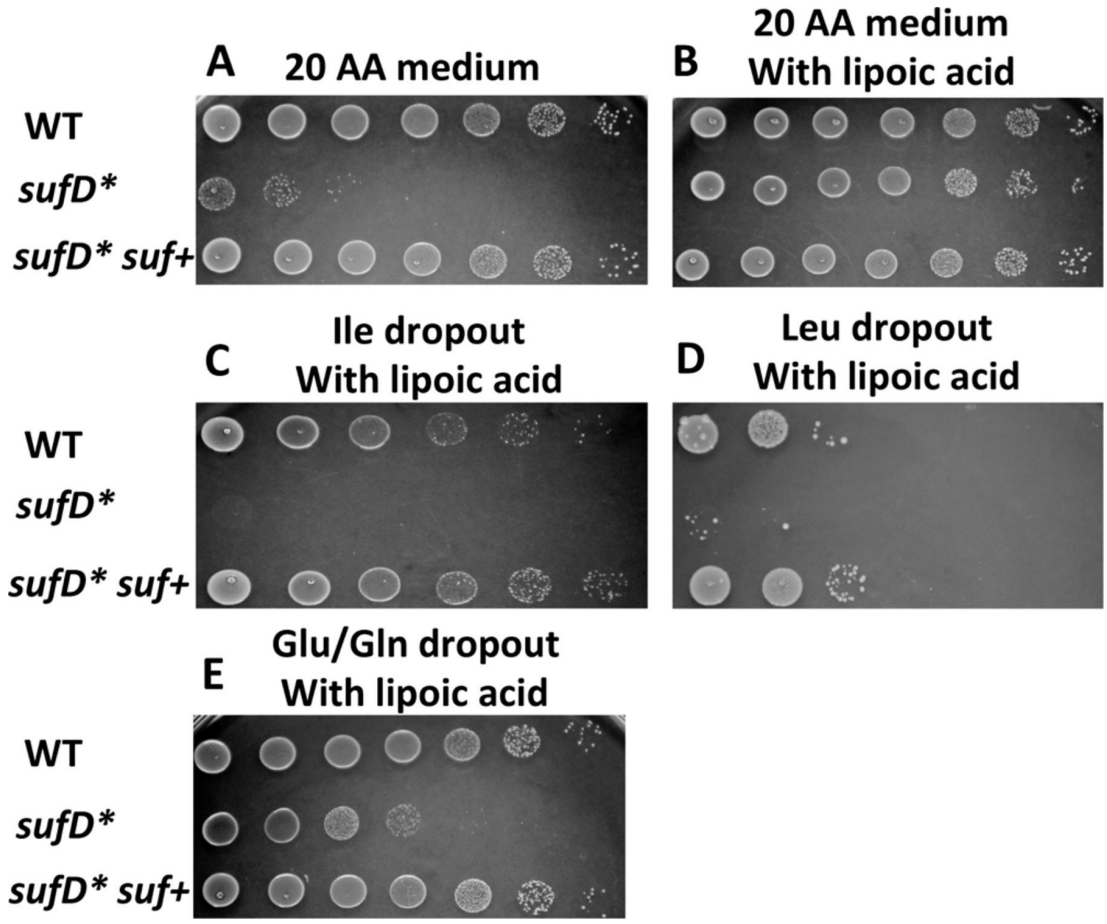

Figure 1.6: Decreased Fe-S cluster synthesis causes decreased growth in media lacking specific amino acids or lipoic acid. Auxotrophic analyses were conducted using the WT, *sufD**, and *sufD* suf*+strains. The strains were grown in TSB before plating on solid chemically defined medium containing the 20 canonical amino acids (A), 20 aa with lipoic acid (B), 19 aa minus isoleucine with lipoic acid (C), 19 aa minus leucine with lipoic acid (D), and 18 aa minus glutamate and glutamine with lipoic acid (E). Images from a representative experiment are shown.

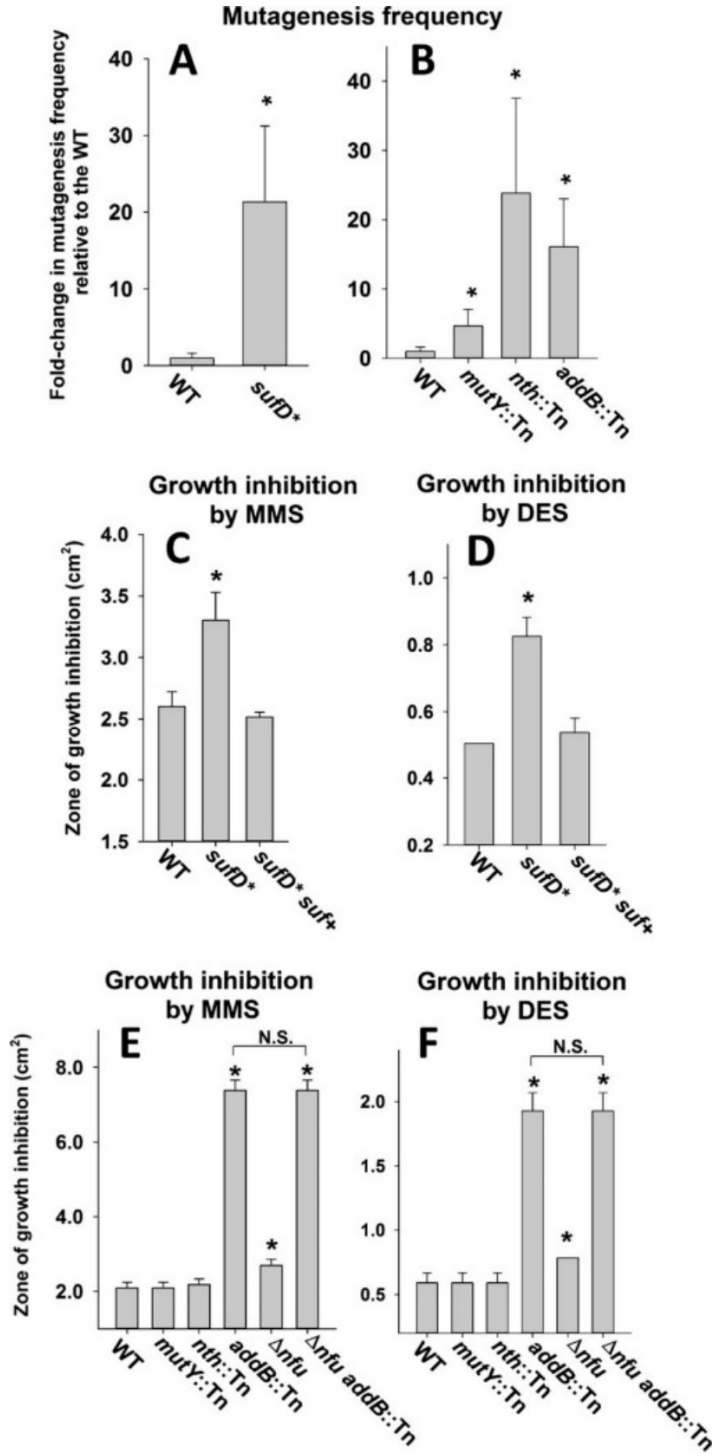

Figure 1.7: Effect of decreased Suf function on DNA metabolism. (A) The frequency of spontaneous rifampin resistance was measured in the WT and *sufD** strains. (B) The frequency of spontaneous rifampin resistance was measured in the

WT, *mutY*::Tn, *nth*::Tn, and *addB*::Tn strains. (C) Sensitivity to MMS was assessed in the WT, *sufD**, and *sufD* suf*$^{+}$ strains. (D) Sensitivity to DES was assessed in the WT, *sufD**, and *sufD* suf*$^{+}$ strains. (E) Sensitivity to MMS was assessed in the WT, *mutY*::Tn, *nth*::Tn, *addB*::Tn, Δ*nfu*, and Δ*nfu addB*::Tn strains. (F) Sensitivity to DES was assessed in the WT, *mutY*::Tn, *nth*::Tn, *addB*::Tn, Δ*nfu*, and Δ*nfu addB*::Tn strains. The data presented in panels A and B represent the averages of 10 biological replicates with standard deviations. The data presented in panels C, D, E, and F represent the averages of biological triplicates with standard deviations. Student *t* tests (two tailed) were performed on the data; *, $P < 0.05$ relative to the WT strain unless otherwise indicated; N.S., not significant ($P > 0.05$).

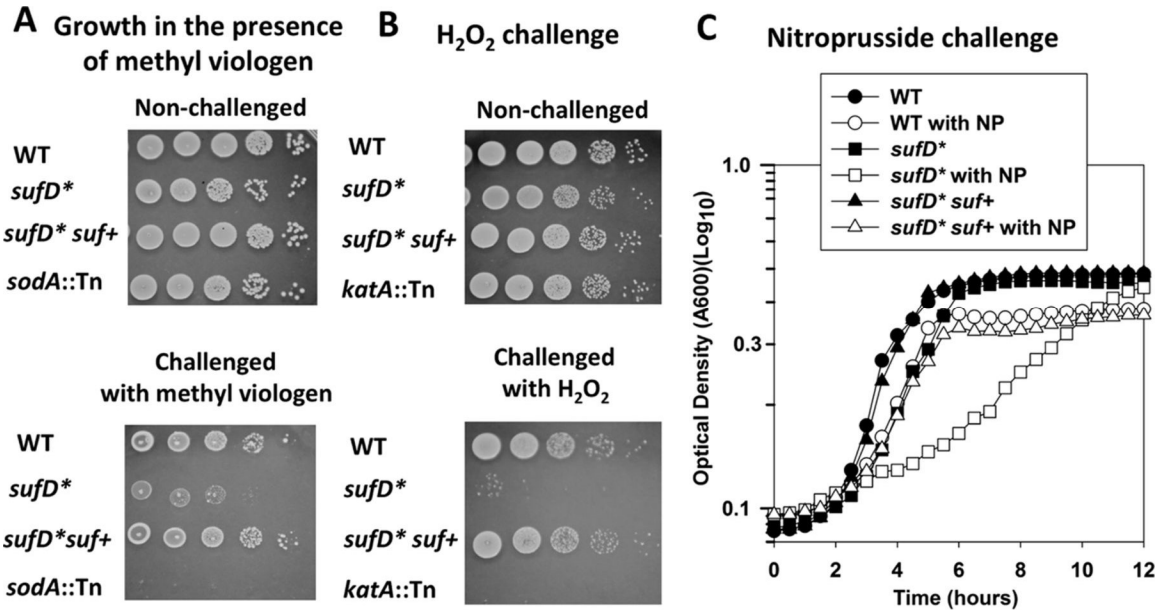

Figure 1.8: Decreased Suf function results in increased sensitivity to RNS and ROS. (A) Methyl viologen sensitivity was monitored in the WT, *sufD**, *sufD* suf*$^+$, and *sodA*::Tn strains. The cells were cultured in TSB before serial dilution and spot plating on solid TSA supplemented with 40 mM methyl viologen or vehicle control. (B) H_2O_2 sensitivity was assessed in the WT, *sufD**, *sufD* suf*$^+$, and *katA*::Tn strains. The cells were challenged with 500 mM H_2O_2 before the reaction was quenched, and the cells were serially diluted and spot plated on solid TSA medium. (C) Nitroprusside (NP) sensitivity was assessed in the WT, *sufD**, and *sufD* suf*$^+$ strains. Representative growth profiles in the presence and absence of 15 mM nitroprusside in TSB medium are shown. The data are from representative experiments.

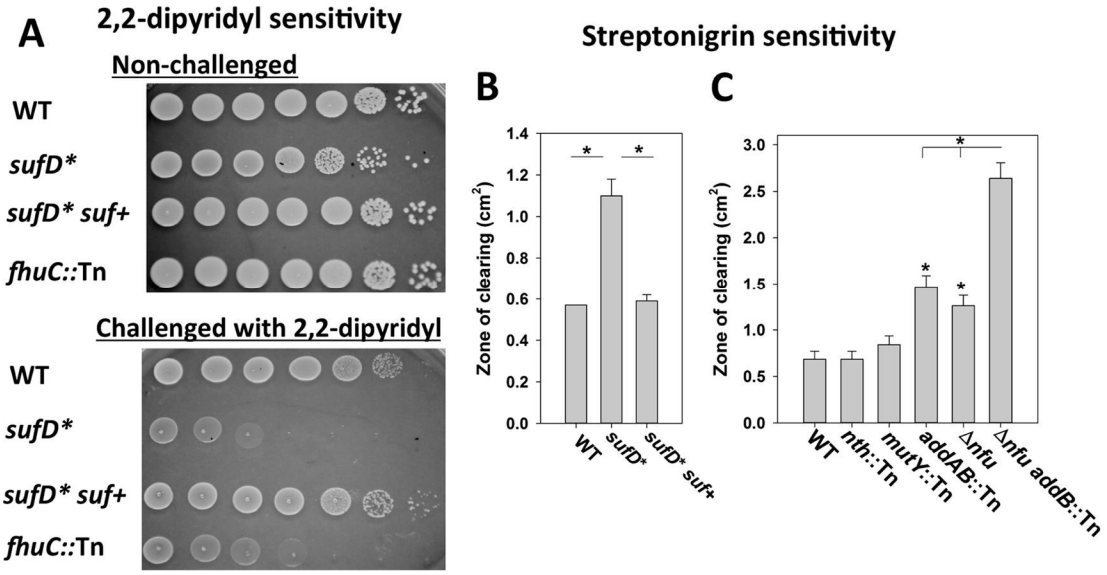

Figure 1.9: Decreased Suf function destabilizes intracellular iron homeostasis. (A) The WT, *sufD**, *sufD** *suf*+, and *fhuC*::Tn strains were spot plated on solid TSA medium with and without 900 mM 2,2-dipyridyl. (B) The WT, *sufD**, and *sufD** *suf*+ strains were plated as top agar overlays on solid TSA, and the zones of growth inhibition resulting from streptonigrin intoxication were measured. (C) The WT, *nth*::Tn, *mutY*::Tn, *addB*::Tn, Δ*nfu*, and Δ*nfu addB*::Tn strains were plated as top agar overlays on solid TSA, and the zones of growth inhibition resulting from streptonigrin intoxication were measured. The data presented in panels B and C represent the averages of biological triplicates with standard deviations. Student *t* tests (two tailed) were performed on the data; *, $P < 0.05$ compared to the WT unless otherwise indicated.

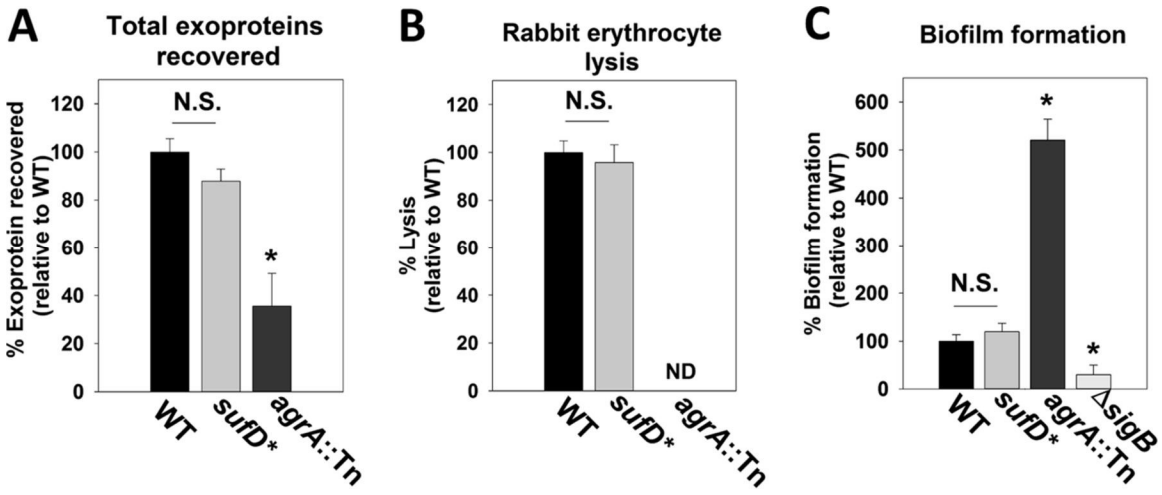

Figure 1.10: Decreased Suf function does not significantly affect exoprotein production or biofilm formation. Total exoprotein production (A), hemolysin activity (B), and biofilm formation (C) were assessed in the WT, *sufD**, *agrA*::Tn, and Δ*sigB* strains. The data presented in panels A and B represent the averages of spent medium supernatants from three biological replicates, and the data in panel C represent averages of eight wells with standard deviations. Student *t* tests (two tailed) were performed on the data; *, $P < 0.05$; N.S., $P > 0.05$ relative to the WT (not significant); ND, not detectable.

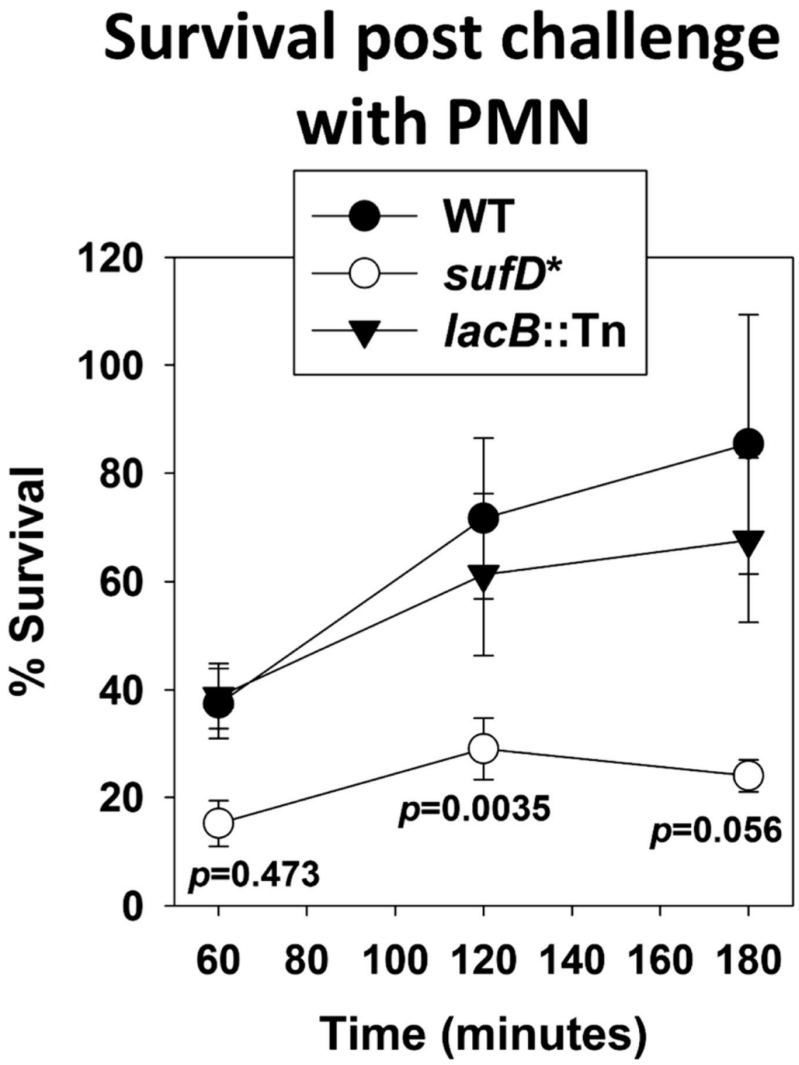

Figure 1.11: A strain with decreased Suf function has decreased survival in neutrophils. The WT, *sufD**, and *lacB*::Tn strains were opsonized with 20% human serum, washed, and then diluted to 2.5 × 10^7 CFU/ml and used to infect 250,000 PMNs per well in a 96-well plate. The neutrophils were lysed upon addition of 1% saponin, and CFU were determined at various time points by plating. The data presented represent the averages of biological triplicates, with error bars representing standard errors of the mean. Student *t* tests (two tailed) were performed on the data, and *P* values are shown for the *sufD** strain relative to the WT.

Chapter 2

Staphylococcus aureus lacking a functional MntABC manganese import system have increased resistance to copper.

Abstract

S. aureus USA300 isolates utilize the *copBL* and *copAZ* operons to prevent copper intoxication. To further understand how copper toxifies *S. aureus*, we created and examined a Δ*copAB* Δ*copBL* mutant strain (*cop*-). The *cop*- strain was sensitive to copper and accumulated intracellular copper. We created and screened a transposon (Tn) mutant library in the *cop*- background. We isolated strains with Tn insertions in *mntABC* that permitted growth in the presence of copper. The *mntA1::Tn* mutations were recessive. Under the growth conditions utilized, MntABC functioned in manganese (Mn) import. When cultured with copper, strains containing the *mntA1::Tn* mutation accumulated less copper than the parent strains. Manganese (II) supplementation improved growth when *cop*- was cultured with copper and this phenotype was dependent upon the presence of MntR, which is a repressor of *mntABC* transcription. A Δ*mntR* strain had an increased copper load and decreased growth in the presence of copper and these phenotypes were abrogated by introduction of *mntA1::Tn*. Over-expression of MntABC increased cellular copper load and increased sensitivity to copper. The presence of *mntA1::Tn* mutation also protected Fe-S enzymes from inactivation by copper. The introduction of a *mntA1::Tn* allele improved growth of both Δ*copAZ* and Δ*copBL* strains from copper intoxication suggesting that the acquisition of a second copper detoxification system protect *S. aureus* from MntABC-dependent

copper intoxication. Taken together, data presented are consistent with a model wherein copper enters *S. aureus* cells via the MntABC importer and poisons Fe-S enzymes.

Introduction

Staphylococcus aureus continues to be a serious public health problem as *S. aureus* infections result in high morbidity and mortality rates (Turner et al. 2019). Although historically known as nosocomial pathogen, there has been an increase in community-acquired (CA) *S. aureus* cases among both immunocompetent and immunocompromised groups (Tenover et al. 2006). These CA *S. aureus* strains often cause skin and soft tissue infections (SSTIs) that can develop into invasive and systemic infections (Turner et al. 2019). Treatment of *S. aureus* infections is complicated due to the ability of this pathogen to evolve and acquire antibiotic resistances (Malachowa and DeLeo 2010). To combat these problems, we need to develop new prevention and therapeutic approaches including the characterization of new promising antimicrobial targets.

Copper (Cu) is gaining popularity as an antimicrobial but killing or preventing growth of microorganisms using copper is an age-old technology. Humans have been using copper to sterilize drinking water and to aid in infection clearance for thousands of years (Dollwet and Sorenson 1985; Grass et al. 2011). As of late, copper is increasingly used as an intrinsic antibacterial and in metallic copper or copper-containing alloys on touch surfaces (Grass et al. 2011). Mammals also use copper to help clear infections (Hodgkinson and Petris 2012). Copper loads increase at sites of inflammation (Beveridge et al. 1985). Copper is

found to accumulate within macrophage intracellular vesicles (Achard et al. 2012) and ultimately in phagosomes (Wagner et al. 2005). Phagosome copper levels increased 20-fold after bacterial phagocytosis (Wagner et al. 2005) and the addition of copper to macrophages increases killing efficiency (White et al. 2009). A genetic depletion of the copper transporter ATP7A suppressed macrophage-dependent bacterial killing suggesting that macrophages that are defective in trafficking copper to the phagolysome have a decreased ability to kill bacterial pathogens (White et al. 2009). Further supporting a role for copper in bacterial clearance, bacterial pathogens, including *S. aureus*, that are defective in exporting copper from the cytosol have decreased survival in macrophages and in other models of infection (Ladomersky et al. 2017; Purves et al. 2018; Zapotoczna et al. 2018; White et al. 2009).

Copper is an important micronutrient in some organisms (Andreini et al. 2008) but, as alluded to above, cytosolic copper overload results in intoxication (Purves et al. 2018). Various mechanisms have been proposed to explain the toxic effects of copper; however, the molecular mechanism(s) of copper poisoning is not entirely clear, and it is likely multifaceted. In support of this, copper stress involves perturbations of many stress and non-stress regulons resulting in multi-dimensional responses (Moore et al. 2005; Baker et al. 2010; Chillappagari et al. 2010; Quintana et al. 2017).

Copper has the ability to redox cycle between the copper (II) and copper (I) oxidation states at physiologically relevant conditions, which expands the list of potential biological ligands (Solomon et al. 2014). Because of this chemistry,

copper has been exploited by organisms for use as a cofactor to facilitate redox chemistry. Whereas copper (I) has low water solubility, copper (II) is water soluble and the most abundant species in aerobic conditions. Aerobically, copper can catalyze the formation of reactive oxygen species through the Haber–Weiss and Fenton reactions (Gunther et al. 1995). However, it was found that increased cytosolic copper loads did not result in increased oxidative DNA damage in *E. coli* (Macomber et al. 2007) and that Fenton chemistry did not contribute to copper-dependent killing of *S. aureus* by a copper-containing surface (Warnes and Keevil 2016). Moreover, copper is more toxic to *E. coli* cultured under anaerobic conditions; however, this is most likely the result of increased cytosolic copper accumulation during anaerobic growth (Tan et al. 2017; Outten et al. 2001). Copper can also damage the outer and/or cytosolic membranes of bacteria (Warnes et al. 2012; Hong et al. 2012).

Metalloproteins often have an essential requirement for their cognate metal cofactor (Imlay 2014). Solvent-accessible protein-associated metal ions can be displaced by oxidative stress or by alternate metals (Xu and Imlay 2012; Gardner and Fridovich 1991; Anjem and Imlay 2012). Metalloproteins can also be mismetalated during maturation or oxidative stress (Waldron and Robinson 2009; Gu and Imlay 2013). Accumulation of copper in the cytosol had been shown to decrease the activities of iron-sulfur (Fe-S) enzymes (Macomber and Imlay 2009; Djoko and McEwan 2013). Biochemical studies found that copper can poison enzymes with solvent-exposed Fe-S clusters bys disrupting the Fe-S cluster (Macomber and Imlay 2009). Copper can also inhibit the assembly of Fe-S proteins

by forming stable complexes with components of the Fe-S cluster synthesis and/or Fe-S protein maturation factors (Chillappagari et al. 2010; Tan et al. 2017, 2014; Brancaccio et al. 2017).

Intoxication of *Streptococcus pneumoniae* by copper was alleviated by the addition of manganese (Mn) to the growth medium (Johnson et al. 2015b). Accumulation of cytosolic copper led to increased expression of nucleotide synthesis pathway including the anaerobic ribonucleotide reductase system (NrdDG) suggesting that cells were starved for deoxynucleotide triphosphates (dNTPs). The aerobic ribonucleotide reductase system (NrdEF) is manganese-dependent (Martin and Imlay 2011). A *S. pneumoniae* Δ*nrdD* mutant was more sensitive than the parent to copper intoxication. These data led to the hypothesis that copper inhibits aerobic dNTP synthesis by mismetalation of NrdF.

S. aureus is predicted to utilize only one cuproprotein, which is the *aa3* cytochrome oxidase (QoxAB) (Powers et al. 1994; Ridge et al. 2008). A Δ*qoxB* mutant has a growth defect during routine laboratory culture suggesting that it is expressed (Hammer et al. 2013). It is unknown if copper must enter *S. aureus* cells to maturate QoxAB, but *S. aureus* does contain mechanisms to help prevent copper intoxication. All *S. aureus* contain the *copAZ* operon (Sitthisak et al. 2007). CopA is a transmembrane P1-type ATPase copper (I) exporter (Argüello et al. 2007) and CopZ is a cytosolic copper (I)-binding chaperone that can deliver copper (I) to CopA for export (Singleton et al. 2009). We and others have recently shown that some *S. aureus* strains also contain the *copBL* operon to aid copper detoxification (Purves et al. 2018; Rosario-Cruz et al. 2019). CopB is a P1-type

ATPase copper exporter and genetic evidence suggests it has a degree of functionally redundancy with CopA (Rosario-Cruz et al. 2019). CopL is an external copper binding lipoprotein that aids in preventing copper from entering the cell (Rosario-Cruz et al. 2019). Some strains also encode a multicopper oxidase (Mco). A *S. aureus* Δ*mco* mutant was more sensitive to copper than the parental strain, but the function of Mco in copper detoxification is unknown (Zapotoczna et al. 2018). *S. aureus* contain *csoR* which encodes for a transcriptional regulator of the *copBL* and *copAZ* operons (Purves et al. 2018; Grossoehme et al. 2011). Upon binding to copper (I), holo-CsoR relieves repression of *copBL* and *copAZ* (Purves et al. 2018; Grossoehme et al. 2011).

During infection, the host restricts the bioavailability of metal ions including manganese (Becker and Skaar 2014). Manganese is important for the infection process because it is involved in a number of regulatory and physiological processes (Juttukonda and Skaar 2015). To overcome manganese limitation, *S. aureus* employ two manganese uptake systems (Horsburgh et al. 2002; Kehl-Fie et al. 2013). The *mntABC* operon encodes for an ATPase to provide energy for uptake (MntA), a permease (MntB), and an extracellular manganese binding lipoprotein (MntC) (Gribenko et al. 2013). The *mntH* gene encodes a manganese permease of the NRAMP family (Que and Helmann 2000). Cytosolic manganese is sensed by the transcriptional regulator MntR. When associated with manganese, holo-MntR represses *mntABC* transcription by binding to the *mntA* promoter (Horsburgh et al. 2002; Glasfeld et al. 2003). Excess cytosolic manganese is toxic

to *S. aureus*. When manganese concentrations reach a critical threshold, excess manganese is exported via MntE (Grunenwald et al. 2019).

The goal of this study was to understand how copper toxifies *S. aureus*. To this end, we constructed a strain that is defective in copper detoxification (*cop*- strain). This strain was sensitive to copper and accumulated cytosolic copper. We screened for *cop*- strains that had increased tolerance to copper. Strains containing transposon (Tn) insertions in *mntA* had increased copper tolerance. The data presented are consistent with the hypothesis that copper enters *S. aureus* cells via the MntABC permease. We show that copper poisons the Fe-S enzyme aconitase *in vitro* and *in vivo*. The *in vivo* effects are mitigated by null mutations in *mntA*. The findings presented herein highlight the troubles that organisms face when trying to acquire an essential micronutrient and may help explain why having redundant tightly regulated systems to uptake metals is beneficial.

Results

A *S. aureus* Δ*copBL* Δ*copAZ* mutant accumulates intracellular copper.

To better understand how copper toxifies *S. aureus*, we created a Δ*copAZ* Δ*copBL* deletion strain in the USA300_LAC background. We compared the growth of the Δ*copAZ* Δ*copBL* strain to that of the wild-type (WT), Δ*copAZ*, and Δ*copBL* strains. When compared to the growth of the WT, the Δ*copAZ* and Δ*copBL* strains were more sensitive to growth on solid medium in the presence of copper with the Δ*copBL* strain being slightly more sensitive than the Δ*copAZ* strain (Figure 2.1A). The Δ*copAZ* Δ*copBL* double mutant was more sensitive to copper than the Δ*copAZ* and Δ*copBL* strains. We henceforth refer to the Δ*copAZ* Δ*copBL* deletion strain as *cop*-.

We hypothesized that the *copAZ* and *copBL* were the only genetically encoded elements in LAC specifically utilized for copper homeostasis. CsoR is a transcriptional repressor that relieves repression when bound to copper (Ma et al. 2009). We created a *cop*- Δ*csoR* strain and found that this strain was as sensitive to copper as the *cop*- strain (Figure 2.1B). Although not conclusive, these data are consistent with the hypothesis that *copAZ* and *copBL* are the only dedicated copper detoxification genes transcriptionally controlled by CsoR in USA300_LAC.

We tested the hypothesis that the *cop*- strain accumulated intracellular copper. We used inductively coupled plasma mass spectrometry (ICP-MS) to monitor total copper load in the WT and *cop*- strains after culturing in the presence and absence of 10 μM copper (II). After co-culture with copper in trypic soy broth (TSB), both strains accumulated copper; however, the *cop*- strain accumulated

copper to a much higher level (Figure 2.1C). There was not a noticeable difference in copper load between the WT and *cop*- strains after culture in TSB.

Mutational analyses provide insight into copper homeostasis.

We built a transposon (Tn) library in the *cop*- strain. We used this pool of Tn mutant strains to conduct a non-biased screen to isolate strains with insertional mutations that grew on solid TSB medium containing 2.5 mM copper (II). We plated cells from the Tn mutant library and 10 resistant strains were picked. After reconstruction and phenotypic verification, we mapped the transposon mutations. The Tn mutations mapped to three locations. Two strains had mutations in *mntA* of the *mntABC* operon. One strain had a mutation in *apt*, which encodes a predicted adenine phosphoribosyltransferase. Seven strains had mutations in *ispA*, which encodes a geranylgeranyl diphosphate synthase II. All mutants provided a similar growth advantage when cultured on copper containing solid medium (Figure 2.2). For the purposes of this study we focused efforts on determining why the *mntA::Tn* strains permitted growth in the presence of copper (II). The *mntA::Tn* insertions were located at the TA/AT sites located at +84 (*mntA1::Tn*) and +91 (*mntA2::Tn*). The *mntA::Tn* mutants phenocopied one another. For simplicity, only the *mntA1::Tn* mutation was further investigated.

The *mntA1::Tn* mutations are recessive.

The *cop- mntA1::Tn* displayed increased growth when compared to the *cop-* strain when cultured in the presence of copper (II) on solid TSB medium (Figure 2.2), as well as in liquid defined medium (Figure 2.3A). When we returned the *mntABC* genes at a secondary chromosomal location *via* episome, the resulting *cop- mntA1::Tn* pLL39_*mntABC* strain grew similar to the *cop-* pLL39 (empty vector) strain. These data verified that mutational inactivation of *mntA* was resulting in the observed growth advantage witnessed and it suggested the *mntA1::Tn* mutations were recessive.

To further explore this idea, we created a *cop-* Δ*mntA::tetR* strain. The *mntA::tetR* mutation provided a growth advantage in medium containing copper (II), but it did not provide as robust growth advantage as the *mntA1::Tn* mutation (Figure 2.3B). We hypothesized that this was due to the *mntA1::Tn* mutation having polar effects on *mntB* and/or *mntC* expression. We compared the growth of the *cop-* Δ*mntA::tetR, cop-* Δ*mntB::tetR, cop- mntC::Tn* strains in the presence and absence of copper (II). Whereas all three mutants showed better growth than the *cop-* strain when cultured with copper (II), the Δ*mntB::tetR* and Δ*mntC::Tn* mutants provided better growth than the Δ*mntA::tetR* mutation (Figure 2.3C). None of the *mnt* mutant strains had a growth defect or growth advantage in the absence of copper under the growth conditions utilized (data not shown).

We tested the hypothesis that the *mntABC* gene products work in conjunction with one another to provide enhanced growth in the presence of copper (II). To this end, we created *cop-* Δ*mntAB::tetR*, and *cop-* Δ*mntABC::tetR*

strains and compared them to the growth of the *cop*- Δ*mntB::tetR* strain. The strains containing the Δ*mntB::tetR*, Δ*mntAB::tetR*, and Δ*mntABC::tetR* mutations phenocopied one another and all three had enhanced growth in the presence of copper (II) when compared to the *cop*- strain (Figure 2.3D). Taken together, these data suggested that the *mntA1::Tn* mutation had polar effects on *mntB* and *mntC* and that mutations in any of the *mntABC* genes was sufficient to suppress the copper (II) sensitivity phenotype of the *cop*- strain.

The *mntA1::Tn* mutation results in decreased copper accumulation

We tested the hypothesis that the *mntA1::Tn* mutation provides enhanced growth in the presence of copper (II) by decreasing intracellular copper accumulation. To this end, we used ICP-MS to monitor intracellular copper loads after a dosing with copper (II). Cultures were grown for eight hours before 0, 1, 5, or 10 uM copper (II) was added. Cultures were incubated for an additional 15, 30, or 60 minutes before cells were harvested. Cells were washed to remove any potentially advantageously bound metal and copper was quantified. Copper accumulated in both strains and it accumulated as a function of time and the concentration of copper used. When compared with *cop*- strain, the *cop*- *mntA1::Tn* mutant accumulated less copper across all copper concentrations of copper utilized (Figure 2.4). For these experiments total copper load was standardized to total sulfur.

MntR represses MntABC in a manganese-dependent manner

Manganese (II) is sensed by the transcriptional regulator MntR, which is predicted to act as a negative and positive regulator of *mntABC* and *mntH*, respectively (Horsburgh et al. 2002; Kehl-Fie et al. 2013). We quantified *mntABC* and *mntH* transcripts in the *cop-* and *cop- mntR::tetR* strains after culturing in the presence and absence of 10 μM manganese (II). The transcription of *mntABC* was repressed in the presence of manganese (II) and this repression was dependent upon the supplementing the growth medium with manganese (II) (Figure 2.5A). Under the growth conditions utilized, neither culturing with manganese (II), or the presence of MntR, had an effect on *mntH* transcription.

We next examined the manganese (II)-dependent transcription of *mntABC*. Treating TSB with Chelex resin decreases the concentrations of divalent metals. We cultured the *cop-* strain in TSB, TSB with 10 μM manganese (II), Chelex treated TSB, or Chelex treated TSB supplemented with 10 μM manganese (II) before isolating RNA and quantified *mntABC* transcripts. The transcription of *mntABC* was repressed when cells were cultured in TSB with manganese (II) medium when compared to cells cultured in TSB (Figure 2.5B). These data suggested that our laboratory TSB medium is not replete with manganese. Culturing in Chelex treated medium increased transcription of *mntABC*. The addition of 10 μM manganese (II) to the Chelex treated medium returned *mntABC* transcription to levels noted in the cells grown in TSB medium containing 10 μM manganese (II). These data suggested that we could further remove manganese from the TSB medium by treatment of Chelex.

We sought to verify a role for MntABC in manganese homeostasis in the growth conditions utilized herein. We cultured the *cop-* and *cop- mntA1::Tn* strains in Chelex-treated TSB before harvesting cells and determining manganese load using ICP-MS (Figure 2.5C). The *cop- mntA1::Tn* mutant had a lower manganese load than the *cop-* strain confirming a role for MntABC in manganese homeostasis.

Derepression of *mntABC* transcription results in increased copper accumulation and toxicity.

We examined the effect of MntR-dependent regulation of *mntABC* on cellular copper loads. The *cop-*, *cop- mntA1::Tn*, *cop- mntR::tetR*, and *cop- mntA1::Tn mntR::tetR* strains were cultured in Chelex-treated TSB before dosing the cells with and without 5 μM copper (II). The cells were incubated for an additional 30 minutes before harvesting, washing away adventitiously associated copper, and quantifying copper. As noted previously, the *cop- mntA1::Tn* strain accumulated less copper than the *cop-* strain (Figure 2.6A). The *cop- mntR::tetR* strain accumulated more copper than the *cop-* strain; however, this copper accumulation was dependent upon a functional MntABC. The *cop- mntA1::Tn mntR::tetR* strain had a copper load that phenocopied that of the *cop- mntA1::Tn* strain.

We examined if depression of *mntABC* transcription would also result in increased sensitivity to copper. The *cop-*, *cop- mntA1::Tn*, *cop- mntR::tetR*, and *cop- mntA1::Tn mntR::tetR* strains were spot-plated on solid TSB containing 0, 1.75, or 2 mM copper (II). The *cop- mntR::tetR* strain was more sensitive to copper (II) than the *cop-* strain suggesting that removal of MntR-dependent repression of

mntABC transcription increased sensitivity to copper (II) (Figure 2.6B). The *cop- mntA1::Tn mntR::tetR* strain phenocopied the *cop- mntA1::Tn* strain.

The findings that MntR modulates copper accumulation and homeostasis via MntABC and that our TSB medium is not replete with manganese led us to hypothesize that we could decrease sensitivity to copper (II) by supplementing the growth medium with manganese (II). We examined the growth of *cop-*, *cop- mntA1::Tn*, *cop- mntR::tetR*, and *cop- mntA1::Tn mntR::tetR* strains with 1.75 or 2 mM copper (II) in the presence and absence of 5 μM manganese (II). The presence of manganese (II) improved the growth of the *cop-* strain when cultured with copper, but not the growth of the *cop- mntR* mutant (Figure 2.6B). The presence of manganese (II) did not alter the copper (II) sensitivities of the *cop- mntA1::Tn* and *cop- mntA1::Tn mntR::tetR* strains. Taken together, these data suggested that MntR-dependent repression of *mntABC* transcription decreased copper accumulation and decreased the sensitivity of the *cop-* strain to copper (II).

Increased MntABC expression results in copper sensitivity and copper accumulation.

We tested the hypotheses that increased *mntABC* expression results in increased copper (II) sensitivity and copper accumulation. We placed *mntABC* under the transcriptional control of a xylose inducible promoter (pEPSA5). When cultured in the presence of copper (II), the *cop-* strain containing pEPSA5_*mntABC* had decreased growth when compared to the *cop-* strain containing the pEPSA5 (empty vector) (Figure 2.7A). The WT strain with pEPSA5_*mntABC* behaved like

the WT strain containing pEPSA5. These experiments had to be completed on solid medium because of a high rate of suppression (data not shown).

We compared the total copper loads of the *cop*- strain containing either pEPSA5_*mntABC* or pEPSA5. The *cop*- strain containing pEPSA5_*mntABC* had an increased copper load compared to the *cop*- strain containing pEPSA5 (Figure 2.7B). These data are consistent with the hypotheses that overproduction of MntABC in the *cop*- strain results in increased copper accumulation and that the WT strain, which contained *copAB* and *copBL*, was able to detoxify copper even when MntABC was over produced.

The lack of a functional MntABC protects enzymes from copper poisoning.

S. aureus utilizes the SufCDSUB machinery to synthesize iron–sulfur (Fe-S) clusters from monoatomic iron (II), sulfur (S^0), and electrons (Roberts et al. 2017). Intracellular copper accumulation can directly and indirectly decrease the activities of enzymes that require solvent-exposed clusters (Macomber and Imlay 2009; Tan et al. 2014). We previously characterized a strain that contains a Tn insertion between the *sufC* and *sufD* genes (*sufD**) of the *suf* operon resulting in decreased transcription of *sufCDSUB* genes downstream of the insertion and a decreased capacity to synthesize Fe-S clusters. We created a *cop*- *sufD** strain to examine the effect of an increased copper load on a strain defective in Fe-S cluster synthesis. When compared to the *cop*- strain, the *cop*- *sufD** strain had a greatly decreased growth when cultured with copper (II) (Figure 2.8A). We introduced a *mntB::tetR* allele into the *cop*- *sufD** strain and assessed growth in the presence

and absence of copper (II). The presence of the *mntB::tetR* allele rescued the growth of the *cop- sufD** strain in the presence of copper (II) (Figure 2.8B).

Previous work found that copper inhibits Ieu and Leu synthesis by inactivation of the Fe-S cluster-dependent dehydratases necessary to synthesize the amino acids. We also noted that the addition of 5 μM copper (II) to defined medium lacking Leu and Ieu amino acids inhibited the growth of the *cop-* strain (Figure 2.8C). The *cop-* strain was capable of growth in defined medium containing 5 μM copper (II) when it was supplemented with Leu and Ieu (data not shown). The *cop- mntA1::Tn* strain was able to grow in defined medium containing 5 μM copper (II) medium lacking Leu and Ieu. These data suggest that the presence of the *mntA1::Tn* mutation protects Fe-S cluster containing dehydratases from inactivation.

We examined the effect of copper (II) on *in vivo* AcnA activity (Beinert et al. 1996). For these experiments, we used strain that contained a null chromosomal *acnA* allele, and a secondary plasmid encoded *acnA* allele that was under the transcriptional control of a xylose inducible promoter (p*acnA*). This helped us control the transcription of *acnA* to possibly prevent any potential effects of copper on *acnA* transcription. Growth in the presence of copper (II) resulted in a concentration-dependent decrease in AcnA activity in the *cop- acnA::tetR* strain containing p*acnA*. AcnA activity was nearly undetectable after culture with 20 μM copper (II) (Figure 2.8D). We next examined the effect of introducing the *mntA1::Tn* mutation on *in vivo* AcnA activity. The *cop- acnA::tetR mntA1::Tn* strain containing p*acnA* had decreased AcnA activity when cultured in the presence of copper (II),

but the decrease in activity was substantially less than that noted for the *cop- acnA::tetR* strain (Figure 2.8D).

We sought to determine if the *S. aureus* AcnA was poisoned by copper (II) *in vitro*. Cell lysates from the *cop-* strain were created anaerobically and then combined with copper (II) before monitoring AcnA activity. The presence of copper (II) decreased AcnA activity in a concentration dependent manor (Figure 2.8E).

Recent work by Johnson et al. reported that the *Streptococcus pneumonia* aerobic manganese-dependent ribonucleotide reductase (NrdEF) is poisoned by copper (Johnson et al. 2015b). *S. aureus* utilizes the NrdEF and NrdDG ribonucleotide reductases primarily during aerobic and anaerobic growth, respectively (Cotruvo and Stubbe 2012; Rabinovitch et al. 2010). We tested the hypothesis that the activity of essential NrdEF is decreased by intracellular copper accumulation. The *cop-* and *cop- nrdD::Tn* strains were spot plated on solid medium with and without copper and the ribonucleotide reductase inhibitor hydroxyurea. Hydroxyurea and copper (II) individually inhibited the growth of the strain aerobically, but no difference was noted between the *cop-* and *cop- nrdD::Tn* strains (Figure 2.9). However, these compounds showed great synergy in inhibiting growth when provided at the same time. The addition of manganese did not significantly affect growth in the presence of copper or hydroxyurea (Figure 2.9).

During anaerobic growth the *cop- nrdD::Tn* strain had a general slow growth phenotype and it was more sensitive to hydroxyurea than the *cop-* strain (Figure 2.9 and data not shown). Both strains had slow growth phenotype in the presence of copper (II) and there was not a significant decrease in growth of the *cop-*

nrdD::Tn strain with copper (II). As noted for aerobic growth the presence of both hydroxyurea and copper resulted in phenotypic synergy and strong growth inhibition. We found that a *cop- nrdG::Tn* strain behaved identically to *cop- nrdD::Tn* strain (data not shown). Taken together, these data suggest that NrdEF is not a primary target of Cu poisoning in *S. aureus*.

The *copBL* and *copAZ* operons protect *S. aureus* from MntABC-dependent copper accumulation.

We previously found that *copAZ* is induced to a higher degree than *copBL* upon copper addition to USA300_LAC cells (Rosario-Cruz et al. 2019). We tested the hypothesis that the acquisition of a secondary copper detoxification system was helping to protect from MntABC-dependent copper accumulation. We found that the Δ*copAZ* strain had a more severe growth defect than the Δ*copBL* strain in the presence of copper (II) (Figure 2.10A) (Figure 2.10B). The introduction of the *mntA1::Tn* mutation improved the growth of the Δ*copAZ* strain in the presence of copper (II), but had less to no effect on the Δ*copBL* strain. No growth difference was noticed when cells grown in media without copper challenge (data not shown).

Discussion

The goal of this study was to further explore copper homeostasis in *S. aureus*. To this end, we created a *S. aureus* strains lacking the CopAZ and CopBL copper detoxification factors. As previously reported, the Δ*copBL* and Δ*copAZ* mutants had intermediate sensitivities to growth in the presence of copper (II) whereas the phenotypes of the Δ*copBL* and Δ*copAZ* deletions displayed genetic synergy. The *cop*- (Δ*copBL* Δ*copAZ*) strain also had a high copper load after dosing with copper (II). CsoR represses copper detoxification systems and a *cop*- Δ*csoR* strain had the same sensitivity to copper (II) as the *cop*- strain. Although not conclusive, these data are consistent with the hypothesis that *copAZ* and *copBL* are the primary copper detoxification genes in USA300_LAC that are under CsoR transcriptional control.

We screened for *cop*- strains that were capable of growth in the presence of a concentration of copper that inhibited the growth of the *cop*- strain. We isolated strains with transposon insertions in *mntA*. The *mntA::Tn* mutations were recessive and strains with Δ*mntA*, Δ*mntB*, or *mntC::Tn* mutations grew in the presence of excess copper (II). The *cop*- *mntA::Tn* strain had decreased copper loads after dosing with copper (II). Under the growth conditions utilized, manganese was limiting in the growth medium resulting in increased *mntABC* transcription, which was dependent upon the manganese-dependent transcriptional repressor MntR. Increased MntABC expression in the *cop*- strain resulted in increased sensitivity to copper (II) and increased cellular copper loads. Lastly, the lack of a functional MntABC system protected cytosolic enzymes from damage by copper.

The data presented herein, in conjunction with our previous work, as well as work from others, has resulted in the following working model for copper homeostasis in *S. aureus* (Figure 2.11). Under manganese deplete conditions, MntABC is expressed and copper enters *S. aureus* cells through the MntABC manganese (II) importer. Once the copper has entered the cell it is sensed by the CsoR transcriptional regulator. Copper association with CsoR results in derepression of the *copAZ* and *copBL* operons. CopA and CopB function as copper (I) export systems. CopZ acts as an intracellular copper (I) binding protein that buffers the cytosol from copper toxicity. Holo-CopZ traffics copper (I) to CopA for export. After export by CopA or CopB, or before copper enters the cell, CopL binds to copper (I) and prevents it from (re)entering.

A number of metals including lead (Pb), silver (Ag), cadmium (Cd) and mercury (Hg) have no described biological roles and are potent poisons of intracellular enzymes (Xu and Imlay 2012; Jarosławiecka and Piotrowska-Seget 2014). For the most part, dedicated import systems for these metals do not exist. It has been hypothesized that these metals enter cells through import systems that function to import alternate compounds deemed useful to the cell (Tynecka et al. 1981; Laddaga and Silver 1985). This is paradoxical because these transporters are expressed to allow entry of essential nutrients while maintaining an electrochemical gradient and preventing the entry of toxic compounds. Cellular systems have evolved to transform and/or efflux these toxic metals thereby decreasing cytosolic concentrations and maintaining homeostasis (Borremans et al. 2001; Gupta et al. 1999; Gaballa and Helmann 2003; Norambuena et al. 2018).

Metals such as zinc, iron, manganese, and copper, often have cellular roles, but cytosolic overload can be toxic (Chandrangsu et al. 2016; Macomber and Imlay 2009; Huang et al. 2017; Guan et al. 2015). The mechanisms of manganese, zinc, iron acquisition have been well defined reviewed by (Palmer and Skaar 2016). Nearly all described ABC transporters only transport in one direction (Wilkens 2015). In support of this, recent work has found that bacteria also contain manganese, zinc, and iron efflux systems to prevent cytosolic accumulation (Gaballa and Helmann 2003; Huang et al. 2017; Guan et al. 2015; Chandrangsu et al. 2017).

Compared to other transition metals, copper uptake pathways are the least understood in bacterial pathogens and many questions remain about how copper enters cells (Begg 2019). Dedicated Cu uptake systems have been described in *Rhodobacter capsulatus* and *Synechocystis* (Ekici et al. 2012; Tottey et al. 2001). *R. capsulatus* CcoA functions to import Cu utilized for cytosolic maturation of a *ccbb*$_3$-type cytochrome oxidase, which is then inserted in the membrane. *S. aureus* is predicted to utilize only one cuproprotein, which is an *aa3* cytochrome oxidase (QoxAB) (Powers et al. 1994). A dedicated Cu import system has not been described for *S. aureus.* The adventitious import of copper through metal importers dedicated to importing alternate metals, such as manganese (II) importers, may provide a mechanism for cells to acquire copper, which is only required, if at all, in trace amounts. These organisms, therefore, must rely on cytosolic copper buffering and efflux to sustain homeostasis. The data presented herein are consistent with the hypothesis that copper enters *S. aureus* cells through the

MntABC transporter, which functions to uptake manganese (II) under deplete conditions (Radin et al. 2019).

Many studies suggest that metal import is a promiscuous process, but few studies have identified and conclusively shown that metal-specific uptake systems inadvertently uptake alternate metals. In *S. aureus*, cadmium (II) is up taken by membrane vesicles and uptake was decreased upon the addition of CCCP, valinomycin, or manganese (II) (Perry and Silver 1982). These data led to the hypothesis that cadmium (II) uptake required the PMF and was entering through a manganese (II) transporter. An alternate study found that a *S. aureus mntA* mutant had increased resistance to cadmium (II) (Horsburgh et al. 2002). These data have been interpreted to suggest that cadmium (II) is transported into *S. aureus* via MntABC (Papp-Wallace and Maguire 2006), but direct evidence for this is lacking.

Studies using other organisms have provided more convincing data that some metal ion transporters can transport more than one metal. *Escherichia coli* strains over-producing the ZIP family Zn importer ZupT resulted in sensitivity to Fe and Co, as well as accumulation of the metals associated with whole cells (Grass et al. 2005). *Mycobacterium smegmatis* cells lacking porins grew poorly in medium that was iron starved and had enhanced growth in medium containing high levels of copper. Over-production of the porin structural gene increased *M. tuberculosis* sensitivity to copper leading to the hypothesis that copper was crossing the outer membrane via a porin (Speer et al. 2013). How copper is crossing the *Mycobacterium* cellular membrane is currently unknown. *Lactobacillus plantarum* accumulates cadmium (II) upon manganese (II) starvation (Archibald and Duong

1984). In fact, cells preferably took up the toxic cadmium (II) to manganese (II) (Archibald and Duong 1984). This effect is nullified upon the addition of the ionophores CCCP and DNP suggesting the a PMF is necessary for import (Hao et al. 1999a). Expression of the MntA P-type ATPase Mn importer from *Lactobacillus plantarum* in *E. coli* increased cadmium (II) and manganese (II) loads (Hao et al.1999b). Iron uptake by manganese-specific NRAMP transporter MntH was investigated. Highly selective for manganese (II), but could transport iron (Kehres et al. 2000). Expression of the *sitABCD* gene products in *E. coli* increased cellular Fe and Mn loads (Sabri et al. 2006) and the *Yersinia pestis* YfeABCD metal transporter was shown to transport both Mn and Fe.

Copper can poison iron-sulfur (Fe-S) proteins by disrupting their integrity and/or by inhibiting their maturation (Macomber and Imlay 2009; Tan et al. 2014). Consistent with this, we found that a strain deficient in synthesizing Fe-S clusters had increased sensitivity to copper. Moreover, the addition of copper resulted in an inability to grow without supplementing the growth medium with the amino acids leu and ile, which is a phenotype common to *S. aureus* strains defective in Fe-S protein maturation (Mashruwala et al. 2015b; Rosario-Cruz et al. 2015; Mashruwala et al. 2016a). Introduction of the *mntB::tetR* allele corrected both phenotypes suggesting that decreasing copper influx protects Fe-S proteins from copper poisoning. Furthermore, in *vivo* and *vitro* incubation with copper (II) inhibited aconitase in a concentration dependent manner. A lower concentration of copper was necessary to inhibit *in vivo* than need for inhibition in cell-free lysates. This maybe be the result of copper poisoning both the Fe-S cluster

synthesis machinery and holo-AcnA *in vivo* resulting in a compounding effect. We recently noted a similar effect in the inhibition of AcnA in *Thermus thermophilus*. The concentration of Hg necessary to inhibit AcnA *in vivo* was less than that necessary to inhibit the enzyme in cell lysates (Norambuena et al. 2019).

A recent study by Johnson et al. examined the mechanisms of copper toxicity in *Streptococcus pneumoniae* (Johnson et al. 2015b). The authors noted that the addition of 50 μM manganese partially rescued the growth of a *S. pneumoniae* Δ*copA* strain in the presence of copper and the addition of 250 μM manganese increased survival in murine lung macrophages. The addition of copper increased transcription of *nrdD*, which encodes for catalytic component of the anaerobic ribonucleotide reductase, as well as *nrdG*, *nrdH* and *nrdR*, which are accessory factors that function in aerobic ribonucleotide reduction. These data suggest that copper stressed cells are starved for reduced deoxynucleotides (dNTPs). The authors demonstrated that a Δ*nrdD* strain has increased sensitivity to copper. A Δ*copA* strain had increased sensitivity to hydroxyurea, which inhibits the aerobic ribonucleotide reductase. The *S. pneumoniae* NrdF is predicted to be manganese-dependent subunit of the class Ib enzyme (NrdEF) (Martin and Imlay 2011). Taken together, these finding led the authors to the hypothesize that copper is causing mis-metalation of NrdF, which is rescued by increasing the concentration of cytosolic manganese.

Like *S. pneumoniae*, *S. aureus* utilizes a class Ib ribonucleotide reductase during aerobic growth (NrdEF) (Cotruvo and Stubbe 2012; Rabinovitch et al. 2010). Data presented herein show that under the culturing conditions utilized, a

S. aureus cop- nrdD::Tn strain did not have a noticeable growth defect or an increased sensitivity to copper or hydroxy urea (when provided at 15 mM) during aerobic growth. However, a synergistic effect was noted when both hydroxyurea and copper were provided in the medium. This effect was noted in both the *cop-* and *cop- nrdD::Tn* strains. During anaerobic growth, where NrdEF expression is predicted to be low, we noted a general growth defect in the *cop- nrdD* strain and the strain had a profound growth defect in the presence of hydroxyurea (15 mM). We hypothesize that this hydroxyurea-dependent growth defect during anaerobic growth was the result of decreased NrdEF expression, which has been demonstrated by others (Masalha et al. 2001). Importantly, we did not witness a significant copper-dependent growth or survival defects in the *cop- nrdD* strain during anaerobic culture. However, as noted for aerobic growth, the phenotypic effects of hydroxyurea and copper supplementation were synergistic and resulted in significant growth defects in the *cop-* and *cop- nrdD::Tn* strains. Supplementing the medium with manganese (II) did not noticeably alter the phenotypes examined. Taken together, we interpret these data to suggest that copper was not greatly inhibiting the growth of *S. aureus* by poisoning NrdEF under the growth conditions utilized; however, when NrdEF function was decreased by copper the ribonucleotide reductase function is decreased by the addition of hydroxyurea.

Like the Johnson et al. study, the data presented herein highlight relationships between manganese and copper homeostasis. We noted that the addition of manganese, at a >10-fold lower concentration than that used by Johnson et al., protected against copper intoxication. This protection was

dependent upon the presence of the manganese sensing transcriptional regulator MntR. A *cop*- Δ*mntR* strain had increased *mntABC* transcription and decreased growth in the presence of copper. The decreased growth of the *cop*- Δ*mntR* was corrected by the introduction of the *mntA1::Tn* mutation. The *cop*- Δ*mntR* strain also had a larger copper load than the *cop*- strain, and again, this phenotype was mitigated by the introduction of *mntA1::Tn*. These data have led us to propose a working model (Figure 2.11) wherein manganese protects *S. aureus* against copper intoxication by binding to MntR and decreasing MntABC expression resulting in decreased copper uptake. The *S. pneumoniae* genome encodes for a predicted MntABC (SP_1648-50) system and MntR (SP_1638). Once these gene products are experimentally validated, it would be interesting to examine what effect the absence of MntABC or MntR have on the ability of manganese to protect *S. pneumoniae* against copper intoxication.

The *mntA::Tn1* mutant provided robust protection from copper to the *cop*- strain, but only very modest effects were witnessed when it was introduced in the WT background (data not shown). We tested the hypothesis that the acquisition of a secondary copper detoxification system was helping to protect from MntABC-dependent copper accumulation. We found that the Δ*copAZ* strain had a more severe growth defect than the Δ*copBL* strain in the presence of copper (II). We previously found that *copAZ* is induced to a greater degree than *copBL* upon copper addition to USA300_LAC cells (Rosario-Cruz et al. 2019). Work by Purves et al. found that a *S. aureus* JE2 *copB::Tn* strain had a large growth defect in RPMI and brain heart infusion broth (BHI) after copper supplementation whereas the

copA::Tn did not (Purves et al. 2018). Interestingly, the introduction of the *mntA1::Tn* mutation improved the growth of both the Δ*copAZ* and Δ*copBL* strains in the presence of copper (II). Strains with the *mntA1::Tn* mutation have decreased copper influx and a lower cellular copper load. These findings support the hypothesis that both the *copBL* and *copAZ* are maintained by USA300 to prevent MntABC-dependent accumulation of cytosolic Cu.

A couple of scenarios could explain these findings. It is possible that strain expressing CopBL has lower cytosolic accumulation. This could be explained by 1) CopL binding copper extracellularly and preventing its entry into the cytosol, and/or 2) the CopB efflux system has a higher affinity for copper than CopAZ resulting in effective removal of copper when cytosolic concentrations are lowered by the introduction of *mntA1::Tn*. Purves et al. found that a *S. aureus* JE2 *copA::Tn* strain did not accumulate copper upon culture with 100 μM copper; however, the copper load was nearly three-times as high in *copB::Tn* mutant (Purves et al. 2018). Further experimentation will be necessary to discern these and other possible scenarios. The results from this study are consistent with the hypothesis that copper is entering *S. aureus* cells through the MntABC Mn-importer which highlight a new aspect for copper homoestasis in *S. aureus.*

Materials and methods

Phusion DNA polymerase, deoxynucleoside triphosphates, the quick DNA ligase kit, and restriction enzymes were purchased from New England BioLabs. The plasmid miniprep kit, gel extraction kit, and RNA Protect were purchased from Qiagen. TRIzol and High-Capacity cDNA reverse transcription kits were purchased from Life Technologies. Oligonucleotides, obtained from Integrated DNA Technologies, are listed in (Table 2.2) DNase I was purchased from Ambion. Lysostaphin was purchased from Ambi Products. TSB was purchased from MP Biomedical. Difco BiTek agar was added (15 g L^{-1}) for solid medium. Tablets to make PBS were purchased from Calbiochem. Distilled and deionized water was used to prepare chemicals, and glassware was often acid washed prior to use. Chelex 100 resin was purchased from Bio-rad. Unless otherwise stated, all chemicals were purchased from Sigma-Aldrich and were of the highest purity obtainable. DNA was sequences by Genewiz (South Plainfield, NJ).

Bacterial strains, media and growth conditions

Unless specified, the *S. aureus* strains used in this study (Table 2.1) were isogenic and constructed in the community associated *S. aureus* MRSA strain USA300_LAC that had cured of the native plasmid pUSA03 that confers erythromycin resistance (Pang et al. 2014).

S. aureus strains were cultured in TSB and grown at 37°C with shaking at 200 rpm. Unless stated otherwise, cells were cultured in 10- or 30-mL capacity culture tubes containing 1 or 7.5 mL of liquid medium, respectively. The chemically defined minimal medium was described previously and where noted was

supplemented with 0.5 μg mL^{-1} lipoic acid (Mashruwala et al 2016). Chelexed TSB was prepared by incubating liquid TSB overnight at 4 °C with Chelex-100 Resin and continuous stirring. The chelated medium was filter sterilized before use. When necessary, antibiotics were added at the final following concentrations: 150 μg mL^{-1} ampicillin (Amp); 30 μg mL^{-1} chloramphenicol (Cm); 10 μg mL^{-1} erythromycin (Erm); 3 μg mL^{-1} tetracycline (Tet); 100 μg mL^{-1} spectinomycin; 150 ng mL^{-1} anhydrotetracycline (Atet). For routine plasmid maintenance, liquid media were supplemented with 10 μg mL^{-1} or 3.3 μg mL^{-1} of chloramphenicol or erythromycin, respectively. The $CuSO_4$ stock was prepared in deionized and distilled water and filter sterilized. Liquid phenotypic analysis was conducted in 96-well microtiter plates containing 200 μL of medium per well using a BioTek 808E visible absorption spectrophotometer. Culture densities were read at 600 nm. The cells used for inoculation were cultured for 18 hours in TSB medium before washing with PBS. The optical densities (OD) of the cell suspensions were adjusted to 2.5 (A600) in PBS. Two microliters of cells were added to 198 μL of medium. For growth analyzes using solid media, strains were cultured for 18 hours in TSB medium before harvesting by centrifugation. Cells were washed with PBS, serial diluted in PBS, and 5 μL aliquots were spotted upon solid media.

Aconitase Enzyme assays

Aconitase (AcnA) assay was conducted as previously described (Mashruwala et al. 2016a). Briefly, Strains were cultured overnight in TSB before washing them with PBS and diluting them to an optical density of 0.05 (A_{600}) in 7.5 mL of fresh liquid chemically defined medium supplemented with 1% xylose and

Cm. Strains were cultured in 30 mL culture tubes for 9 hours. Cells were harvested by centrifugation, washed with PBS, and pellets stored at -80 °C. Protein concentrations were determined using a copper bicinchoninic acid based colorimetric assay modified for a 96-well plate. Aconitase *invirtro* assay was done by assaying cells free lysate to increasing doses of copper. Copper (II) or equivalent amount of water was added to tubes containing lysates anaerobically to get 0, 25, 50, 100 μM final concentration. Tubes were incubated for 20 minutes before assaying for aconitase activity.

RNA isolation and quantification of mRNA transcripts.

Bacterial strains were cultured for 18 hours in TSB and diluted to a final OD of 0.1 (A_{600}) in 30 mL of fresh TSB or Chelex-treated TSB. The cells were cultured in 250 mL flasks and incubated with shaking till growth reached an OD of 0.8 (A600). One mL was transferred to 10 mL capacity tubes in triplicates and 10 μM $MnCl_2$ final concentration was added to manganese treated group. Both manganese treated and non-treated cultures were then incubated for 15, 30, and 60 minutes and harvested. Harvested cells were treated with RNAProtect (Qiagen) for 10 min at room temperature, pelleted by centrifugation, and stored at -80 °C. Cell pellets were thawed and washed twice with 0.5 mL of lysis buffer (20 mM RNase-free Sodium acetate, 1 mM EDTA, 0.5% SDS). The cells were lysed by the addition of 4 μg lysostaphin and incubated for 40 min at 37 °C until confluent lysis was observed. RNA was isolated using TRIzol reagent according to the manufacturer's instructions. DNA was digested with the Turbo DNA-free kit. The cDNA libraries were constructed using isolated RNA as a template and a High

Capacity RNA-to-cDNA kit. An Applied Biosystems StepOnePlus thermocycler and Power SYBR green PCR master mix (Applied Biosystems) were used to quantify DNA abundance. The primer pairs were designed using Primer Express 3.0 software (Applied Biosystems). Primers are listed in (Table 2.2).

Whole cell metal quantification

S. aureus were subuculted in triplicate, from 18 hour grown overnights, to an OD of 0.05 (A_{600}) in 7.5 mL of chelexed TSB in a 30 mL capacity culture tubes. Cultures were incubated with shaking for 8 hrs, before 0-10 µM $CuSO_4$ was added. After 15, 30, or 60 minutes of incubation, samples were transferred into pre-weighted metals free propylene tubes and cells were pelleted by centrifugation using a prechilled table top centrifuge (Eppendorf, Hauppauge, NY). Pellets were washed three times with 10 mL of ice-cold PBS. After decanting the PBS, a fourth spin was conducted to help separate the pellets from any remaining liquid, which was removed using metals free pipettes. Tubes were weighed again to quantify the weight of the cell pellets. All samples were kept at -80 °C or on dry ice until processing.

Cell pellets were acid digested with 2 mL Optima grade nitric acid (ThermoFisher, Waltham, MA) and 500 µL hydrogen peroxide (Sigma, St. Louis, MO) for 24 h at 60 °C. After digestion, 10 mL UltraPure water (Invitrogen, Carlsbad, CA) was added to each sample. Elemental quantification on acid-digested liquid samples was performed using an Agilent 7700 inductively coupled plasma mass spectrometer (Agilent, Santa Clara, CA). The following settings were fixed for the analysis Cell Entrance = -40 V, Cell Exit = -60 V, Plate Bias = -60 V, OctP Bias =

-18 V, and collision cell Helium Flow = 4.5 mL min^{-1}. Optimal voltages for Extract 2, Omega Bias, Omega Lens, OctP RF, and Deflect were determined empirically before each sample set was analyzed. Element calibration curves were generated using ARISTAR ICP Standard Mix (VWR). Samples were introduced by peristaltic pump with 0.5 mm internal diameter tubing through a MicroMist borosilicate glass nebulizer (Agilent). Samples were initially up taken at 0.5 rps for 30 seconds followed by 30 seconds at 0.1 rps to stabilize the signal. Samples were analyzed in Spectrum mode at 0.1 rps collecting three points across each peak and performing three replicates of 100 sweeps for each element analyzed. Sampling probe and tubing were rinsed for 20 s at 0.5 rps with 2 % nitric acid between each sample. Data were acquired and analyzed using the Agilent Mass Hunter Workstation Software version A.01.02.

Transposon library construction, mutant selection, and Tn location determination.

The transposon library was constructed in the *cop*- strain as previously described by Grosser et al. (Bae et al. 2004 ; Grosser et al. 2018). Briefly, pMG020 (harboring transposase) was transformed into RN4220 and plated and incubated on TSA Tet (10 µg/mL) at 30° C. Single colonies were selected and grown in TSB Tet (10 µg/mL) at 30° C. The *cop*- strain carrying pBursa was transduced with pMG020 and selected with TSA-Cm-Tet at 30° C. Individual colonies were struck on Cm-Tet plates. Individual colonies were suspended in 200 µL sterile water and 15 µL aliquots were spread onto TSA plates containing 10 µg mL^{-1} Erm and incubated at 43 °C for 24 hours to allow for transposition. In total, colonies from

170 Petri plates containing approximately 3000 colonies each were pooled using TSB 10 μg mL^{-1} Erm with 25% glycerol. Aliquots were thoroughly mixed by vortexing and combined into a single pool of transposon mutants. This mutant library was cultured for 2 hours with shaking at 43 °C before 1 mL aliquots were frozen and stored at -80 °C.

To select for copper resistant mutants, an aliquot of the *cop*- Tn library was thawed, diluted 1/200, and 100 μL were plated on TSA plates containing 2.5 mM $CuSO_4$. Plates were incubated at 37 °C for 5 days and monitored daily. The total colony forming units plated was also determined by plating to TSA. Single colonies from the TSA-copper plates were struck on TSA-Erm plates. Individual colonies cultured overnight in TSB and the copper resistance phenotype was verified by serial dilution and spot plating on TSA-copper medium. Strains displaying increased growth when compared to the *cop*- strain were reconstructed and phenotypically verified.

The protocol outlined by Fey et al. was used to determine the locations of transposon insertions (Fey et al. 2013). Briefly, cells were lysed using lysostaphin and genomic DNA was purified. The DNA was digested using AciI and the resulting DNA fragments were ligated using quick ligase kit and PCR reactions were preformed using the Tn buster and Martn-ermR primers. The PCR products were gel purified and sequenced to identify the transposon genome junction sites.

Recombinant DNA and genetic techniques

JMB1100 chromosomal DNA was used as a template for PCR reactions. *Escherichia coli* PX5α (Protein Express) was used as cloning host for plasmid propagation. Plasmids were isolated and transformed into *S. aureus* strain RN4220 using standard protocol. All transductions were conducted using phage 80α (ref) and selected in the presence of 2 mM citrate. All strains were verified by PCR and/or sequencing. DNA sequencing was conducted by Genewiz (South Plainfield, NJ).

Creation of plasmids and mutant strains

Construction of plasmids for mutant generation or genetic complementation was done using yeast homologous recombination cloning as previously outlined (Joska et al. 2014; Mashruwala et al. 2015a). The following primer pairs were used to create the amplicons necessary to make pJB38_Δ*copAZ*: Ycc Pjb38 for and YCC CopAZ rev; CopAZ Up for and copAZ up rev; copAZ dwn for and pJB38 copAZ rev. The amplified PCR fragments were combined with an EcoRI linearized pJB38 plasmid and transformed into competent *Saccharomyces cerevisiae* FY2. To create pEPSA_*mntABC*, pEPSA5_*citB_FLAG* (Mashruwala et al. 2015b) was linearized with NheI and MluI. The *mntABC* insert was amplified using primers pEPmntABCfor and mntABCYCCrev, combined with vector, and transformed into competent *Saccharomyces cerevisiae* FY2. For all *tetR* insertion mutants, the tetracycline cassette was amplified from strain JMB1432. To generate all *mnt* pJB38 vectors, pJB38_Δ*rseA* (a pJB38 plasmid that carries yeast cassette and

Δ*rseA*) was linearized using NheI and MluI, which was combined with amplicons and transformed into competent *Saccharomyces cerevisiae* FY2. The following primer pairs were used to create the amplicons necessary to make pJB38_*ΔmntR::tetR*: YccmntRfor and mntRtetRrev; tetRmntRfor and pJB38mntRrev. The following primer pairs were used to create the amplicons necessary to make pJB38_*ΔmntA::tetR*: YCCmntAfor and mntAtetRrev; mntAtetRfor and tetRmntArev; tetRmntAfor and pJB38mntArev. The following primer pairs were used to create the amplicons necessary to make pJB38_*ΔmntB::tetR*: YCCmntBfor and mntBtetRrev; mntBtetRfor and tetRmntBrev; tetRmntBfor and pJB38mntArev. The following primer pairs were used to create the amplicons necessary to make pJB38_*ΔmntAB::tetR:* YCCmntAfor and mntAtetRrev; mntAtetRfor and tetRmntABrev;tetRmntABfor and pJB38mntArev. The following primer pairs were used to create the amplicons necessary to make pJB38_Δ*mntABC*::*tetR* were YCCmntABCfor and mntABCtetRrev; mntABCtetRfor and tetRmntABCrev; tetRmntABCfor and pJB38mntABCrev. The following primer pairs were used to create the amplicons necessary to make pLL39_*mntABC*: pLLYCC5 and mntABCYCC3; YccmntABC and mntABCpLL39. The pLL39 vector was linearized with SalI, combined with PCR amplicons, and transformed into *Saccharomyces cerevisiae* FY2. The *pLL39_ mntABC* construct was transformed into RN4220 containing pLL2787 and integrated onto the chromosome at the Φ11 *attB* site as previously described (Luong and Lee 2007). Episome integration was verified using the Scv8 and Scv9 primers. Mutant strains were constructed using the pJB38 allelic exchange vectors

as described previously (Rosario-Cruz et al. 2015). The *cop*- strain was created using strain JMB7901 *ΔcopBL* (ΔSAUSA300_0078-0079) and pJB38_Δ*copAZ*.

Table 2.1 Microbial strains and plasmids used in this study.

Name	Chromosomal Genotype	Allele or strain reference
***S. aureus* USA300 LAC strains**		
JMB1100	USA300 wild-type strain- LAC	AR Horswill
JMB1432	*fur::tetR*	(Horsburgh et al. 2001a; Mashruwala and Boyd 2017)
JMB 8571	Δ*copAZ* (SAUSA300_2494-5)	This study
JMB 9620	Δ*copAZ mntA1::Tn* (*ermB*) (SAUSA300_0620)	This study
JMB 7901	Δ*copBL* (SAUSA300_0078-9)	(Rosario-Cruz et al. 2019)
JMB 9621	Δ*copBL mntA1::Tn* (*ermB*) (SAUSA300_0620)	This study
JMB 8573	Δ*copBL* Δ*copAZ* (*cop-*)	This study
JMB 8914	*cop- mntA1::Tn* (*ermB*) (SAUSA300_0620)	This study
JMB 8915	*cop- mntA2::Tn* (*ermB*) (SAUSA300_0620)	This study
JMB 8898	*cop- ispA::Tn* (*ermB*) (SAUSA300_1470)	This study
JMB 8902	*cop- apt::Tn* (*ermB*) (SAUSA300_1591)	This study
JMB 9313	*mntA1*::*Tn* (*ermB*) (SAUSA300_0620)	This study
JMB 8965	*cop- mntC::Tn* (ermB) (SAUSA300_0618)	This study
JMB 9201	*cop-* Δ*mntA::tetR*	This study
JMB 9208	*cop-* Δ*mntB::tetR* (SAUSA300_0619)	This study
JMB 9325	*cop-* Δ*mntABC::tetR* (SAUSA300_0619-21)	This study
JMB 9151	*cop-* Δ*mntR:tetR* (SAUSA300_0621)	This study
JMB 9244	*cop-* Δ*mntR:tetR mntA1::Tn* (*ermB*)	This study
JMB 8625	*cop- sufD**	This study and (Roberts et al. 2017)
JMB 9604	*cop- sufD** Δ*mntB::tetR*	This study and (Roberts et al. 2017)
JMB 9535	*cop- attP::pLL39*	This study
JMB 8804	*cop- nrdD::Tn (ermB)* (SAUSA300_2551)	This study
JMB 9534	*cop- mntA1::Tn* (*ermB*) *attP::pLL39*	This study
JMB 9469	*cop- mntA1::Tn* (*ermB*) *attP::pLL39_mntABC*	This study
JMB 9320	*cop- acnA::tetR*	This study and (Somerville et al. 2002)
JMB 9517	*cop- mntA1::Tn* (*ermB*) *acnA::tetR*	This study and (Somerville et al. 2002)
JMB 8723	*cop- csoR::Tn*	This study
Other microbial strains		
S. aureus RN4220	Restriction minus for transformation	(Kreiswirth et al. 1983)
Escherichia coli PX5α	Used for molecular cloning	Protein Express
Saccharomyces cerevisiae FY2	Used for YCC cloning	(Joska et al. 2014)

Plasmids used in this study

Name	Function	Reference
pJB38	Construction of gene deletions	(Bose et al. 2013)
pJB38_Δ*mntA::tet*	Construction of *mntA* deletion	This study
pJB38_Δ*mntB::tet*	Construction of *mntB* deletion	This study
pJB38_Δ*mntABC::tet*	Construction of *mntABC* deletion	This study
pJB38_Δ*mntR::tet*	Construction of gene deletion	This study
pEPSA5	Xylose inducible promoter	(Forsyth et al. 2002)
pEPSA5_*mntABC*	*mntABC* under xylose inducible promoter	This study
pEPSA5_*acnA_FLAG*	AcnA expression	(Mashruwala et al. 2015b)
pLL39	Genetic complementation	(Luong and Lee 2007)
pLL39_*mntABC*	*mntA::Tn* complement	This study
pMG020	Tn library generation	(Grosser et al. 2018)
pBursa	Tn library generation	(Bae et al. 2008)
pLL2787	Use to generate *attP::pLL39* integrant	(Luong and Lee 2007)

Abbreviations: Tn, transposon

Table 2.2 Oligonucleotides used in this study

Primer name	Sequence
Ycc Pjb38 forward	AATAGGCGTATCACGAGGCCCTTTCGTCTTCAAGAATTCGGTGGCACTTTTCGGGGAAA
YCC CopAZ rev	GGACCTAATTGTGGATTCTACACGCTAGCGCACATTAGGACCGTTATAGTTACGCTAT
CopAZ Up for	ATAGCGTAACTATAACGGTCCTAATGTGCGCTAGCGTGTAGAATCCACAATTAGGTCC
CopAZ up rev	CGACATCGTAACCTTGATCTTCACGCGTGTCATACCAGTGATATCTAATGTTG
CopAZ dwn for	CAACATTAGATATCACTGGTATGACACGCGTGAAGATCAAGGTTACGATGTCG
pJB38 CopAZ rev	CTAGAGGATCCCCGGGTACCGAGCTCGAATTCGACAATGTTGAAGGTGTCGCTGG
YccmntRfor	AGCGTAACTATAACGGTCCTAATGTGCGCTAGCAAGATTCTAATTCTAAATCGCTTAAT
mntRtetRrev	TTTCTTCATCATCGGTCATAAAATCCGACGCGTACTTTCACCTCACATACATTGTCTAT
tetRmntRfor	GTATATAAACATTCTCAAAGGGATTTCTAAAATAAAGAAGCCATAAAGATATCCATGAT
pJB38mntRrev	TAGAGGATCCCCGGGTACCGAGCTCGAATTCTATTATGTTATTGATAGGTTTAGCGTCG
mntRtetRfor	ATAGACAATGTATGTGAGGTGAAAGTACGCGTCGGATTTTATGACCGATGATGAAGAAA
tetRmntRrev	ATCATGGATATCTTTATGGCTTCTTTATTTTAGAAATCCCTTTGAGAATGTTTATATAC
YCCmntAfor	ATAGCGTAACTATAACGGTCCTAATGTGCGCTAGCCCAGCGTCCGAGTCCACAGTGGGA
mntAtetRfor	CTTTTAATTAGGAGGTATAAACGACGCGTCGGATTTTATGACCGATGATGAAGAAAAGA
mntAtetRrev	TCTTTTCTTCATCATCGGTCATAAAATCCGACGCGTCGTTTATACCTCCTAATTAAAAG
tetRmntAfor	ATATAAACATTCTCAAAGGGATTTCTAACCACCATGATCTATCAAAAGCAAAGCAATAC
tetRmntArev	GTATTGCTTTGCTTTTGATAGATCATGGTGGTTAGAAATCCCTTTGAGAATGTTTATAT
pJB38mntArev	ACTCTAGAGGATCCCCGGGTACCGAGCTCGAATTCTGTGGCCTAAAATATTGGAGATAC
tetRmntABrev	GGTACTAATTTTTTCATGTTAAACTTCCTCGTTAGAAATCCCTTTGAGAATGTTTATAT
tetRmntABfor	ATATAAACATTCTCAAAGGGATTTCTAACGAGGAAGTTTAACATGAAAAAATTAGTACC
YCCmntABCfor	ATAGCGTAACTATAACGGTCCTAATGTGCGCTAGCCGTTATTGTTGCAGCTTGTTATAT
mntABCtetRrev	TCTTTTCTTCATCATCGGTCATAAAATCCGACGCGTTTCTAACAAACGTTTATACCTCC
mntABCtetRfor	GGAGGTATAAACGTTTGTTAGAAACGCGTCGGATTTTATGACCGATGATGAAGAAAAGA
tetRmntABCrev	TCTTACTTCATTAAAACACAGCGTGTTATTAGAAATCCCTTTGAGAATGTTTATATA
tetRmntABCfor	TATATAAACATTCTCAAAGGGATTTCTAATAACACGCTGTGTTTTAATGAAGTAAGA
pJB38mntABCrev	ACTCTAGAGGATCCCCGGGTACCGAGCTCGAATTCAGTAGGGAGAACAGTTGTCCAATC
pJB38mntABCrev	ACTCTAGAGGATCCCCGGGTACCGAGCTCGAATTCAGATGAAGTATCAGAAGGTACAGC
pEPmntABCfor	CCTCTAGAGTCGACTTAGGAGGATGATTATTTTTGTTAGAAACAAAAGATTTAAATCTG
mntABCYCCrev	GCGTAACTTTTCCCCGAAAAGTGCCACCACGCGTGGTAATATATATTTAACGCACGATA
pLLYCC5	CTGTAATGGGCCCAATCACTAGTGAATTCCCGAAGCGGTGGCACTTTTCGGGGAAA
mntABCYCC3	AAAGAGGACTATTTAAAGGCAATCCTTACGCTATTATACCCTGTTATCCCTA
YccmntABC	TAGGGATAACAGGGTAATATAGCGTAAGGATTGCCTTTAAATAGTCCTCTTT
2 mntABCpLL39	GTGCTAAAGAAGTTGTAGGTAATAAAAAGCTTGCCAATATTTTAGGTTGCATCAACATC
Rt_mntC Fwd	GCAGTGATAAGTCAAATGGCAAATT
Rt_mntC rev	TCTCCACCAACATTTTTAGCCATA
Rt_mntA fwd	ATACCAGTACGCGGCGAAATA
Rt_mntA rev	AGGGAAGATTTACCAGCACCATT
Rt_mntB fwd	TCACGCAGTATTACCTGGTGTTG
Rt_mntB rev	ACCAGTTATAAGTGCGCCTACAAA
Rt_mntH fwd	TTAGTCGCTGTTGGTTACATGGA
Rt_mntH rev	GCGCCACCTTGCATTGAT
16sfwdRT	TGAAAGCCCACGGCTCAA
16srevRT	TTCTGCACTCAAGTTTTCCAGTTT
gyrAfor	GGACGTCAACGTATTGTTGTCACT
gyrARev	CGAGCTCTGCAATTTTTTCAATC
SCV8	GCACATAATTGCTCACAGCCA
SCV9	GCTGATCTAACAATCCAATCCA
Tn Buster	GCTTTTTCTAAATGTTTTTTAAGTAAATCAAGTACC
Martn-ermR	AAACTGATTTTTAGTAAACAGTTGACGATATTC

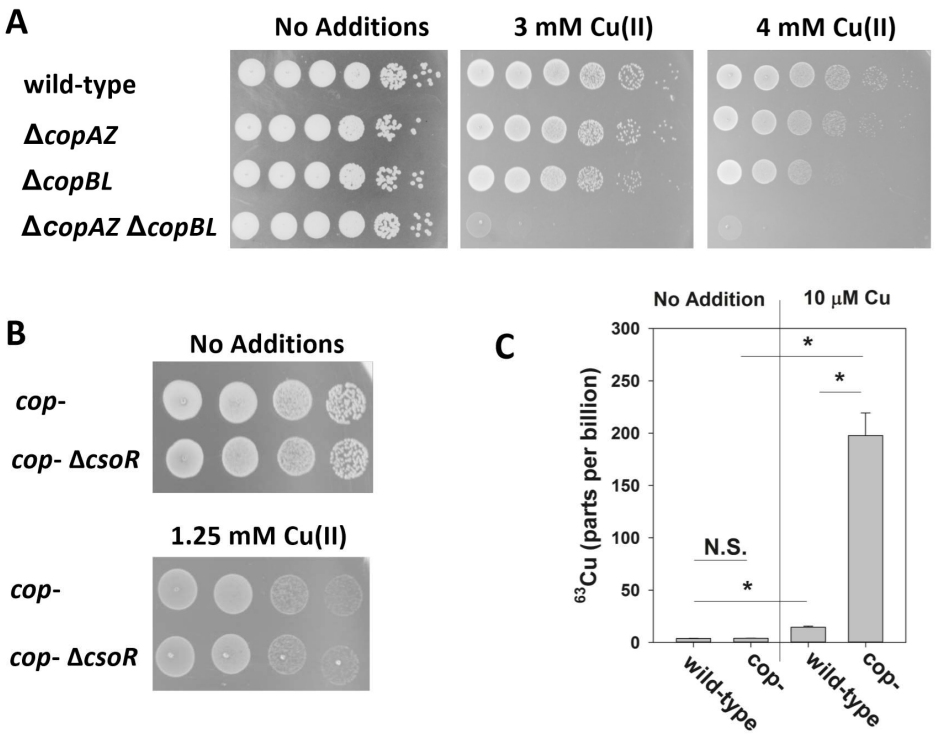

Figure 2.1: A *S. aureus* Δ*copBL* Δ*copAZ* strain accumulates copper.

Panel A; copper sensitivity of *S. aureus* strains lacking copper detoxification systems. Spot plate analysis of wild-type (JMB1100), Δ*copAZ* (JMB8571), Δ*copBL* (JMB7901), and Δ*copAZ* Δ*copBL* (*cop*-) (JMB8573). Overnight cultures were serial diluted and spot plated on TSB medium containing various concentrations of copper. Photos from a representative experiment are shown. Panel B; spot plate analysis of *cop*- (JMB8573) and *cop- csoR::Tn* (JMB8723). Panel C; Total ^{63}Cu load was determined in the WT and *cop*- (JMB8573) strains using inductively coupled plasma mass spectrometry after growth in TSB medium in the presence and absence of 10 μM copper. The data represent the mean of three biological replicates and errors are presented as standard deviations. Paired student t-tests were performed on the samples and N.S. denotes not significant ($p > 0.1$) and * denotes $p \leq 0.05$.

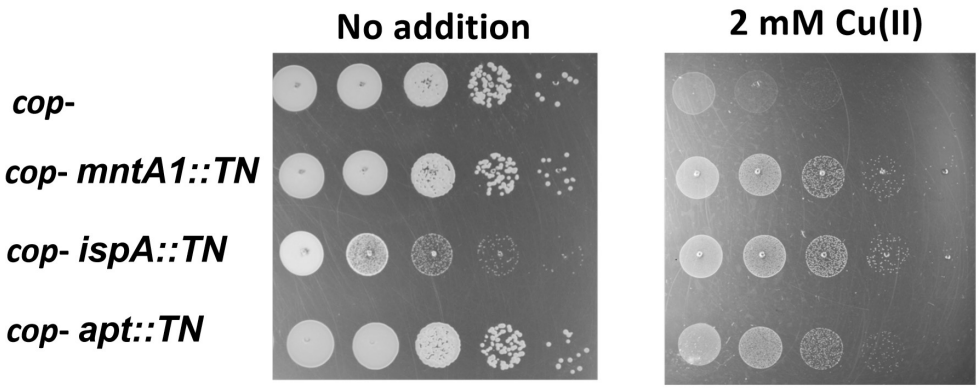

Figure 2.2: *S. aureus* strains with individual transposon insertions have increased growth in the presence of copper

Overnight cultures of the *cop-* (JMB8573), *cop- mntA1::Tn* (JMB8914), *cop- apt::Tn* (JMB 8902), and *cop- ispA::Tn* (JMB8898) strains were serial diluted and spot plated on TSB medium containing 0 or 2 mM copper (II). Photos from a representative experiment are shown.

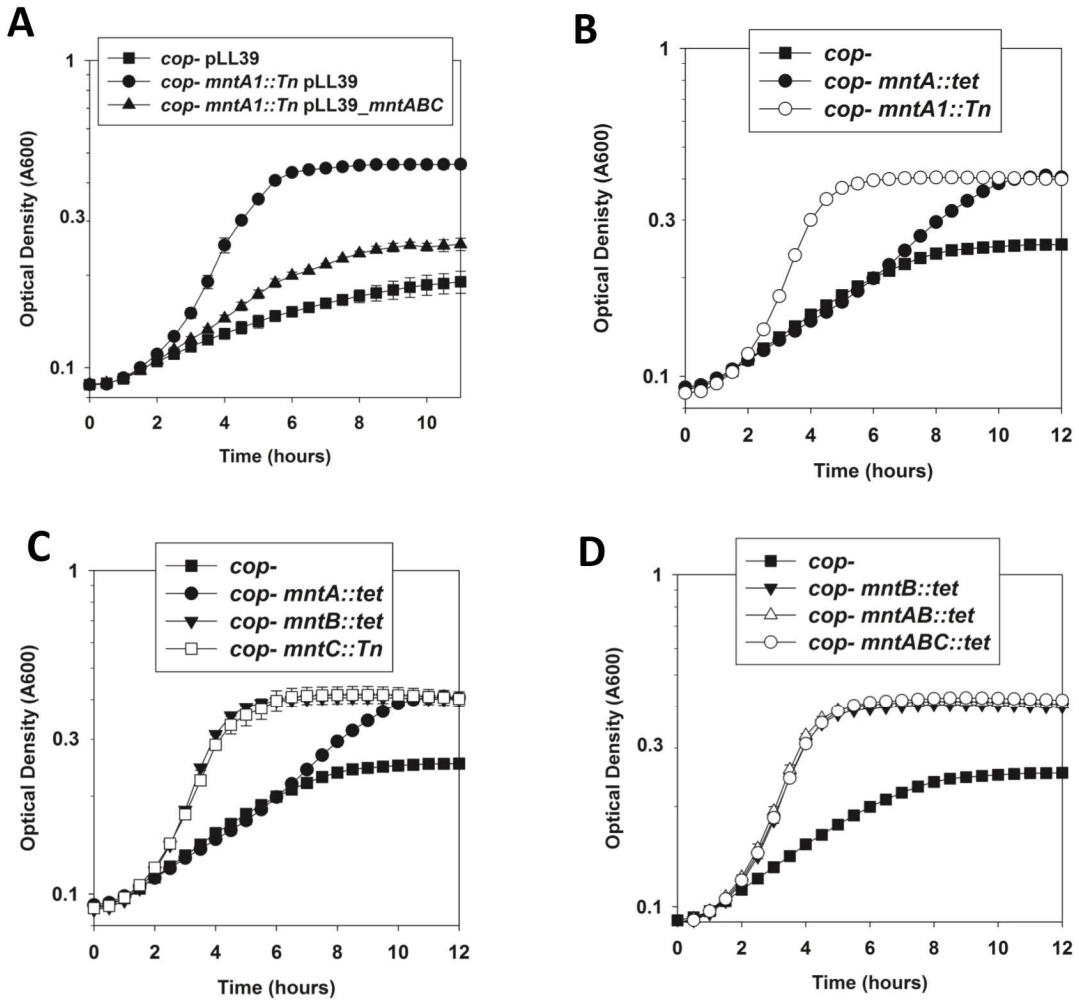

Figure 2.3: The *mntA1::Tn* mutation is recessive and null mutants in *mntA*, *mntB*, or *mntC* promote growth in the presence of copper (II)

Growth was monitored in chemically defined media containing 20 amino acids (AA) supplemented with lipoic acid with 20 μM copper and without copper. Panel A; genetic complementation of the copper (II) resistance phenotype of the *cop- mntA1::Tn* strain. Growth of the *cop-* pLL39 (squares; JMB9535), *cop- mntA1::Tn* pLL39 (circles; JMB9534), and *cop- mntA1::Tn* pLL39_*mntABC* (triangles; JMB9469) is shown. Panel B; A Δ*mntA::tetR* allele partially protected against

copper (II) intoxication. Growth of the *cop-* (squares; JMB8573), Δ*mntA::tetR* (black circles; JMB 9201), and *mntA1::Tn* insertion (white circles; JMB8914) are shown. Panel C; non-functional *mntA::tetR*, *mntB::tetR*, and *mntC::Tn* alleles improve the growth of the *cop-* strain in the presence of copper (II). Growth of the *cop-* (filled squares; JMB8573), *cop-* Δ*mntA::tetR* (circles; JMB 9201), *cop-* Δ*mntB::tetR* (triangles; JMB9208), and *cop- mntC::Tn* (white squares; JMB 8965) are shown. Panel D; the phenotypes associated with null mutants in *mntA*, *mntB*, and *mntC* are not genetically additive. Growth of the *cop-* (squares; JMB8573), Δ*mntA::tetR* (filled circles; JMB 9201), and Δ*mntB::tetR* (filled triangles; JMB9208), Δ*mntAB::tetR* (open triangles; JMB9246), Δ*mntABC::tetR* (open cirles; JMB9324) are shown. The data represent the mean of two biological replicates and errors are presented as standard deviations. Error bars are presented for all data, but often obscured by the symbol.

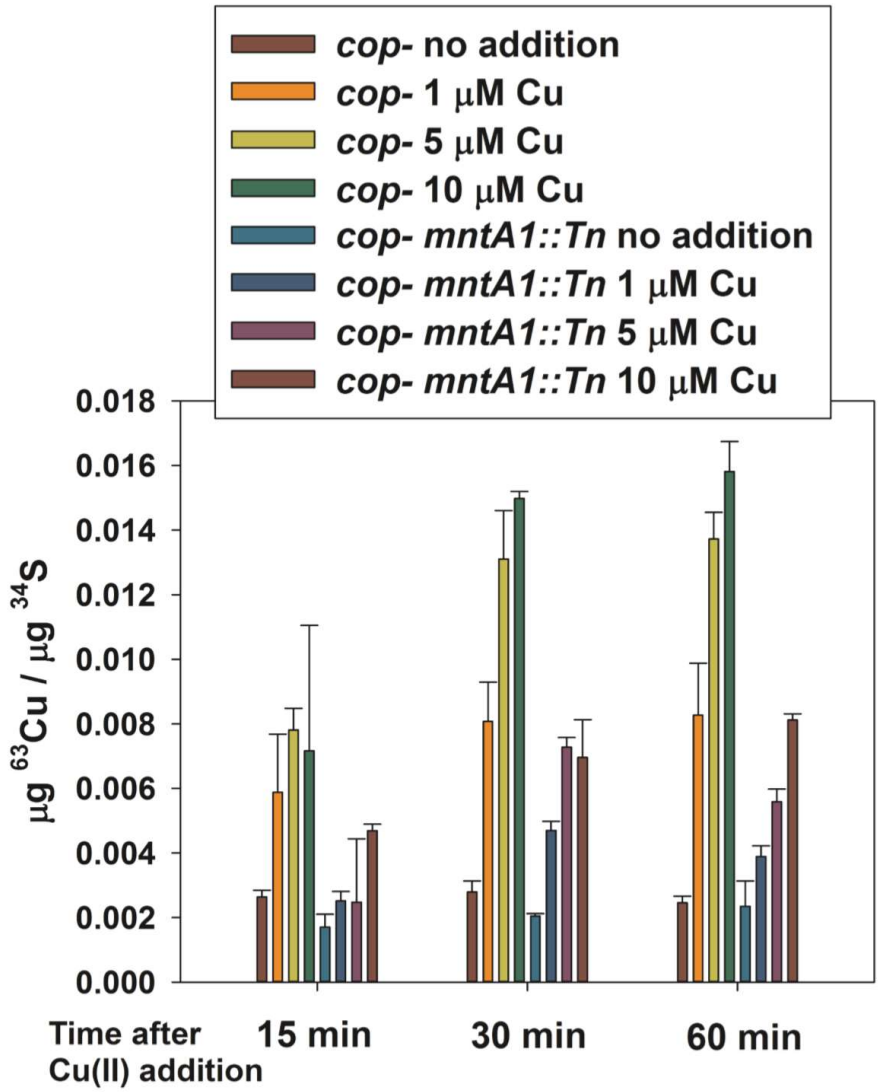

Figure 2.4: The *cop- mntA1::Tn* strain accumulate less copper post challenge.

Cultures of *cop-* (JMB8573) and *cop- mntA1::Tn* mutant (JMB8914) were subclustered into chelated TSB for 8 hours and challenged with 1,5, and 10 μM copper (II). Samples were incubated for an additional 15, 30, or 60 minutes before harvesting and determining copper load by ICP-MS.

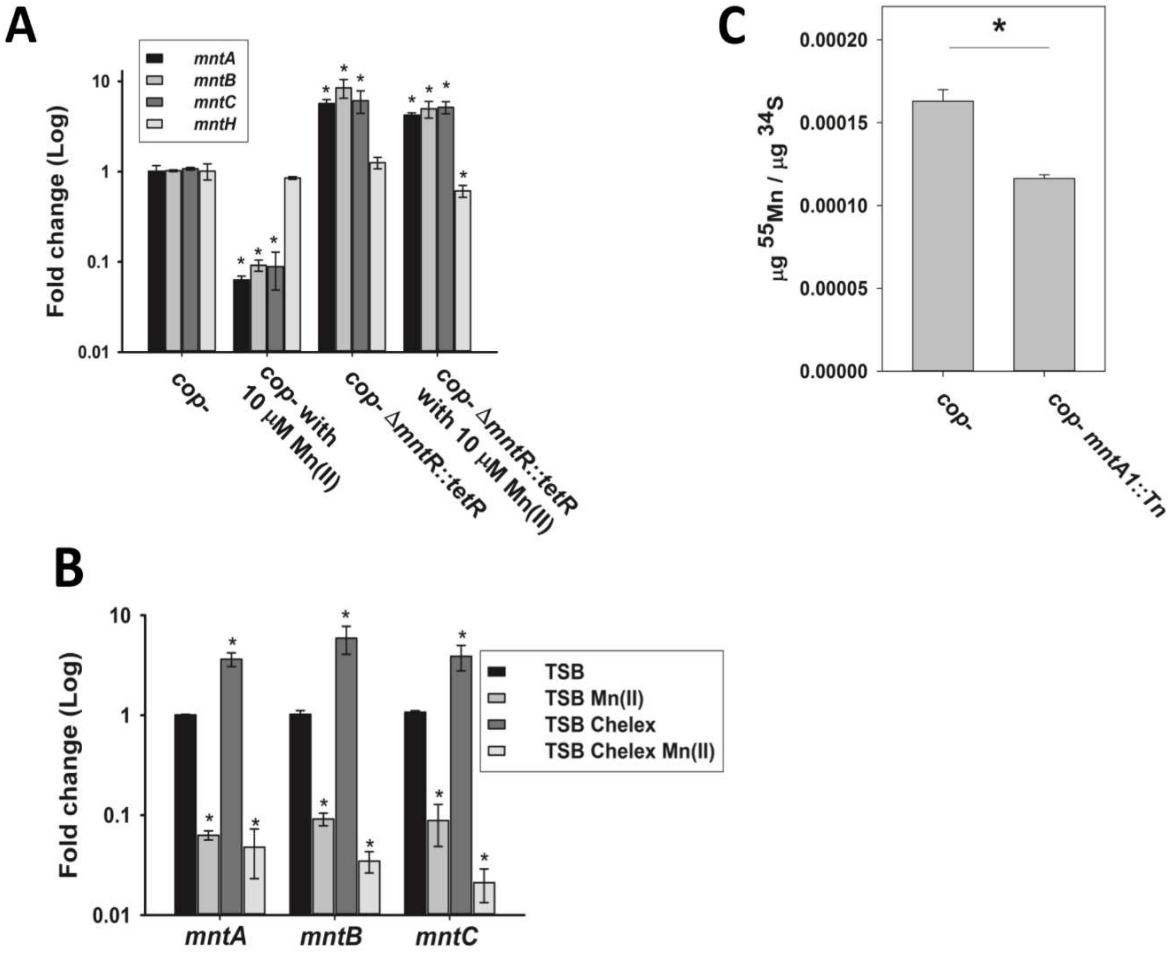

Figure 2.5: MntR represses transcription of the *mntABC* in a manganese-dependent manner. Panel A; MntR represses transcription of *mntABC*, but not *mntH*, in manganese (II) replete conditions. The data show fold-induction of *mntA*, *mntB*, *mntC*, and *mntH* in the *cop*- (JMB8573) and *cop*- Δ*mntR::tetR* (JMB9151) strains. The strains were cultured in TSB with and without 10 μM manganese (II) before RNA was isolated and transcripts quantified. Panel B; Data represent fold-induction of *mntA*, *mntB*, and *mntC* in the *cop*- (JMB8573) strain after culture in TSB, TSB with 10 μM manganese (II), Chelex treated TSB, or Chelex treated TSB

with 10 μM manganese (II). Panel C; The *cop- mntA1::Tn* strain accumulates less manganese than the *cop-* strain. Total manganese was quantified in the *cop-* (JMB8573) and *cop- mntA1::Tn* (JMB8914) strains using ICP-MS after the strains were cultured for 8 hours in Chelex-treated TSB. The data presented in Panels A, B, and C represent the average of biological triplicates with errors presented as standard deviations. Paired student t-tests were performed on the samples and N.S. denotes not significant ($p > 0.1$) and * denotes $p \leq 0.05$.

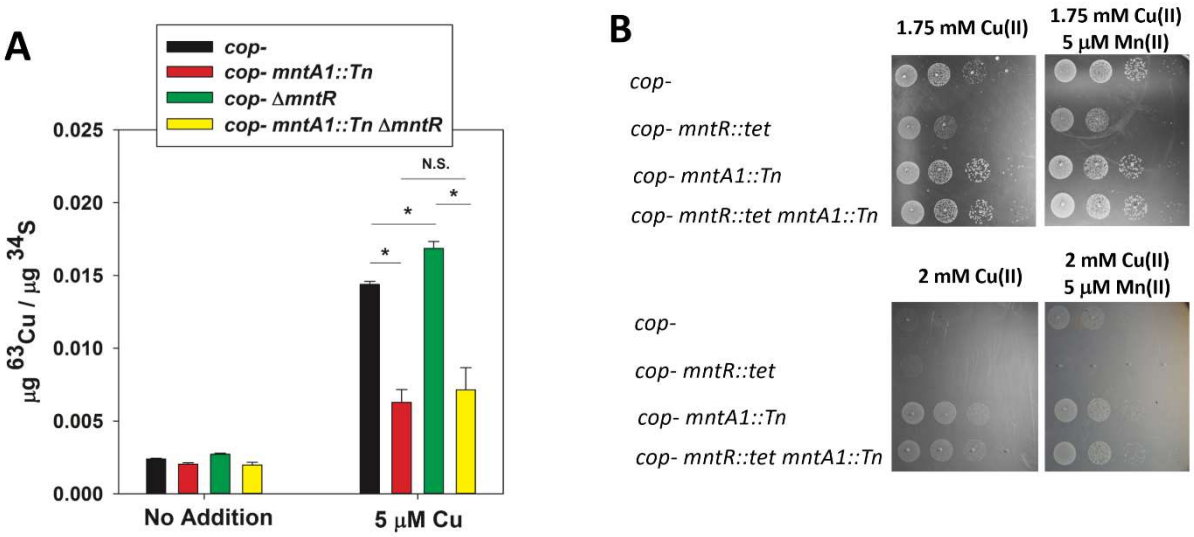

Figure 2.6: Derepression of the mntABC operon results in an increased copper load and copper sensitivity. Panel A; the *cop-* (JMB8573), *cop- mntA1::Tn* (JMB8914), *cop-* Δ*mntR::tet* (JMB9151), and *cop-* Δ*mntR::tet mntA1::Tn* (JMB99244) strains were cultured in Chelex-treated TSB for 8 hours before challenge with 5 µM copper for 60 minutes before harvesting and quantifying total copper loads using ICP-MS. Panel B; *cop-* (JMB8573), *cop- mntA1::Tn* (JMB8914), *cop-* Δ*mntR::tet* (JMB9151), and *cop-* Δ*mntR::tet mntA1::Tn* (JMB9244) strains were spot plated on solid TSB medium with 1.7 or 2 mM copper and 0 or 5 µM manganese.

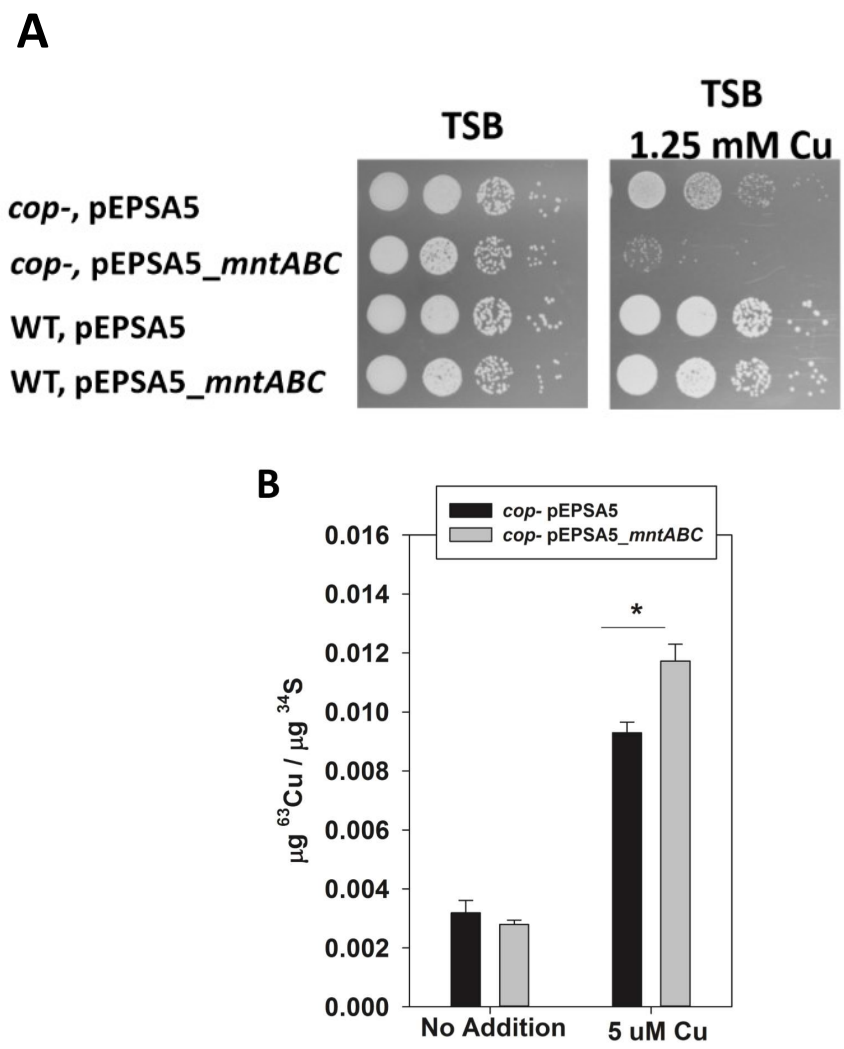

Figure 2.7: Over-production of MntABC increases sensitivity to copper and increases the cellular copper load. Panel A; the *cop-* pEPSA5 (JMB9062) , *cop-* pEPSA5_*mntABC* (JMB9397), WT pEPSA5 (JMB1304), and WT pEPSA5_*mntABC* (JMB9478) overnight cultures were serial diluted and spot platted on TSB solid media containing 0.08 % xylose with and without 1.25 mM copper (II). Panel B; the *cop-* pEPSA5 (JMB9062) and *cop-* pEPSA5_*mntABC* (JMB9397) strains were grown in Chelex-treated TSB for 8 hours before challenge with 5 µM copper (II) for 15 min. Cells were harvested and copper quantified using ICP-MS.

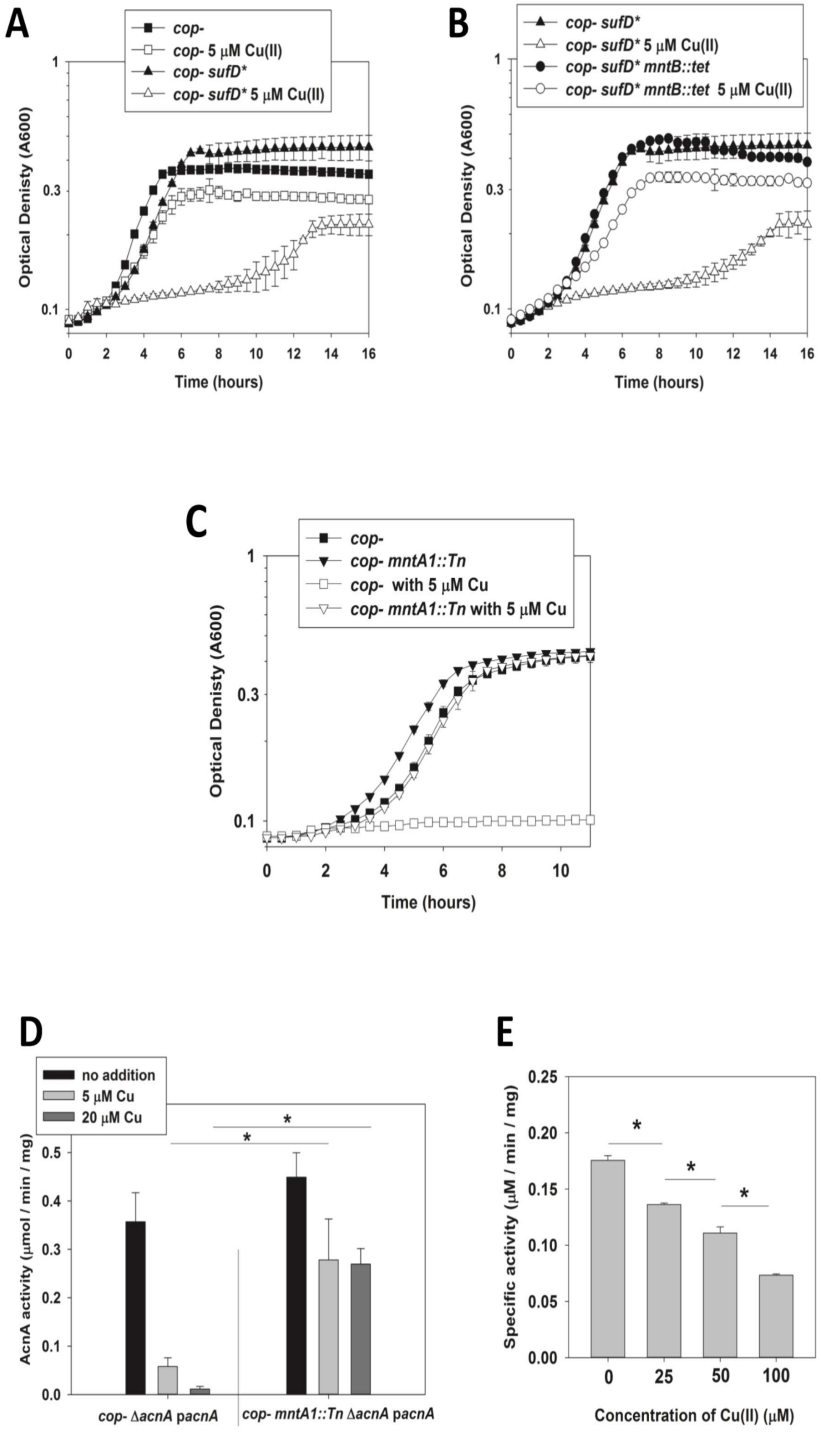

Figure 2.8: Defective MntABC protects iron-sulfur proteins from copper poisoning. Panel A; Growth of the *cop-* (JMB8573) and *cop- sufD** (JMB8625) strains were monitored in defined medium in the presence and absence of 5 μM

copper (II). Panel B; Growth of the *cop- sufD** (JMB8625) *cop- sufD** Δ*mntB::tetR* (JMB9604) strains was monitored in defined medium in the presence and absence of 5 μM copper (II). Growth in panels A and B was monitored in chemically defined media containing 20 amino acids (AA) supplemented with lipoic acid. The data represent the average of biological duplicates and error is expressed as standard deviations. Panel C; Growth of the *cop-* (JMB8573) and *cop- mntA1::Tn* (JMB8914) strains in defined medium containing 18 amino acid medium lacking leucine and isoleucine with and without 5 μM copper (II). Panel D; AcnA activity was monitored in cell-free lysates from the *cop- acnA::tetR* and *cop- acnA::tetR mntA1::Tn* strains containing p*acnA* (JMB9320 and JMB9517) after culture in presence of 0-20 μM copper (II). Panel E. AcnA activity was monitored in cell-lysates generated from the *cop-* strain growth without copper. The lysates were treated with copper before assaying AcnA. The data in panels A-C represent the average of biological duplicates with error expressed as standard deviations. The data in panels D and E represent the average of biological triplicates with error expressed as standard deviations. Paired student t-tests were performed on the samples in D and E and N.S. denotes not significant ($p > 0.1$) and * denotes $p \leq 0.05$.

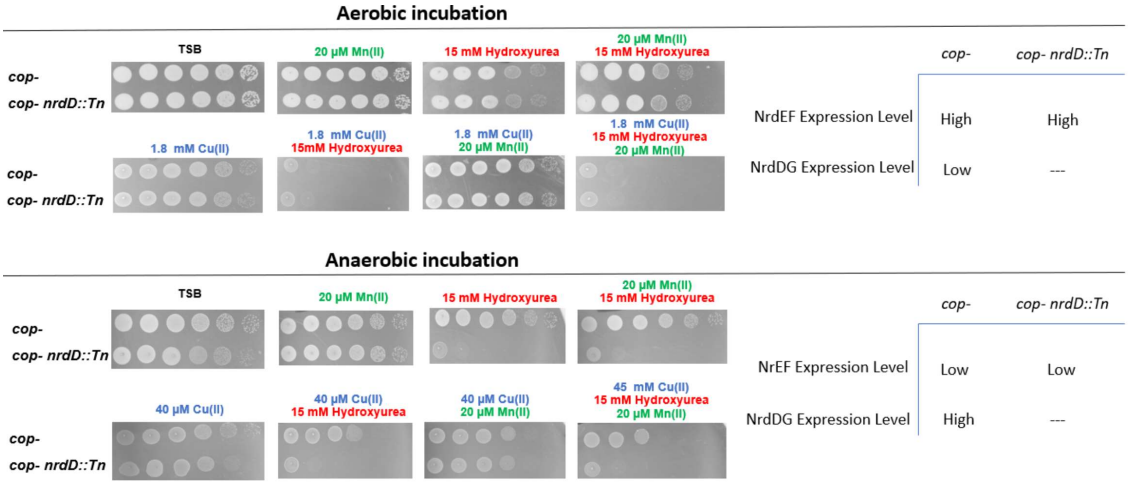

Figure 2.9: Effect of copper and hydroxyurea on cell growth. The *cop-* (JMB8573) and *cop- nrdD::Tn* (JMB8804) strains were spot plated on TSB plates containing combinations of copper, hydroxyurea, and manganese. Plates were then incubated aerobically and anaerobically. The diagram of the right side depicts predicted expression levels based on previous studies (Cotruvo and Stubbe 2012; Rabinovitch et al. 2010).

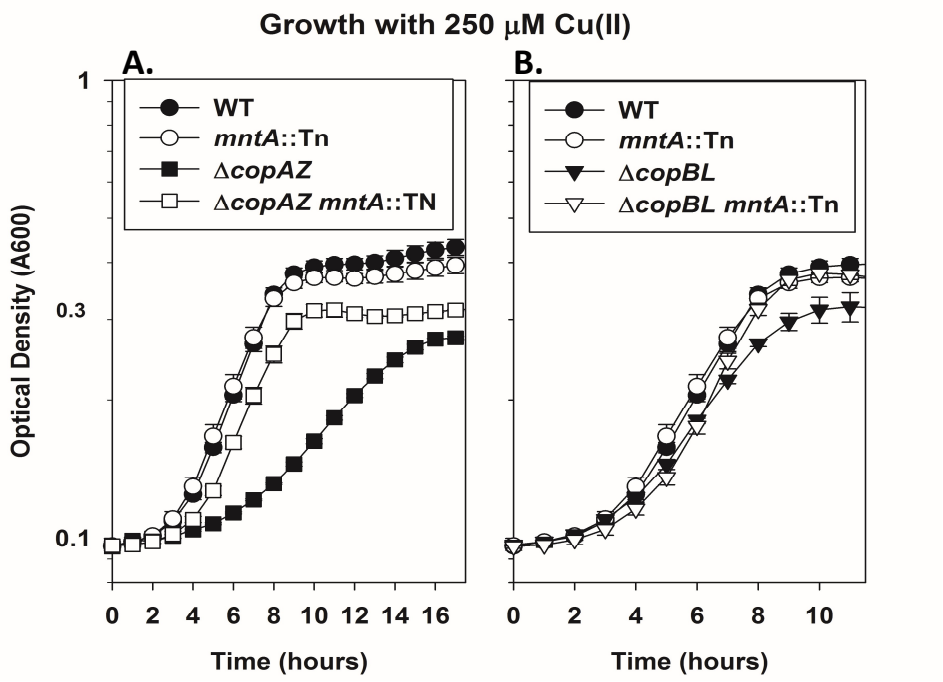

Figure 2.10: *copAZ*, but not *copBL* protects cells from MntABC-dependent copper intoxication. Panel A; copper sensitivity of *S. aureus* strains lacking copper detoxification systems. WT (JMB1100), *mntA1:Tn* (JMB9313), Δ*copAZ* (JMB8571), Δ*copAZ mntA1::Tn* (JMB9620). Panel B; WT (JMB1100), *mntA1:Tn* (JMB9313) Δ*copBL* (JMB7901), and Δ*copBL mntA1::Tn* (JMB9621). Strains were monitored in defined medium in the presence and absence of 250 μM copper (II). Growth in panels A and B was monitored in chemically defined media containing 20 amino acids (AA) supplemented with lipoic acid. The data represent the average of biological duplicates and error is expressed as standard deviations.

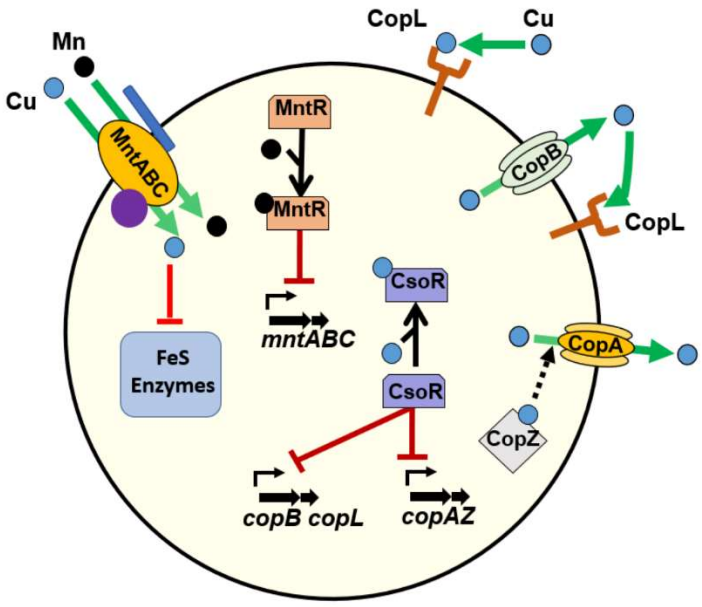

Figure 2.11: Working model for copper ion homeostasis in *Staphylococcus aureus*. Under manganese deplete conditions, MntR derepresses *mntABC* transcription and MntABC is expressed. Copper enters *S. aureus* cells through the MntABC manganese (II) importer. Once the copper ions have entered the cell they are sensed by the CsoR transcriptional regulator. Copper association with CsoR results in derepression of the *copAZ* and *copBL* operons. CopA and CopB function as copper (I) export systems. CopZ acts as an intracellular copper (I) binding protein that buffers the cytosol from copper toxicity. Holo-CopZ traffics copper (I) to CopA for export. After export by CopA or CopB, or before copper enters the cell, CopL binds to copper (I) and prevents it from (re)entering.

Concluding remarks and future directions

This study was initiated to investigate essential elements for survival at the host-pathogen interface. Fe-S cluster biogenesis targeting and utilizing copper toxicity are promising therapeutic approaches against pathogens including *S. aureus* (Summarized in Figure-D.1, D.2)

The ability of *S. aureus* to continuously evolve antibiotic resistance signify the need to investigate alternative therapeutic targets. Iron-sulfur clusters are necessary for almost all pathogens. The work presented in chapter-1 elucidated that Suf-dependent Fe-S cluster biosynthesis is essential for *S. aureus* pathogenicity and survival. Disruption of this pathway had broad metabolic anomalies and reduced survival upon challenge with human PMNs. Consequently, it is of interest to identify potential Suf pathway inhibitors and for further characterization of Fe-S cluster assembly in *S. aureus*. Metals such as copper and ROS can target Fe-S related processes. This can be exploited further by investigating the effects of engineered antimicrobials that selectively disturb metals homoeostasis and ROS mitigation.

S. aureus can form small colony variants strains that can persist in infection settings. These strains can avoid immune responses and antibiotics and may retain infection intracellularly (Ellington et al. 2006; Garzoni and Kelley 2009). Consequently, the Fe-S therapeutic approach should consider the nature of the infection and the ability of the Fe-S targeting molecule to penetrate to the site of infection. Several FDA approved drugs can generate ROS or NOS stresses (reviewed by (Vernis et al. 2017). These compounds could be exploited further or

modified to selectively toxify cells by targeting Fe-S protein maturation. Moreover, Fe-S protein maturation can be targeted aerobically and anaerobically by metals such as copper which widens the scope of Fe-S targeting strategies.

Studies investigated Fe-S targeting compounds that affect ROS (Huang et al. 2016; Chen et al. 2011), Fe-S biogenesis (Choby et al. 2016), Fe-S trafficking, and dysregulation of microbes Fe-S levels sensing (for example ROS produced by cellular respiratory modulates Fe-S Cluster sensitivity to primaquine (Lalève et al. 2015). Therefore, shifting the physiology of the pathogen to relay more on Fe-S related processes and concurrently targeting Fe-S systems could attenuate the infection.

The Suf components are distant from the Fe-S machinery of eukaryotes (reviewed in (Dellibovi-Ragheb etal. 2013; Lill 2009).Therefore, targeting Fe-S synthesis or Fe-S containing proteins in bacteria is an advantageous approach. Combining Fe-S biogenesis inhibitors or Fe-S targeting compounds with other conventional therapeutic approaches could have a synergic effect and improve the prognosis of infection. Clinical trials in animal models of infection could further elucidate the synergy of Suf targeting therapy with conventional antibiotics and immune responses. In our lab, we started to test FDA approved library of medications against Suf deficient strains hoping to find a chemical that selectively inhibits the Suf pathway. However, due to time constrains and the limited amount of provided chemicals, we were unable to finish this project. Determining an already approved FDA chemical can speed the process of releasing this medicine to clinical use. In collaboration with others, our lab investigated new molecules that

target Fe-S assembly (Choby et al. 2016). Metals and metal-complexes are potential antimicrobial alternatives or to supplement conventional antibiotics treatment. Copper, aluminum (Singh et al. 2005), and cobalt (Ranquet et al. 2007; Thorgersen and Downs 2007) can be a promising Fe-S protein targeting metals. Other metals have been shown to target Fe-S cluster requiring dehydratases including silver(I), mercury (II), cadmium(II), and zinc(II) (Xu and Imlay 2012). Due to their toxic effects on the host, developing a special metals delivery system to the site of infection is essential.

The work in chapter 2 elucidated a novel copper killing mechanism in response to manganese deficiencies. Both metals are essential for many cellular processes. Copper (Cu) is an ancient antimicrobial compound and has been used as intrinsic antimicrobial to prevent the growth of microbes including *S. aureus*. The data presented can be utilized in the treatment and prevention efforts. Copper homeostasis is a promising alternative therapy against pathogens. Cells have more tolerance to manganese compared to copper which is maintained at very low levels inside cells. To moderate copper entrance through MntABC, it is reasonable to propose that *S. aureus* evolved two copper exporting systems. Limiting manganese and dosing with copper is a promising approach. Strains deficient in copper defenses are more susceptible to macrophage killing (White et al. 2009; Johnson et al. 2015a).

Our data suggest that copper targets both Fe-S proteins and probably Fe-S biogenesis processes. *S. aureus* utilizes the SufCDSUB machinery for building

Fe-S cofactors. It would be interesting to test if copper binds to SufCDSUB components and disrupt their binding characteristics.

Utilizing engineered chemical molecules that selectively disrupt the efficacy of copper exporting or detoxification proteins could increase the efficacy of copper-dependent killing mechanisms of the host. Similarly, disruption of manganese sensing and derepressing uptake of copper through MntABC could pose prognostic advantages for anti-microbial resistance pathogens. Under the growth conditions we utilized, we noticed that *mntH* and *mntR* mutants are sensitive to copper because *mntABC* is most likely de-repressed in these strains. Deletion of *mntH* decreased *S. aureus* burden in mice liver (Kehl-Fie et al. 2013). Copper and other metals can bind to MntR with variable affinities and modulate its DNA binding kinetics (Lieser et al. 2003; Golynskiy et al. 2006). Therefore, disturbing manganese-copper homeostasis and MntR metals binding selectivity is a valid research approach.

Iron and manganese homeostasis are overlapping (Grunenwald et al. 2019; Lieser et al. 2003; Horsburgh et al 2001a). Some importers are thought to have a bifunctional activity for manganese and iron (Dashper et al. 2005; Cartron et al. 2006). The ICPMS analysis showed that MntA mutant had less iron load compared to *cop*- strain (Data not shown). MntR and Fur are key metals regulators and they cross-regulate numerous genes. Although they are recognized for manganese and iron uptake regulation, they can bind other metals including copper (Lorenzo et al. 1987; Mills and Marletta 2005; Lieser et al. 2003). Mutating either one of these regulators increased sensitivity to copper (data not shown). It would be interesting

to build and test a transposon library in mutants lacking these major regulators to further understand the connections between the systems involved in copper, manganese, and iron homeostasis. Furthermore, Ferric uptake regulator controls Fe-S related processes through the iron-sparing-response, which permits the cell to arrange iron usage by reducing the synthesis of less important iron-containing proteins (Smaldone et al. 2012). Copper theoretically can bind to Ferric uptake regulator or MntR and change their binding regulons. It would be interesting to investigate this possibility.

Transposon analysis showed that seven strains had mutations in *ispA*, which encodes a geranylgeranyl diphosphate synthase II, and one strain had a mutation in *apt*, which encodes a predicted adenine phosphoribosyltransferase. Mutations in *ispA* and *apt* decreased *S. aureus* sensitivity to copper. Our lab is currently investigating the molecular mechanism of these two genes in copper resistance. There is no enough information about the functions of *apt* except its relatedness to purine nucleotide metabolism. It has been shown that *ispA* abrogation in *S. aureus* caused changes in the regulation of numerous genes of which many are related to cell envelop structure such as lipoproteins and fatty acids. The composition of fatty acids in cell envelope was towards longer fatty acids and increased membrane fluidity (Krute et al. 2015). Copper can cause membrane depolarization and lipids peroxidation. It would be interesting to measure the membrane fluidity and lipids profile of *ispA* mutant and link it to copper toxicity. This can be tested by the addition of selected fatty acids to media containing copper and/or genetic additivity of *ispA* mutant with fatty acids

pathways. Once confirmed, IspA overexpression should lead to less copper uptake which should be consistent with membrane fatty acids architecture restoration. Fatty acids analysis and membrane fluidity probe 1,6-diphenyl-1,3,5-hexatriene (DPH) can verify results.

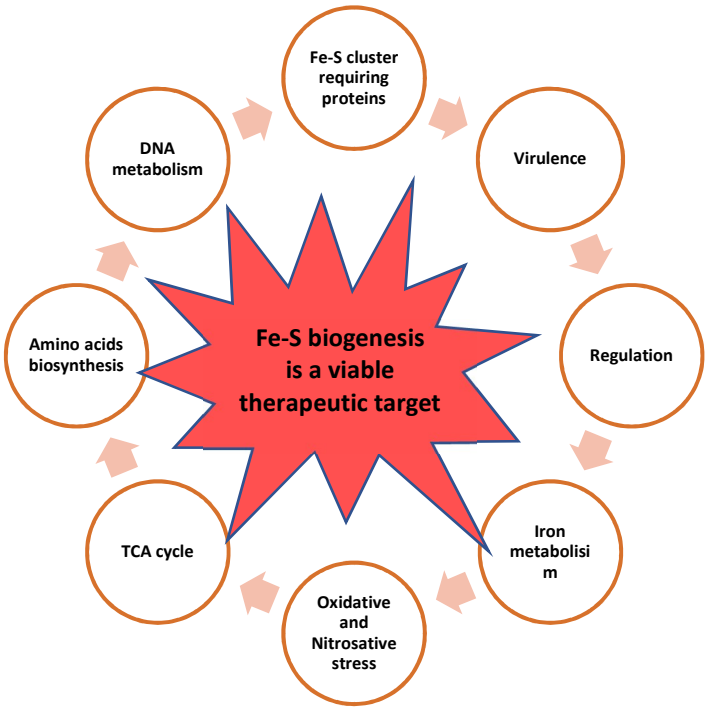

Figure-D-1: Fe-S biogenesis is a viable therapeutic target

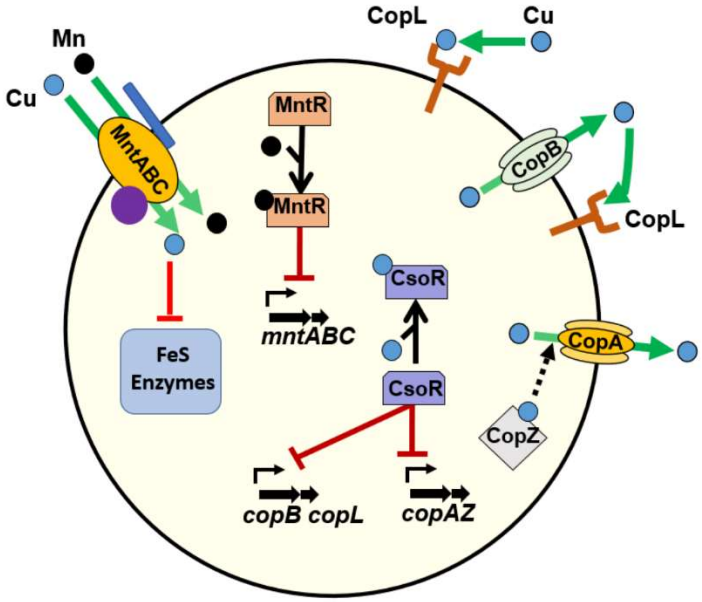

Figure-D-2: Proposed models for copper toxicity and metal ion homeostasis: Altered MntABC activity influences sensitivity to copper.

References:

Achard MES, Stafford SL, Bokil NJ, Chartres J, Bernhardt P V, Schembri MA, Sweet MJ, McEwan AG (2012) Copper redistribution in murine macrophages in response to *Salmonella* infection. Biochem *J* 444:51–7 .

Ahuja S, Rougé L, Swem DL, Sudhamsu J, Wu P, Russell SJ, Alexander MK, Tam C, Nishiyama M, Starovasnik MA, Koth CM (2015) Structural analysis of bacterial ABC transporter inhibition by an antibody fragment. Structure 23:713–723

Akerley BJ, Rubin EJ, Novick VL, Amaya K, Judson N, Mekalanos JJ (2002) A genome-scale analysis for identification of genes required for growth or survival of *Haemophilus influenzae*. Proc Natl Acad Sci U S A 99:966–71 .

Altschul SF, Gish W, Miller W, Myers EW, Lipman DJ (1990) Basic local alignment search tool. J Mol Biol 215:403–410 .

Anderson AS, Scully IL, Timofeyeva Y, Murphy E, McNeil LK, Mininni T, Nuñez L, Carriere M, Singer C, Dilts DA, Jansen KU (2012) *Staphylococcus aureus* manganese transport protein C is a highly conserved cell surface protein that elicits protective immunity against *S. aureus* and *Staphylococcus epidermidis*. J Infect Dis 205:1688–96

Ando M, Manabe YC, Converse PJ, Miyazaki E, Harrison R, Murphy JR, Bishai WR (2003) Characterization of the role of the divalent metal ion-dependent transcriptional repressor MntR in the virulence of *Staphylococcus aureus*. Infect Immun 71:2584–90 .

Andreini C, Banci L, Bertini I, Rosato A (2008) Occurrence of Copper Proteins through the Three Domains of Life: A Bioinformatic Approach. J Proteome Res 7:209–216 .

Anjem A, Imlay JA (2012) Mononuclear iron enzymes are primary targets of hydrogen peroxide stress. J Biol Chem 287: 15544–56.

Arce Miranda JE, Sotomayor CE, Albesa I, Paraje MG (2011) Oxidative and nitrosative stress in *Staphylococcus aureus* biofilm. FEMS Microbiol Lett 315:23–29 .

Archibald FS, Duong MN (1984) Manganese acquisition by *Lactobacillus plantarum*. J Bacteriol 158:1–8.

Argüello JM, Eren E, González-Guerrero M (2007) The structure and function of heavy metal transport P1B-ATPases. BioMetals 20:233–48.

Baba T, Ara T, Hasegawa M, Takai Y, Okumura Y, Baba M, Datsenko KA, Tomita M, Wanner BL, Mori H (2006) Construction of *Escherichia coli* K-12 in-frame, single-gene knockout mutants: The Keio collection. Mol Syst Biol 2: 2006.0008.

Bachman MA, Breen P, Deornellas V, Mu Q, Zhao L, Wu W, Cavalcoli JD, Mobley HLT (2015) Genome-wide identification of *Klebsiella pneumoniae* fitness

genes during lung infection. MBio 6:e00775 .

Bae, T., Banger, A. K., Wallace, A., Glass, E. M., Aslund, F., Schneewind, O., and Missiakas, D. M. (2004) *Staphylococcus aureus* virulence genes identified by bursa aurealis mutagenesis and nematode killing. Proc Natl Acad Sci U S A 101: 12312-12317

Bae T, Glass EM, Schneewind O, Missiakas D (2008) Generating a collection of insertion mutations in the *Staphylococcus aureus* genome using *bursa aurealis*. Methods in molecular biology 416:103–116.

Bags A, Neilands JB (1987) Ferric uptake regulation protein acts as a repressor, employing iron(ii) as a cofactor to bind the operator of an iron transport operon in *Escherichia coli*. Biochemistry 26:5471–5477 .

Baker J, Sengupta M, Jayaswal RK, Morrissey JA (2011) The *Staphylococcus aureus* CsoR regulates both chromosomal and plasmid-encoded copper resistance mechanisms. Environ Microbiol 13:2495–2507 .

Baker J, Sitthisak S, Sengupta M, Johnson M, Jayaswal RK, Morrissey JA (2010) Copper stress induces a global stress response in *Staphylococcus aureus* and represses *sae* and *agr* expression and biofilm formation. Appl Environ Microbiol 76:150–60 .

Ballal A, Manna AC (2010) Control of thioredoxin reductase gene (*trxB*) transcription by SarA in *Staphylococcus aureus*. J Bacteriol 192:336–45 .

Barras F, Loiseau L, Py B (2005) How *Escherichia coli* and *Saccharomyces cerevisiae* build Fe/S Proteins. Adv Microb Physiol 50:41–101.

Barrett FF, McGehee RF, Finland M (1968) Methicillin-resistant *Staphylococcus aureus* at Boston City Hospital: Bacteriologic and epidemiologic observations. N Engl J Med 279: 441–48.

Bartlett AH, Hulten KG (2010) *Staphylococcus aureus* pathogenesis. Pediatr Infect Dis J 29:860–861 .

Beasley FC, Vinés ED, Grigg JC, Zheng Q, Liu S, Lajoie GA, Murphy MEP, Heinrichs DE (2009) Characterization of staphyloferrin A biosynthetic and transport mutants in *Staphylococcus aureus*. Mol Microbiol 72:947–963 .

Becker KW, Skaar EP (2014) Metal limitation and toxicity at the interface between host and pathogen. FEMS Microbiology Reviews 38(6): 1235-249.

Begg SL (2019) The role of metal ions in the virulence and viability of bacterial pathogens. Biochem Soc Trans 47 (1): 77–87.

Beinert H (2000) Iron-sulfur proteins: Ancient structures, still full of surprises. J. Biol. Inorg. Chem *5:2–15.*

Beinert, H., Kennedy, M. C., and Stout, C. D. (1996) Aconitase as iron-sulfur protein, enzyme, and iron-regulatory protein. *Chemical reviews* **96**, 2335-2373.

Beveridge SJ, Garrett IR, Whitehouse MW, Vernon-Roberts B, Brooks PM (1985) Biodistribution of 64Cu in inflamed rats following administration of two anti-inflammatory copper complexes. Agents Actions 17 (1): 104–11.

Blevins JS, Beenken KE, Elasri MO, Hurlburt BK, Smeltzer MS (2002) Strain-dependent differences in the regulatory roles of *sarA* and *agr* in *Staphylococcus aureus*. Infect Immun 70:470–80 .

Boles BR, Horswill AR (2008) *agr*-Mediated dispersal of *Staphylococcus aureus* Biofilms. PLoS Pathog 4:e1000052 .

Boles BR, Thoendel M, Roth AJ, Horswill AR (2010) Identification of genes Involved in polysaccharide-Independent *Staphylococcus aureus* Biofilm Formation. PLoS One 5:e10146 .

Bolzán AD, Bianchi MS (2001) Genotoxicity of streptonigrin: a review. Mutat Res Mutat Res 488:25–37.

Borremans B, Hobman JL, Provoost A, Brown NL, Van Der Lelie D (2001) Cloning and functional analysis of the *pbr* lead resistance determinant of *Ralstonia metallidurans* CH34. J Bacteriol 183 (19): 5651–58.

Bose JL, Fey PD, Bayles KW (2013) Genetic Tools to enhance the study of gene function and regulation in *Staphylococcus aureus*. Appl Environ Microbiol 79:2218 .

Boyd ES, Thomas KM, Dai Y, Boyd JM, Outten FW (2014) Interplay between oxygen and Fe–S cluster biogenesis: Insights from the Suf pathway. Biochemistry 53:5834–5847 .

Brancaccio D, Gallo A, Piccioli M, Novellino E, Ciofi-Baffoni S, Banci L (2017) [4Fe-4S] cluster assembly in mitochondria and its impairment by copper. J Am Chem Soc 139(2):719–30.

Carr AL, Daley MJ, Givens Merkel K, Rose DT (2018) Clinical utility of methicillin-resistant *Staphylococcus aureus* nasal screening for antimicrobial stewardship: a review of current literature. Pharmacother J Hum Pharmacol Drug Ther 38:1216–1228 .

Cartron ML, Maddocks S, Gillingham P, Craven CJ, Andrews SC (2006) Feo - transport of ferrous iron into bacteria. BioMetals 19:143–157

Cervantes-Cervantes MP, Víctor Calderón-Salinas J, Albores A, Luis Muñoz-Sánchez J (2005) Copper increases the damage to DNA and proteins caused by reactive oxygen species. Biological Trace Element Research 103 (3): 229–48.

Chahal HK, Outten FW (2012) Separate FeS scaffold and carrier functions for SufB2C2 and SufA during *in vitro* maturation of [2Fe2S] Fdx. J Inorg Biochem 116:126–134 .

Chandrangsu P, Helmann JD, Fuangthong M, Helmann J, Helmann J, Stocks C (2016) Intracellular Zn(II) Intoxication Leads to Dysregulation of the PerR Regulon Resulting in Heme Toxicity in *Bacillus subtilis*. PLOS Genet

12:e1006515 .

Chandrangsu P, Rensing C, Helmann JD (2017) Corrigendum: Metal homeostasis and resistance in bacteria. Nat Rev Microbiol 15:379–379.

Changela A, Chen K, Xue Y, Holschen J, Outten CE, O'Halloran T V, Mondragon A (2003) Molecular basis of selectivity and sensitivity in metal-ion recognition by CueR. Science (80-) 301:1383–1387

Chaturvedi KS, Hung CS, Crowley JR, Stapleton AE, Henderson JP (2012) The siderophore yersiniabactin binds copper to protect pathogens during infection. Nat Chem Biol 8:731–36 .

Chaudhuri RR, Allen AG, Owen PJ, Shalom G, Stone K, Harrison M, Burgis TA, Lockyer M, Garcia-Lara J, Foster SJ, Pleasance SJ, Peters SE, Maskell DJ, Charles IG (2009) Comprehensive identification of essential *Staphylococcus aureus* genes using Transposon-Mediated Differential Hybridisation (TMDH). BMC Genomics 10:291.

Chen G, Chen Z, Hu Y, Huang P (2011) Inhibition of mitochondrial respiration and rapid depletion of mitochondrial glutathione by β-phenethyl isothiocyanate: mechanisms for anti-leukemia activity. Antioxid Redox Signal 15:2911–21 .

Chillappagari S, Seubert A, Trip H, Kuipers OP, Marahiel MA, Miethke M (2010) Copper stress affects iron homeostasis by destabilizing iron-sulfur cluster formation in *Bacillus subtilis*. J Bacteriol 192:2512–24 .

Choby JE, Mike LA, Mashruwala AA, Dutter BF, Dunman PM, Sulikowski GA, Boyd JM, Skaar EP (2016) A small-molecule inhibitor of iron-sulfur cluster assembly uncovers a link between virulence regulation and metabolism in *Staphylococcus aureus*. Cell Chem Biol 23:1351–1361 .

Clauditz A, Resch A, Wieland K-P, Peschel A, Götz F (2006) Staphyloxanthin plays a role in the fitness of *Staphylococcus aureus* and its ability to cope with oxidative stress. Infect Immun 74:4950–3 .

Cockayne A, Hill PJ, Powell NB, Bishop K, Sims C, Williams P (1998) Molecular cloning of a 32-kilodalton lipoprotein component of a novel iron-regulated *Staphylococcus epidermidis* ABC transporter. Infect Immun 66:3767–74

Corbin BD, Seeley EH, Raab A, Feldmann J, Miller MR, Torres VJ, Anderson KL, Dattilo BM, Dunman PM, Gerads R, Caprioli RM, Nacken W, Chazin WJ, Skaar EP (2008) Metal chelation and inhibition of bacterial growth in tissue abscesses. Science 319:962–965 .

Cosgrove SE, Sakoulas G, Perencevich EN, Schwaber MJ, Karchmer AW, Carmeli Y (2003) comparison of mortality associated with methicillin-resistant and methicillin-susceptible *Staphylococcus aureus* bacteremia: A meta-analysis. Clin Infect Dis 36:53–59 .

Cotruvo JA, Stubbe J (2012) Metallation and mismetallation of iron and manganese proteins *in vitro* and *in vivo*: The class i ribonucleotide reductases as a case study. Metallomics 4: 1020– 1036.

Dashper SG, Butler CA, Lissel JP, Paolini RA, Hoffmann B, Veith PD, O'Brien-Simpson NM, Snelgrove SL, Tsiros JT, Reynolds EC (2005) A novel *Porphyromonas gingivalis* FeoB plays a role in manganese accumulation. J Biol Chem 280:28095–102 .

Daum RS (2007) clinical practice Skin and Soft-Tissue Infections Caused by Methicillin-Resistant *Staphylococcus aureus.* N Engl J Med. 357: 380-390.

David MZ, Daum RS (2010) Community-Associated Methicillin-Resistant *Staphylococcus aureus*: Epidemiology and Clinical Consequences of an Emerging Epidemic. Clin Microbiol Rev 23:616–687 .

DeGraff W, Hahn SM, Mitchell JB, Krishna MC (1994) Free radical modes of cytotoxicity of adriamycin® and streptonigrin. Biochem Pharmacol 48:1427–1435 .

delCardayre SB, Stock KP, Newton GL, Fahey RC, Davies JE (1998) Coenzyme A disulfide reductase, the primary low molecular weight disulfide reductase from *Staphylococcus aureus*. Purification and characterization of the native enzyme. J Biol Chem 273:5744–51 .

Dellibovi-Ragheb TA, Gisselberg JE, Prigge ST (2013) Parasites FeS up: iron-sulfur cluster biogenesis in eukaryotic pathogens. PLoS Pathog 9:e1003227.

Dembek M, Barquist L, Boinett CJ, Cain AK, Mayho M, Lawley TD, Fairweather NF, Fagan RP (2015) High-throughput analysis of gene essentiality and sporulation in *Clostridium difficile*. MBio 6:e02383 .

den Heijer CD, van Bijnen EM, Paget WJ, Pringle M, Goossens H, Bruggeman CA, Schellevis FG, Stobberingh EE (2013) Prevalence and resistance of commensal *Staphylococcus aureus*, including meticillin-resistant *S. aureus*, in nine European countries: a cross-sectional study. Lancet Infect Dis 13:409–415 .

Diep BA, Gill SR, Chang RF, Phan TH, Chen JH, Davidson MG, Lin F, Lin J, Carleton HA, Mongodin EF, Sensabaugh GF, Perdreau-Remington F (2006) Complete genome sequence of USA300, an epidemic clone of community-acquired meticillin-resistant *Staphylococcus aureus*. Lancet 367:731–739 .

Djoko KY, Chong LX, Wedd AG, Xiao Z (2010) Reaction mechanisms of the Multicopper Oxidase CueO from *Escherichia coli* support its functional role as a cuprous oxidase. J Am Chem Soc 132:2005–2015 .

Djoko KY, McEwan AG (2013) Antimicrobial action of copper is amplified *via* inhibition of heme biosynthesis. ACS Chem Biol 8:2217–2223 .

Dollwet HHA, Sorenson JRJ (1985) Historic use of copper-compounds in medicine. Trace Elem Med 2 (2): 80–87.

Dougall DK (1974) Evidence for the presence of glutamate synthase in extracts of carrot cells cultures. Biochem Biophys Res Commun 58:639–646 .

Duan X, Yang J, Ren B, Tan G, Ding H (2009) Reactivity of nitric oxide with the [4Fe-4S] cluster of dihydroxyacid dehydratase from *Escherichia coli*. Biochem

J 417:783–9 .

DuMont AL, Yoong P, Surewaard BGJ, Benson MA, Nijland R, van Strijp JAG, Torres VJ (2013) *Staphylococcus aureus* elaborates leukocidin AB to mediate escape from within human neutrophils. Infect Immun 81:1830–41 .

Eidem TM, Lounsbury N, Emery JF, Bulger J, Smith A, Abou-Gharbia M, Childers W, Dunman PM (2015) Small-molecule inhibitors of *Staphylococcus aureus* RnpA-mediated RNA turnover and tRNA processing. Antimicrob Agents Chemother 59:2016–2028 .

Ekici S, Yang H, Koch H-G, Daldal F (2012) Novel Transporter Required for Biogenesis of cbb3-Type Cytochrome c Oxidase in Rhodobacter capsulatus. MBio 3: .

Ellington JK, Harris M, Hudson MC, Vishin S, Webb LX, Sherertz R (2006) Intracellular*Staphylococcus aureus* and antibiotic resistance: Implications for treatment of Staphylococcal osteomyelitis. J Orthop Res 24:87–93 .

Ellison RT (1994) The effects of lactoferrin on gram-negative bacteria. Adv Exp Med Biol 357:71–90.

Ezekiel Dh, Hutchins Je (1968) Mutations affecting RNA polymerase associated with rifampicin resistance in *Escherichia coli*. Nature 220:276–277 .

Fahey RC (2013) Glutathione analogs in prokaryotes . Biochim Biophys. Acta Gen 1830(5):3182–3198.

Fang Z, Dos Santos PC (2015) Protective role of bacillithiol in superoxide stress and Fe-S metabolism in *Bacillus subtilis*. Microbiologyopen 4:616–31 .

Festa RA, Thiele DJ (2011) Copper: An essential metal in biology. CURBIO 21:R877–R883 .

Fey PD, Endres JL, Yajjala VK, Widhelm TJ, Boissy RJ, Bose JL, Bayles KW (2013) A genetic resource for rapid and comprehensive phenotype screening of nonessential *Staphylococcus aureus* genes. MBio 4:e00537-12.

Fillat MF (2014) The *fur* (ferric uptake regulator) superfamily: Diversity and versatility of key transcriptional regulators. Arch Biochem Biophys 546:41–52.

Finney LA, O'Halloran T V (2003) Transition metal speciation in the cell: insights from the chemistry of metal ion receptors. Science 300:931–6 .

Flint DH, Emptage MH (1988) Dihydroxy acid dehydratase from spinach contains a [2Fe-2S] cluster. J Biol Chem 263:3558–3564.

Flint DH, Tuminello JF, Emptage MH (1993) The inactivation of Fe-S cluster containing hydro-lyases by superoxide. J Biol Chem 268:22369–22376 .

Forsyth RA, Haselbeck RJ, Ohlsen KL, Yamamoto RT, Xu H, Trawick JD, Wall D, Wang L, Brown-Driver V, Froelich JM, C. KG, King P, McCarthy M, Malone C, Misiner B, Robbins D, Tan Z, Zhu Z, Carr G, Mosca DA, Zamudio C, Foulkes JG, Zyskind JW (2002) A genome-wide strategy for the identification of essential genes in *Staphylococcus aureus*. Mol Microbiol 43:1387–1400 .

Friedman DB, Stauff DL, Pishchany G, Whitwell CW, Torres VJ, Skaar EP (2006) *Staphylococcus aureus* redirects central metabolism to increase iron availability. PLoS Pathog 2:e87.

Fu W, Handleyg SO, Cunninghamg RP, Johnson MK (1992) The role of the iron-sulfur cluster in *Escherichia coli* endonuclease III. A resonance raman study.. J Biol Chem 267:16135–16137.

Gaballa A, Helmann JD (2003) *Bacillus subtilis* CPx-type ATPases: characterization of Cd, Zn, Co and Cu efflux systems. Biometals 16: 497–505.

Gallagher LA, Ramage E, Jacobs MA, Kaul R, Brittnacher M, Manoil C (2007) A comprehensive transposon mutant library of *Francisella novicida*, a bioweapon surrogate. Proc Natl Acad Sci U S A 104:1009–1014.

Gallagher LA, Ramage E, Weiss EJ, Radey M, Hayden HS, Held KG, Huse HK, Zurawski D V, Brittnacher MJ, Manoil C (2015) Resources for genetic and genomic analysis of emerging pathogen *Acinetobacter baumannii*. J Bacteriol 197:2027–35 .

Garcia YM, Barwinska-Sendra A, Tarrant E, Skaar EP, Waldron KJ, Kehl-Fie TE (2017) A superoxide dismutase capable of functioning with iron or manganese promotes the resistance of *Staphylococcus aureus* to calprotectin and nutritional immunity. PLOS Pathog 13:e1006125 .

Gardner PR, Fridovich I (1991) Superoxide sensitivity of the *Escherichia coli* aconitase. J Biol Chem. 266 (29): 19328–33.

Garsin DA, Urbach J, Huguet-Tapia JC, Peters JE, Ausubel FM (2004) Construction of an *Enterococcus faecalis Tn917*-mediated-gene-disruption library offers insight into *Tn917* insertion patterns. J Bacteriol 186:7280–9 .

Garzoni C, Kelley WL (2009) *Staphylococcus aureus*: new evidence for intracellular persistence. Trends Microbiol 17:59–65 .

Gertz S, Engelmann S, Schmid R, Ziebandt AK, Tischer K, Scharf C, Hacker J, Hecker M (2000) Characterization of the *sigma*(B) regulon in *Staphylococcus aureus*. J Bacteriol 182:6983–91 .

Glasfeld A, Guedon E, Helmann JD, Brennan RG (2003) Structure of the manganese-bound manganese transport regulator of *Bacillus subtilis.* Nature structural biology.10: 652–657.

Golynskiy M V, Gunderson WA, Hendrich MP, Cohen SM (2006) Metal binding studies and EPR spectroscopy of the manganese transport regulator MntR. Biochemistry 45:15359–15372 .

Gralnick JA, Downs DM (2003) The YggX protein of *Salmonella enterica* is involved in Fe(ii) trafficking and minimizes the DNA damage caused by hydroxyl radicals. Residue CYS-7 is essential for YggX function. Journal of Biological Chemistry 278(23), 20708–20715.

Grass G, Franke S, Taudte N, Nies DH, Kucharski LM, Maguire ME, Rensing C (2005) The metal permease ZupT from *Escherichia coli* is a transporter with a

broad substrate spectrum. J Bacteriol 187:1604–1611 .

Grass G, Rensing C, Solioz M (2011) Metallic copper as an antimicrobial surface. Appl Environ Microbiol 77:1541–7 .

Gribenko A, Mosyak L, Ghosh S, Parris K, Svenson K, Moran J, Chu L, Li S, Liu T, Woods VL, Jansen KU, Green BA, Anderson AS, Matsuka Y V. (2013) Three-dimensional structure and biophysical characterization of *Staphylococcus aureus* cell surface antigen–manganese transporter MntC. J Mol Biol 425:3429–3445 .

Grosser MR, Paluscio E, Thurlow LR, Dillon MM, Cooper VS, Kawula TH, Richardson AR (2018) Genetic requirements for *Staphylococcus aureus* nitric oxide resistance and virulence. PLOS Pathog 14:e1006907 .

Grossi L, D'Angelo S (2005) Sodium nitroprusside: Mechanism of NO release mediated by sulfhydryl-containing molecules. J Med Chem 48:2622–2626 .

Grossoehme N, Kehl-Fie TE, Ma Z, Adams KW, Cowart DM, Scott RA, Skaar EP, Giedroc DP (2011) Control of copper resistance and inorganic sulfur metabolism by paralogous regulators in *Staphylococcus aureus*. J Biol Chem 286:13522–31 .

Grunenwald CM, Choby JE, Juttukonda LJ, Beavers WN, Weiss A, Torres VJ, Skaar EP, Sperandio V, Fey P (2019) Manganese detoxification by MntE is critical for resistance to oxidative stress and virulence of *Staphylococcus aureus*. MBio 10 (1).

Gu M, Imlay JA (2013) Superoxide poisons mononuclear iron enzymes by causing mismetallation. Mol Microbiol 89(1): 123–134.

Guan G, Pinochet-Barros A, Gaballa A, Patel SJ, Argüello JM, Helmann JD (2015) PfeT, a P1B4 -type ATPase, effluxes ferrous iron and protects *Bacillus subtilis* against iron intoxication. Mol Microbiol 98:787–803 .

Gunther MR, Hanna PM, Mason RP, Cohen MS (1995) Hydroxyl radical formation from cuprous ion and hydrogen peroxide: a spin-trapping study. Arch Biochem Biophys 316:515–522 .

Gupta A, Matsui K, Lo JF, Silver S (1999) Molecular basis for resistance to silver cations in *Salmonella*. Nat Med 5:183–188 .

Hammer ND, Reniere ML, Cassat JE, Zhang Y, Hirsch AO, Hood MI, Skaar EP (2013) Two heme-dependent terminal oxidases power *Staphylococcus aureus* organ-specific colonization of the vertebrate host. MBio 4:1–9 .

Handke LD, Gribenko A V, Timofeyeva Y, Scully IL, Anderson AS (2018) MntC-dependent manganese transport is essential for *Staphylococcus aureus* oxidative stress resistance and virulence. mSphere 3:e00336-18 .

Hao Z, Chen S, Wilson DB (1999a) Cloning, expression, and characterization of cadmium and manganese uptake genes from *Lactobacillus plantarum*. Appl Environ Microbiol 65(11):4746–4752.

Hao Z, Reiske HR, Wilson DB (1999b) Characterization of cadmium uptake in *Lactobacillus plantarum* and isolation of cadmium and manganese uptake mutants. Appl Environ Microbiol 65:4741–4745.

Hartman B, Tomasz A (1981) Altered penicillin-binding proteins in methicillin-resistant strains of *Staphylococcus aureus*. Antimicrob Agents Chemother 19:726–35.

Hartman BJ, Tomasz A (1984) Low-affinity penicillin-binding protein associated with beta-lactam resistance in *Staphylococcus aureus*. J Bacteriol 158:513–6

Hentze MW, Argos P (1991) Homology between IRE-BP, a regulatory RNA-binding protein, aconitase, and isopropylmalate isomerase. Nucleic Acids Res 19:1739–1740 .

Hodgkinson V, Petris MJ (2012) Copper homeostasis at the host-pathogen interface. J Biol Chem 287:13549–13555 .

Hong R, Kang TY, Michels CA, Gadura N (2012) Membrane lipid peroxidation in copper alloy-mediated contact killing of *Escherichia coli*. Appl Environ Microbiol 78:1776–1784 .

Horsburgh MJ, Clements MO, Crossley H, Ingham E, Foster SJ (2001a) PerR controls oxidative stress resistance and iron storage proteins and is required for virulence in *Staphylococcus aureus*. Infect Immun 69:3744–54 .

Horsburgh MJ, Ingham E, Foster SJ (2001b) In *Staphylococcus aureus*, Fur is an interactive regulator with PerR, contributes to virulence, and Is necessary for oxidative stress resistance through positive regulation of catalase and iron homeostasis. J Bacteriol 183:468–75 .

Horsburgh MJ, Wharton SJ, Cox AG, Ingham E, Peacock S, Foster SJ (2002) MntR modulates expression of the PerR regulon and superoxide resistance in *Staphylococcus aureus* through control of manganese uptake. Mol Microbiol 44:1269–1286 .

Huang M-E, Facca C, Fatmi Z, Baïlle D, Bénakli S, Vernis L (2016) DNA replication inhibitor hydroxyurea alters Fe-S centers by producing reactive oxygen species *in vivo*. Scientific Reports 6:29361.

Huang X, Shin JH, Pinochet-Barros A, Su TT, Helmann JD (2017) *Bacillus subtilis* MntR coordinates the transcriptional regulation of manganese uptake and efflux systems. Mol Microbiol 103(2), 253–268.

Huet G, Daffé M, Saves I (2005) Identification of the *Mycobacterium tuberculosis* SUF machinery as the exclusive mycobacterial system of [Fe-S] cluster assembly: evidence for its implication in the pathogen's survival. J Bacteriol 187:6137–46 .

Imlay JA (2014) The mismetallation of enzymes during oxidative stress. J. Biol. Chem **289**:28121–28128.

Imlay JA (2003) Pathways of oxidative damage. Annu Rev Microbiol 57:395–418.

Ito T, Hiramatsu K, Oliveira DC, De Lencastre H, Zhang K, Westh H, O'Brien F, Giffard PM, Coleman D, Tenover FC, Boyle-Vavra S, Skov RL, Enright MC, Kreiswirth B, Kwan SK, Grundmann H, Laurent F, Sollid JE, Kearns AM, Goering R, John JF, Daum R, Soderquist B (2009) Classification of S*taphylococcal Cassette Chromosome mec* (SCCmec): Guidelines for reporting novel SCCmec elements. Antimicrob. Agents Chemother. 53:4961–4967.

Jang S, Imlay JA (2007) Micromolar intracellular hydrogen peroxide disrupts metabolism by damaging iron-sulfur enzymes. J Biol Chem 282:929–37 .

Jarosławiecka A, Piotrowska-Seget Z (2014) Lead resistance in micro-organisms. Microbiol. (United Kingdom) 160:12–25

Jevons MP (1961) "Celbenin"-resistant staphylococci. BMJ 1:124–125 .

Ji Y, Woodnutt G, Rosenberg M, Burnham MKR (2002) Identification of essential genes in *Staphylococcus aureus* using inducible antisense RNA. Methods Enzymol 358:123–128 .

Johnson M, Sengupta M, Purves J, Tarrant E, Williams PH, Cockayne A, Muthaiyan A, Stephenson R, Ledala N, Wilkinson BJ, Jayaswal RK, Morrissey JA (2011) Fur is required for the activation of virulence gene expression through the induction of the sae regulatory system in *Staphylococcus aureus*. Int J Med Microbiol 301:44–52 .

Johnson MDL, Kehl-Fie TE, Klein R, Kelly J, Burnham C, Mann B, Rosch JW (2015a) Role of copper efflux in pneumococcal pathogenesis and resistance to macrophage-mediated immune clearance. Infect Immun 83:1684–94 .

Johnson MDL, Kehl-Fie TE, Rosch JW (2015b) Copper intoxication inhibits aerobic nucleotide synthesis in *Streptococcus pneumoniae*. Metallomics 7:786–794 .

Joska TM, Mashruwala A, Boyd JM, Belden WJ (2014) A universal cloning method based on yeast homologous recombination that is simple, efficient, and versatile. Journal of Microbiological Methods, 100(1), 46–51.

Juttukonda LJ, Skaar EP (2015) Manganese homeostasis and utilization in pathogenic bacteria. Mol Microbiol 97:216–28 .

Kamp HD, Patimalla-Dipali B, Lazinski DW, Wallace-Gadsden F, Camilli A (2013) Gene fitness landscapes of *Vibrio cholerae* at important stages of its life cycle. PLoS Pathog 9:e1003800 .

Kashmiri ZN, Mankar SA (2014) Free radicals and oxidative stress in bacteria. IntJCurrMicrobiolAppSci 3:34–40

Kehl-Fie TE, Zhang Y, Moore JL, Farrand AJ, Hood MI, Rathi S, Chazin WJ, Caprioli RM, Skaar EP (2013) MntABC and MntH contribute to systemic *Staphylococcus aureus* infection by competing with calprotectin for nutrient manganese. Infect Immun 81(9), 3395–3405.

Kehres DG, Zaharik ML, Finlay BB, Maguire ME (2000) The NRAMP proteins of Salmonella typhimurium and *Escherichia coli* are selective manganese

transporters involved in the response to reactive oxygen. Mol. Microbiol. 36:1085–1100

Kennedy MC, Emptage MH, Dreyer JL, Beinert H (1983) The role of iron in the activation-inactivation of aconitase. J Biol Chem 258:11098–11105

Keyer K, Imlay JA (1996) Superoxide accelerates DNA damage by elevating free-iron levels. Proc. Natl. Acad. Sci. U. S. A. 93(24), 13635–40.

Klein BA, Tenorio EL, Lazinski DW, Camilli A, Duncan MJ, Hu LT (2012) Identification of essential genes of the periodontal pathogen *Porphyromonas gingivalis*. BMC Genomics 13:578 .

Klevens RM (2007) Invasive methicillin-resistant *Staphylococcus aureus* infections in the united states. JAMA 298:1763 .

Kluytmans J, Van Belkum A, Verbrugh H (1997) Nasal carriage of *Staphylococcus aureus*: epidemiology, underlying mechanisms, and associated risks. *Clin. Microbiol. Rev.* 10, 505–520.

Knuth K, Niesalla H, Hueck CJ, Fuchs TM (2004) Large-scale identification of essential *Salmonella* genes by trapping lethal insertions. Mol Microbiol 51:1729–1744 .

Kobayashi K, Ehrlich SD, Albertini A, Amati G, Andersen KK, Arnaud M, Asai K, Ashikaga S, Aymerich S, Bessieres P, Boland F, Brignell SC, Bron S, Bunai K, Chapuis J, Christiansen LC, Danchin A, Debarbouille M, Dervyn E, Deuerling E, Devine K, Devine SK, Dreesen O, Errington J, Fillinger S, Foster SJ, Fujita Y, Galizzi A, Gardan R, Eschevins C, Fukushima T, Haga K, Harwood CR, Hecker M, Hosoya D, Hullo MF, Kakeshita H, Karamata D, Kasahara Y, Kawamura F, Koga K, Koski P, Kuwana R, Imamura D, Ishimaru M, Ishikawa S, Ishio I, Le Coq D, Masson A, Mauel C, Meima R, Mellado RP, Moir A, Moriya S, Nagakawa E, Nanamiya H, Nakai S, Nygaard P, Ogura M, Ohanan T, O'Reilly M, O'Rourke M, Pragai Z, Pooley HM, Rapoport G, Rawlins JP, Rivas LA, Rivolta C, Sadaie A, Sadaie Y, Sarvas M, Sato T, Saxild HH, Scanlan E, Schumann W, Seegers JFML, Sekiguchi J, Sekowska A, Seror SJ, Simon M, Stragier P, Studer R, Takamatsu H, Tanaka T, Takeuchi M, Thomaides HB, Vagner V, van Dijl JM, Watabe K, Wipat A, Yamamoto H, Yamamoto M, Yamamoto Y, Yamane K, Yata K, Yoshida K, Yoshikawa H, Zuber U, Ogasawara N (2003) Essential *Bacillus subtilis* genes. Proc Natl Acad Sci 100:4678–4683 .

Kreiswirth BN, Löfdahl S, Betley MJ, O'Reilly M, Schlievert PM, Bergdoll MS, Novick RP (1983) The toxic shock syndrome exotoxin structural gene is not detectably transmitted by a prophage. Nature 305:709–712 .

Krute CN, Carroll RK, Rivera FE, Weiss A, Young RM, Shilling A, Botlani M, Varma S, Baker BJ, Shaw LN (2015) The disruption of prenylation leads to pleiotropic rearrangements in cellular behavior in *Staphylococcus aureus*. Mol Microbiol 95:819–832 .

Laddaga RA, Silver S (1985) Cadmium uptake in *Escherichia coli* K-12. J Bacteriol

162:1100–1105.

Ladomersky E., Khan, A., Shanbhag, V., Cavet, J. S., Chan, J., Weisman, G. A., and Petris, M. J. (2017) Host and Pathogen Copper-Transporting P-Type ATPases Function Antagonistically during Salmonella Infection. Infect Immun 85.

Lalève A, Vallières C, Golinelli-Cohen M-P, Bouton C, Song Z, Pawlik G, Tindall SM, Avery S V, Clain J, Meunier B (2015) The antimalarial drug primaquine targets Fe-S cluster proteins and yeast respiratory growth. Redox Biol 7:21–29 .

Lauderdale KJ, Boles BR, Cheung AL, Horswill AR (2009) Interconnections between Sigma B, *agr*, and proteolytic activity in *Staphylococcus aureus* biofilm maturation. Infect Immun 77:1623–35 .

Layer G, Gaddam SA, Ayala-Castro CN, Ollagnier-de Choudens S, Lascoux D, Fontecave M, Outten FW (2007) SufE transfers sulfur from SufS to SufB for iron-sulfur cluster assembly. J Biol Chem 282:13342–50 .

Le Breton Y, Belew AT, Valdes KM, Islam E, Curry P, Tettelin H, Shirtliff ME, El-Sayed NM, McIver KS (2015) Essential genes in the core genome of the human pathogen *Streptococcus pyogenes*. Sci Rep 5:9838 .

Ledala N, Zhang B, Seravalli J, Powers R, Somerville GA (2014) Influence of iron and aeration on *Staphylococcus aureus* growth, metabolism, and transcription. J Bacteriol 196:2178–2189 .

Lee J-W, Soonsanga S, Helmann JD, Gottesman S (2007) A complex thiolate switch regulates the *Bacillus subtilis* organic peroxide sensor OhrR. Proc Natl Acad Sci U S A 104: 8743–8748.

Lee SA, Gallagher LA, Thongdee M, Staudinger BJ, Lippman S, Singh PK, Manoil C (2015) General and condition-specific essential functions of Pseudomonas aeruginosa. Proc Natl Acad Sci U S A 112:5189–94 .

Lei MG, Cue D, Roux CM, Dunman PM, Lee CY (2011) Rsp inhibits attachment and biofilm formation by repressing fnbA in *Staphylococcus aureus* MW2. J Bacteriol 193:5231–5241 .

Lewis K (2013) Platforms for antibiotic discovery. Nat Rev Drug Discov 12:371–387 .

Li, H., Handsaker, B., Wysoker, A., Fennell, T., Ruan, J., Homer, N., … 1000 Genome Project Data Processing Subgroup (2009). The Sequence Alignment/Map format and SAMtools. Bioinformatics 25(16):2078–2079.

Lieser SA, Davis TC, Helmann JD, Cohen SM (2003) DNA-binding and oligomerization studies of the manganese(ii) metalloregulatory protein MntR from *Bacillus subtilis*. Biochemistry 42:12634–12642 .

Lill R (2009) Function and biogenesis of iron–sulphur proteins. Nature 460:831–838 .

Lin L, Pantapalangkoor P, Tan B, Bruhn KW, Ho T, Nielsen T, Skaar EP, Zhang Y, Bai R, Wang A, Doherty TM, Spellberg B (2014) Transferrin iron starvation therapy for lethal bacterial and fungal infections. J Infect Dis 210:254–64 .

Lodise TP, McKinnon PS (2007) Burden of methicillin-resistant *Staphylococcus aureus*: Focus on clinical and economic outcomes. Pharmacotherapy 27:1001–1012

Lorenzo VDE, Wee S, Herrero M, Neilands JB (1987) Operator Sequences of the Aerobactin Operon of Plasmid ColV-K30 Binding the Ferric Uptake Regulation (*fur*) Repressor. J Bacteriol 169:2624–2630

Luong TT, Lee CY (2007) Improved single-copy integration vectors for *Staphylococcus aureus*. J Microbiol Methods 70:186–190 .

Ma Z, Cowart DM, Scott RA, Giedroc DP (2009) Molecular insights into the metal selectivity of the copper(i)-sensing repressor CsoR from *Bacillus subtilis*. Biochemistry 48:3325–3334 .

Macomber L, Imlay JA (2009) The iron-sulfur clusters of dehydratases are primary intracellular targets of copper toxicity. Proc Natl Acad Sci 106:8344–8349 .

Macomber L, Rensing C, Imlay JA (2007) Intracellular copper does not catalyze the formation of oxidative dna damage in *Escherichia coli*. J Bacteriol 189:1616–1626 .

Malachowa N, DeLeo FR (2010) Mobile genetic elements of *Staphylococcus aureus*. Cell Mol Life Sci 67:3057–71 .

Maringanti S, Imlay JA (1999) An intracellular iron chelator pleiotropically suppresses enzymatic and growth defects of superoxide dismutase-deficient *Escherichia coli.* Journal of Bacteriology, 181(12): 3792–3802.

Martin JE, Giedroc DP (2016) Functional determinants of metal ion transport and selectivity in paralogous cation diffusion facilitator transporters CzcD and MntE in *Streptococcus pneumoniae*. J Bacteriol 198(7), 1066–1076.

Martin JE, Imlay JA (2011) The alternative aerobic ribonucleotide reductase of *Escherichia coli*, NrdEF, is a manganese-dependent enzyme that enables cell replication during periods of iron starvation. Mol Microbiol 80:319–334 .

Masalha M, Borovok I, Schreiber R, Aharonowitz Y, Cohen G (2001) Analysis of transcription of the *Staphylococcus aureus* aerobic class Ib and anaerobic class III ribonucleotide reductase genes in response to oxygen. J Bacteriol 183:7260–72 .

Mashruwala AA, Bhatt S, Poudel S, Boyd ES, Boyd JM (2016a) The DUF59 containing protein SufT is involved in the maturation of iron-sulfur (fes) proteins during conditions of high fes cofactor demand in *Staphylococcus aureus*. PLOS Genet 12:e1006233 .

Mashruwala AA, Boyd JM (2015a) *De Novo* Assembly of Plasmids Using Yeast Recombinational Cloning. Methods Mol Biol 1373: 33–41.

Mashruwala AA, Boyd JM (2017) The *Staphylococcus aureus* SrrAB regulatory system modulates hydrogen peroxide resistance factors, which imparts protection to aconitase during aerobic growth. PLoS One 12:e0170283 .

Mashruwala AA, Pang YY, Rosario-Cruz Z, Chahal HK, Benson MA, Mike LA, Skaar EP, Torres VJ, Nauseef WM, Boyd JM (2015b) Nfu facilitates the maturation of iron-sulfur proteins and participates in virulence in *S taphylococcus aureus*. Mol Microbiol 95:383–409 .

Mashruwala AA, Roberts CA, Bhatt S, May KL, Carroll RK, Shaw LN, Boyd JM (2016b) *Staphylococcus aureus* SufT: an essential iron-sulphur cluster assembly factor in cells experiencing a high-demand for lipoic acid. Mol Microbiol 102(6), 1099–1119.

Metris, A., Reuter, M., Gaskin, D. J., Baranyi, J., & van Vliet, A. H. (2011). *In vivo* and in silico determination of essential genes of *Campylobacter jejuni*. BMC genomics, 12, 535.

Miller RE (1974) Glutamate synthase from *Escherichia coli*—An iron-sulfur flavoprotein: Separation and analysis of non-identical subunits. Biochim Biophys Acta - Enzymol 364:243–249 .

Mills SA, Marletta MA (2005) Metal binding characteristics and role of iron oxidation in the ferric uptake regulator from *Escherichia coli*. Biochemistry 44:13553–13559 .

Moore CM, Gaballa A, Hui M, Ye RW, Helmann JD (2005) Genetic and physiological responses of *Bacillus subtilis* to metal ion stress. Mol Microbiol 57:27–40 .

Morrissey JA, Cockayne A, Brummell K, Williams P (2004) The Staphylococcal ferritins are differentially regulated in response to iron and manganese and *via* PerR and Fur. Infect Immun 72:972–979 .

Moule MG, Hemsley CM, Seet Q, Guerra-Assunção JA, Lim J, Sarkar-Tyson M, Clark TG, Tan PBO, Titball RW, Cuccui J, Wren BW (2014) Genome-wide saturation mutagenesis of *Burkholderia pseudomallei K96243* predicts essential genes and novel targets for antimicrobial development. MBio 5:e00926-13 .

Müller P, Müller-Anstett M, Wagener J, Gao Q, Kaesler S, Schaller M, Biedermann T, Götz F (2010) The *Staphylococcus aureus* lipoprotein SitC colocalizes with Toll-like receptor 2 (TLR2) in murine keratinocytes and elicits intracellular TLR2 accumulation. Infect Immun 78:4243–50 .

Nachin L, El Hassouni M, Loiseau L, Expert D, Barras F (2001) SoxR-dependent response to oxidative stress and virulence of *Erwinia chrysanthemi*: the key role of SufC, an orphan ABC ATPase. Mol Microbiol 39:960–972 .

Nair D, Memmi G, Hernandez D, Bard J, Beaume M, Gill S, Francois P, Cheung AL (2011) Whole-genome sequencing of *Staphylococcus aureus* strain RN4220, a key laboratory strain used in virulence research, identifies mutations that affect not only virulence factors but also the fitness of the strain.

J Bacteriol 193:2332–5 .

Nauseef WM (2007) How human neutrophils kill and degrade microbes: an integrated view. Immunol Rev 219:88–102 .

Newton GL, Rawat M, La Clair JJ, Jothivasan VK, Budiarto T, Hamilton CJ, Claiborne A, Helmann JD, Fahey RC (2009) Bacillithiol is an antioxidant thiol produced in *Bacilli*. Nat Chem Biol 5:625–627 .

Norambuena J, Hanson TE, Barkay T, Boyd JM (2019) Superoxide dismutase and pseudocatalase increase tolerance to Hg(II) in *Thermus thermophilus* HB27 by maintaining the reduced bacillithiol pool. MBio 10:e00183-19 .

Norambuena J, Wang Y, Hanson T, Boyd JM, Barkay T (2018) Low-molecular-weight thiols and thioredoxins are important players in Hg(II) resistance in *Thermus thermophilus HB27*. Appl Environ Microbiol 84:e01931-17.

Novick RP (1963) Analysis by Transduction of Mutations affecting Penicillinase Formation in *Staphylococcus aureus.* J. Gen. Microbiol. 33:121-136.

Ogston A (1984) “On Abscesses”. Reviews of Infectious Diseases 6:122–128 .

Ollagnier-de Choudens S, Fontecave M (1999) The lipoate synthase from *Escherichia coli* is an iron-sulfur protein. FEBS Lett 453:25–28 .

Olson BJSC, Markwell J (2007) Assays for determination of protein concentration. Curr Protoc Pharmacol 38:A.3A.1-A.3A.29 .

Osman D, Cavet JS (2008) Copper homeostasis in bacteria. Adv. Appl. Microbiol. 65: 217–247.

Osmundson J, Dewell S, Darst SA (2013) RNA-Seq reveals differential gene expression in *Staphylococcus aureus* with single-nucleotide resolution. PLoS One 8:e76572.

Otto M (2008) Staphylococcal Biofilms. Curr Top Microbiol Immunol 322: 207–228.

Outten FW, Huffman DL, Hale JA, O’Halloran T V (2001) The independent *cue* and *cus* systems confer copper tolerance during aerobic and anaerobic growth in *Escherichia coli*. J Biol Chem 276:30670–7 .

Palmer LD, Skaar EP (2016) Transition metals and virulence in bacteria. Annu Rev Genet 50:67–91 .

Pané-Farré J, Jonas B, Förstner K, Engelmann S, Hecker M (2006) The *σB* regulon in *Staphylococcus aureus* and its regulation. Int J Med Microbiol 296:237–258 .

Pang YY, Schwartz J, Bloomberg S, Boyd JM, Horswill AR, Nauseef WM (2014) Methionine sulfoxide reductases protect against oxidative stress in S*taphylococcus aureus* encountering exogenous oxidants and human neutrophils. J Innate Immun 6:353–364 .

Papp-Wallace KM, Maguire ME (2006) Manganese transport and the role of manganese in virulence. Annu Rev Microbiol 60:187–209 .

Perry RD, Silver S (1982) Cadmium and manganese transport in *Staphylococcus aureus* membrane vesicles. J Bacteriol 150:973–976

Peters K, Pazos M, Edoo Z, Hugonnet J-E, Martorana AM, Polissi A, VanNieuwenhze MS, Arthur M, Vollmer W (2018) Copper inhibits peptidoglycan LD-transpeptidases suppressing β-lactam resistance due to bypass of penicillin-binding proteins. Proc Natl Acad Sci U S A 115:10786–10791 .

Pham AN, Xing G, Miller CJ, Waite TD (2013) Fenton-like copper redox chemistry revisited: Hydrogen peroxide and superoxide mediation of copper-catalyzed oxidant production. J Catal 301:54–64 .

Porello SL, Cannon MJ, David SS (1998) A substrate recognition role for the [4Fe-4S]2+ cluster of the DNA repair glycosylase MutY. Biochemistry 37:6465–6475 .

Posada AC, Kolar SL, Dusi RG, Francois P, Roberts AA, Hamilton CJ, Liu GY, Cheung A (2014) Importance of bacillithiol in the oxidative stress response of *Staphylococcus aureus*. Infect Immun 82:316–32 .

Powers L, Lauraeus M, Reddy KS, Chance B, Wikström M (1994) Structure of the binuclear heme iron-copper site in the quinol-oxidizing cytochrome *aa3* from *Bacillus subtilis*. Biochim Biophys Acta - Bioenerg 1183:504–512 .

Prinz WA, Åslund F, Holmgren A, Beckwith J (1997) The role of the thioredoxin and glutaredoxin pathways in reducing protein disulfide bonds in the *Escherichia coli* cytoplasm. J Biol Chem 272:15661–15667 .

Proctor RA, Van Langevelde P, Kristjansson M, Maslow JN, Arbeit RD (1995) Persistent and Relapsing Infections Associated with Small-Colony Variants of *Staphylococcus aureus.* Clinical Infectious Diseases 20(1): 95–102.

Purves J, Thomas J, Riboldi GP, Zapotoczna M, Tarrant E, Andrew PW, Londoño A, Planet PJ, Geoghegan JA, Waldron KJ, Morrissey JA (2018) A horizontally gene transferred copper resistance locus confers hyper-resistance to antibacterial copper toxicity and enables survival of community acquired methicillin resistant *Staphylococcus aureus* USA300 in macrophages. Environ Microbiol 20:1576–1589 .

Py B, Barras F (2010) Building Fe–S proteins: bacterial strategies. Nat. Rev. Microbiol 8:436-446 .

Que Q, Helmann JD (2000) Manganese homestasis in *Bacillus subtilis* is regulated by MntR, a bifunctional regulator related to the diphtheria toxin repressor family of proteins. Mol Microbiol 35: 1454–1468.

Quintana J, Novoa-Aponte L, Argüello JM (2017) Copper homeostasis networks in the bacterium *Pseudomonas aeruginosa*. Journal of Biological Chemistry 292: 15691–15704.

Rabinovitch I, Yanku M, Yeheskel A, Cohen G, Borovok I, Aharonowitz Y (2010) *Staphylococcus aureus* NrdH redoxin is a reductant of the class Ib

ribonucleotide reductase. J Bacteriol 192:4963–4972 .

Radin JN, Zhu J, Brazel EB, McDevitt CA, Kehl-Fie TE (2019) Synergy between nutritional immunity and independent host defenses contributes to the importance of the MntABC manganese transporter during *Staphylococcus aureus* infection. Infect Immun 87:e00642-18 .

Ranquet C, Ollagnier-de-Choudens S, Loiseau L, Barras F, Fontecave M (2007). Cobalt stress in *Escherichia coli*. The effect on the iron-sulfur proteins. J Biol Chem 282:30442–30451 .

Rauen U, Springer A, Weisheit D, Petrat F, Korth H-G, de Groot H, Sustmann R (2007) Assessment of chelatable mitochondrial iron by using mitochondrion-selective fluorescent iron indicators with different iron-binding affinities. ChemBioChem 8:341–352 .

Recsei P, Kreiswirth B, O'Reilly M, Schlievert P, Gruss A, Novick RP (1986) Regulation of exoprotein gene expression in *Staphylococcus aureus* by *agr*. MGG Mol Gen Genet 202:58–61 .

Ridge PG, Zhang Y, Gladyshev VN (2008) Comparative genomic analyses of copper transporters and cuproproteomes reveal evolutionary dynamics of copper utilization and its link to oxygen. PLoS ONE, 3(1).

Roberts CA, Al-Tameemi HM, Mashruwala AA, Rosario-Cruz Z, Chauhan U, Sause WE, Torres VJ, Belden WJ, Boyd JM (2017) The Suf iron-sulfur cluster biosynthetic system is essential in *Staphylococcus aureus*, and decreased suf function results in global metabolic defects and reduced survival in human neutrophils. Infect Immun 85:e00100-17 .

Robinson JT, Thorvaldsdóttir H, Winckler W, Guttman M, Lander ES, Getz G, Mesirov JP (2011) Integrative genomics viewer. Nat Biotechnol 29:24–26 .

Roche B, Aussel L, Ezraty B, Mandin P, Py B, Barras F (2013) Reprint of: Iron/sulfur proteins biogenesis in prokaryotes: formation, regulation and diversity. Biochim Biophys Acta 1827:923–37 .

Rosario-Cruz Z, Boyd JM (2016) Physiological roles of bacillithiol in intracellular metal processing. Curr Genet 62:59–65 .

Rosario-Cruz Z, Chahal HK, Mike LA, Skaar EP, Boyd JM (2015) Bacillithiol has a role in Fe-S cluster biogenesis in *S taphylococcus aureus*. Mol Microbiol 98:218–242 .

Rosario-Cruz Z, Eletsky A, Daigham NS, Al-Tameemi H, Swapna GVT, Kahn PC, Szyperski T, Montelione GT, Boyd JM (2019) The *copBL* operon protects *Staphylococcus aureus* from copper toxicity: CopL is an extracellular membrane-associated copper-binding protein. J Biol Chem jbc.RA118.004723 .

Rowland JL, Niederweis M (2012) Resistance mechanisms of *Mycobacterium tuberculosis* against phagosomal copper overload. Tuberculosis 92:202–210.

Rubino JT, Chenkin MP, Keller M, Riggs-Gelasco P, Franz KJ (2011) A

comparison of methionine, histidine and cysteine in copper(i)-binding peptides reveals differences relevant to copper uptake by organisms in diverse environments. Metallomics 3:61–73 .

Sabri M, Léveillé S, Dozois CM (2006) A SitABCD homologue from an avian pathogenic *Escherichia coli* strain mediates transport of iron and manganese and resistance to hydrogen peroxide. Microbiology 152:745–758 .

Sadykov MR, Mattes TA, Luong TT, Zhu Y, Day SR, Sifri CD, Lee CY, Somerville GA (2010) Tricarboxylic acid cycle-dependent synthesis of *Staphylococcus aureus* Type 5 and 8 capsular polysaccharides. J Bacteriol 192:1459–62 .

Saini A, Mapolelo DT, Chahal HK, Johnson MK, Outten FW (2010) SufD and SufC ATPase activity are required for iron acquisition during in vivo Fe-S cluster formation on SufB. Biochemistry 49:9402–9412 .

Salama NR, Shepherd B, Falkow S (2004) Global transposon mutagenesis and essential gene analysis of *Helicobacter pylori*. J Bacteriol 186:7926–35 .

Salomon E, Keren N, Kanteev M, Adir N (2011) Manganese in biological systems: transport and function. PATAI'S Chem Funct Groups 1–16 .

Santiago M, Matano LM, Moussa SH, Gilmore MS, Walker S, Meredith TC (2015) A new platform for ultra-high density *Staphylococcus aureus* transposon libraries. BMC Genomics 16:252 .

Sebulsky MT, Hohnstein D, Hunter MD, Heinrichs DE (2000) Identification and characterization of a membrane permease involved in iron-hydroxamate transport in *Staphylococcus aureus*. J Bacteriol 182:4394–400 .

Selbach B, Earles E, Dos Santos PC (2010) Kinetic analysis of the bisubstrate cysteine desulfurase *sufs* from *Bacillus subtilis*. Biochemistry 49:8794–8802.

Selbach BP, Chung AH, Scott AD, George SJ, Cramer SP, Dos Santos PC (2014) Fe-S cluster biogenesis in gram-positive bacteria: SufU is a zinc-dependent sulfur transfer protein. Biochemistry 53:152–160 .

Seo SW, Kim D, Latif H, O'Brien EJ, Szubin R, Palsson BO (2014) Deciphering Fur transcriptional regulatory network highlights its complex role beyond iron metabolism in *Escherichia coli*. Nat Commun 5:4910 .

Shi X, Festa RA, Ioerger TR, Butler-Wu S, Sacchettini JC, Darwin KH, Samanovic MI (2014) The Copper-Responsive RicR Regulon Contributes to Mycobacterium tuberculosis Virulence. MBio 5:e00876-13 .

Singh R, Beriault R, Middaugh J, Hamel R, Chenier D, Appanna VD, Kalyuzhnyi S (2005) Aluminum-tolerant *Pseudomonas fluorescens*: ROS toxicity and enhanced NADPH production. Extremophiles 9:367–373 .

Singleton C, Hearnshaw S, Zhou L, Le Brun NE, Hemmings AM (2009) Mechanistic insights into Cu(I) cluster transfer between the chaperone CopZ and its cognate Cu(I)-transporting P-type ATPase, CopA. Biochem J 424:347–356 .

Sitthisak S, Howieson K, Amezola C, Jayaswal RK (2005) Characterization of a multicopper oxidase gene from *Staphylococcus aureus*. Appl Environ Microbiol 71:5650–3 .

Sitthisak S, Knutsson L, Webb JW, Jayaswal RK (2007) Molecular characterization of the copper transport system in Staphylococus aureus. Microbiology 153:4274–4283 .

Skaar EP, Humayun M, Bae T, DeBord KL, Schneewind O (2004) Iron-source preference of *Staphylococcus aureus* infections. Science 305:1626–1628 .

Skinner D, Keefer CS (1941) Significance of bacteremia caused by *Staphylococcus aureus*. Arch Intern Med 68:851-875.

Smaldone GT, Revelles O, Gaballa A, Sauer U, Antelmann H, Helmann JD (2012) A global investigation of the *Bacillus subtilis* iron-sparing response identifies major changes in metabolism. J Bacteriol 194:2594–2605 .

Smith MN, Brotherton AL, Lusardi K, Tan CA, Hammond DA (2019) Systematic review of the clinical utility of methicillin-resistant *Staphylococcus aureus* (MRSA) nasal screening for mrsa pneumonia. Ann Pharmacother *53*(6): 627–638.

Solomon EI, Heppner DE, Johnston EM, Ginsbach JW, Cirera J, Qayyum M, Kieber-Emmons MT, Kjaergaard CH, Hadt RG, Tian L (2014) Copper active sites in biology. Chem Rev 114(7): 3659–3853.

Somerville GA, Chaussee MS, Morgan CI, Fitzgerald JR, Dorward DW, Reitzer LJ, Musser JM (2002) *Staphylococcus aureus* aconitase inactivation unexpectedly inhibits post-exponential-phase growth and enhances stationary-phase survival. Infect Immun 70:6373–82 .

Speer A, Rowland JL, Haeili M, Niederweis M, Wolschendorf F (2013) Porins increase copper susceptibility of *Mycobacterium tuberculosis*. J Bacteriol 195:5133–40 .

Speziali CD, Dale SE, Henderson JA, Vinés ED, Heinrichs DE (2006) Requirement of *Staphylococcus aureus* ATP-binding cassette-ATPase FhuC for iron-restricted growth and evidence that it functions with more than one iron transporter. J Bacteriol 188:2048–55 .

Stoll H, Dengjel J, Nerz C, Götz F (2005) *Staphylococcus aureus* deficient in lipidation of prelipoproteins is attenuated in growth and immune activation. Infect Immun 73:2411–2423 .

Sun F, Ji Q, Jones MB, Deng X, Liang H, Frank B, Telser J, Peterson SN, Bae T, He C (2012) AirSR, a [2Fe-2S] cluster-containing two-component system, mediates global oxygen sensing and redox signaling in *Staphylococcus aureus*. J Am Chem Soc 134:305–14 .

Takahashi Y, Tokumoto U (2002) A third bacterial system for the assembly of iron-sulfur clusters with homologs in archaea and plastids. J Biol Chem 277:28380–3 .

Tan G, Cheng Z, Pang Y, Landry AP, Li J, Lu J, Ding H (2014) Copper binding in IscA inhibits iron-sulphur cluster assembly in *Escherichia coli*. Mol Microbiol *93*(4): 629–644.

Tan G, Yang J, Li T, Zhao J, Sun S, Li X, Lin C, Li J, Zhou H, Lyu J, Ding H (2017) Anaerobic copper toxicity and iron-sulfur cluster biogenesis in *Escherichia coli*. Appl Environ Microbiol 83:e00867-17 .

Tenover FC, McDougal LK, Goering R V., Killgore G, Projan SJ, Patel JB, Dunman PM (2006) Characterization of a strain of community-associated methicillin-resistant *Staphylococcus aureus* widely disseminated in the United States. J Clin Microbiol 44(1):108–118.

Thorgersen MP, Downs DM (2007) Cobalt targets multiple metabolic processes in *Salmonella enterica*. J Bacteriol 189:7774–81 .

Tottey S, Rich PR, Rondet SAM, Robinson NJ (2001) Two menkes-type ATPases supply copper for photosynthesis in *Synechocystis* PCC 6803. J Biol Chem 276:19999–20004.

Traber K, Novick R (2006) A slipped-mispairing mutation in AgrA of laboratory strains and clinical isolates results in delayed activation of *agr* and failure to translate δ- and α-haemolysins. Mol Microbiol 59:1519–1530 .

Trapnell C, Roberts A, Goff L, Pertea G, Kim D, Kelley DR, Pimentel H, Salzberg SL, Rinn JL, Pachter L (2012) Differential gene and transcript expression analysis of RNA-seq experiments with TopHat and Cufflinks. Nat Protoc 7:562–578 .

Trapnell C, Williams BA, Pertea G, Mortazavi A, Kwan G, van Baren MJ, Salzberg SL, Wold BJ, Pachter L (2010) Transcript assembly and quantification by RNA-Seq reveals unannotated transcripts and isoform switching during cell differentiation. Nat Biotechnol 28:511–515 .

Turner NA, Sharma-Kuinkel BK, Maskarinec SA, Eichenberger EM, Shah PP, Carugati M, Holland TL, Fowler VG (2019) Methicillin-resistant *Staphylococcus aureus*: an overview of basic and clinical research. Nat Rev Microbiol 1 .

Tynecka Z, Gos Z, Zajac J (1981) Reduced cadmium transport determined by a resistance plasmid in *Staphylococcus aureus*. J Bacteriol 147:305–312

Uribe-Querol E, Rosales C (2017) Control of phagocytosis by microbial pathogens. Front Immunol 8:1368 .

Uziel O, Borovok I, Schreiber R, Cohen G, Aharonowitz Y (2004) Transcriptional regulation of the *Staphylococcus aureus* thioredoxin and thioredoxin reductase genes in response to oxygen and disulfide stress. J Bacteriol 186:326–334 .

Valentino MD, Foulston L, Sadaka A, Kos VN, Villet RA, Santa Maria J, Lazinski DW, Camilli A, Walker S, Hooper DC, Gilmore MS (2014) Genes contributing to *Staphylococcus aureus* fitness in abscess- and infection-related ecologies.

MBio 5:e01729-14 .

van Opijnen T, Camilli A (2012) A fine scale phenotype-genotype virulence map of a bacterial pathogen. Genome Res 22:2541–51 .

Vanoni MA, Curti B (2008) Structure–function studies of glutamate synthases: A class of self-regulated iron-sulfur flavoenzymes essential for nitrogen assimilation. IUBMB Life 60:287–300 .

Veeranagouda Y, Husain F, Tenorio EL, Wexler HM (2014) Identification of genes required for the survival of *B. fragilis* using massive parallel sequencing of a saturated transposon mutant library. BMC Genomics 15:429 .

Vernis L, El Banna N, Baïlle D, Hatem E, Heneman A, Huang ME (2017) Fe-S clusters emerging as targets of therapeutic drugs. Oxid Med Cell Longev 2017: .

Wagner D, Maser J, Lai B, Cai Z, Barry CE, Höner Zu Bentrup K, Russell DG, Bermudez LE (2005) Elemental analysis of *Mycobacterium avium*, *Mycobacterium tuberculosis*, and *Mycobacterium smegmatis* containing phagosomes indicates pathogen-induced microenvironments within the host cell's endosomal system. J Immunol 174:1491–500 .

Waldron KJ, Robinson NJ (2009) How do bacterial cells ensure that metalloproteins get the correct metal? Nature Rev. Microbiol **7:**25–35

Warnes SL, Caves V, Keevil CW (2012) Mechanism of copper surface toxicity in *Escherichia coli* O157:H7 and *Salmonella* involves immediate membrane depolarization followed by slower rate of DNA destruction which differs from that observed for Gram-positive bacteria. Environ Microbiol 14:1730–43 .

Warnes SL, Keevil CW (2016) Lack of involvement of fenton chemistry in death of methicillin-resistant and methicillin-sensitive strains of *Staphylococcus aureus* and destruction of their genomes on wet or dry copper alloy surfaces. Appl Environ Microbiol 82:2132–2136 .

Whellan DJ, Ellis SJ, Kraus WE, Hawthorne K, Piña IL, Keteyian SJ, Kitzman DW, Cooper L, Lee K, Connor CMO (2014) Copper active sites in biology. Chem Rev 114:3659–3853 .

White C, Lee J, Kambe T, Fritsche K, Petris MJ (2009) A role for the ATP7A copper-transporting ATPase in macrophage bactericidal activity. J Biol Chem 284:33949–56 .

White JR, Yeowell HN (1982) Iron enhances the bactericidal action of streptonigrin. Biochem Biophys Res Commun 106:407–411 .

Wilcox M, Al-Obeid S, Gales A, Kozlov R, Martínez-Orozco JA, Rossi F, Sidorenko S, Blondeau J (2019) Reporting elevated vancomycin minimum inhibitory concentration in methicillin-resistant *Staphylococcus aureus* : consensus by an International Working Group. Future Microbiol 14(4): 345–352.

Wilkens S (2015) Structure and mechanism of ABC transporters. F1000Prime Rep 7:14 .

Williams RE (1963) Healthy carriage of *Staphylococcus aureus*: its prevalence and importance. Bacteriol Rev 27:56–71

Wollers S, Layer G, Garcia-Serres R, Signor L, Clemancey M, Latour J-M, Fontecave M, Ollagnier de Choudens S (2010) Iron-sulfur (Fe-S) cluster assembly: the SufBCD complex is a new type of Fe-S scaffold with a flavin redox cofactor. J Biol Chem 285:23331–41 .

Xiong A, Singh VK, Cabrera G, Jayaswal RK (2000) Molecular characterization of the ferric-uptake regulator, Fur, from *Staphylococcus aureus*. Microbiology 146:659–668

Xu FF, Imlay JA (2012) Silver(I), Mercury(II), Cadmium(II), and Zinc(II) target exposed enzymic iron-sulfur clusters when they toxify *Escherichia coli*. Appl Environ Microbiol 78:3614–3621 .

Yeeles JTP, Cammack R, Dillingham MS (2009) An iron-sulfur cluster is essential for the binding of broken DNA by AddAB-type helicase-nucleases. J Biol Chem 284:7746–55 .

Yuvaniyama P, Agar JN, Cash VL, Johnson MK, Dean DR (2000) NifS-directed assembly of a transient [2Fe-2S] cluster within the NifU protein. Proc Natl Acad Sci U S A 97:599–604 .

Zapotoczna M, Riboldi GP, Moustafa AM, Dickson E, Narechania A, Morrissey JA, Planet PJ, Holden MTG, Waldron KJ, Geoghegan JA (2018) Mobile-genetic-element-encoded hypertolerance to copper protects *Staphylococcus aureus* from killing by host phagocytes. MBio 9:e00550-18.

Zheng L, Cash VL, Flint DH, Dean DR (1998) Assembly of iron-sulfur clusters. Identification of an iscSUA-hscBA-fdx gene cluster from *Azotobacter vinelandii*. J Biol Chem 273:13264–72 .